Surface chemistry of Burrup Rock art at the Yara monitoring sites 2019

Report for Yara Pilbara Nitrates by
CBG Solutions

Prepared by Dr Ian D MacLeod
Heritage Conservation Solutions

Draft report
Version 1.8

9 October 2019

Figure 1: View of the TAN plant from site 23

Contents

Executive Summary

- Measurements in August 2019 were conducted on gabbro sites (7, 22 & 23) and granophyre sites (5, 6 & 21) with the sites determined through the CSIRO monitoring program. An additional set of measurements were taken at site 4 and an adjacent rock. At the climbing man site pH measurements only were made and at the adjacent rock a suite of pH and chloride measurements were conducted.
- In addition to the surface pH and chloride, the redox voltages were measured at the Yara monitoring points and at site 4 and its adjacent rock. From the intercept values of the regression lines between the Pourbaix plots it has been possible to determine the dissolution mechanisms on the rock surfaces
- There was measurable soluble iron detected at all the washed rock surfaces.
- There is a correlation of increased colour difference between the engravings and the host rock with the mean pH and differences occur between parent rock types.
- Twenty-eight sets of measurements of colour show that nearly 96% show NO colour difference between 2019 and 2018. The differences are only definite the differences between 2019 an d2018 for site 4 spot 1. The only significant difference in colour between the 2019 and 2017 data was found for site 23 spot 3.
- The only site with a measurable amount of boron in the wash solution was for the Deep Gorge site which indicates that there is not a problem with mobilisation of chlorite at all the other sites
- Prolonged dry spells lead to accumulation of wind-borne sea salts which resist acidification. Light rainfall events have taken place in the past year and all the sites, except site 4, have increased acidification.
- The mean nitrate concentration in wash solutions was 6.3 ppm in 2003, 4.5 ppm in 2004 and 0.6 ppm in 2017, 0.7 ± 0.4 ppm for 2018 while for 2019 the mean value was the same as in the previous year at 0.71± 0.36 ppm.
- There is a need to continue surface measurements and washing of rocks to ensure that the sites are stable.

Background

To comply with the regulations concerning retention of its operating licence, EPBC 2008/4546, Yara Pilbara Nitrates engaged CBG Solutions to develop appropriate methodologies to conduct colour monitoring measurements on the six sites surrounding the ammonia and ammonium nitrate plants in the Burrup (Figure 1). The lead consultant (Warren Fish) conducted meetings with the management team from Yara to develop the timetable and to engage with key community members of the Murujuga Aboriginal Corporation for permission to come to country August 2019 to repeat the colour measurements done in previous years by the CSIRO team. MacLeod retired from the Western Australian Museum in 2016 and is now the Principal of Heritage Conservation Solutions and has published peer-reviewed papers on the conservation of Aboriginal rock art and has 40-years' experience in materials conservation (Appendix I).

During the first phase (2003-2004) of research into the condition of the rock surfaces in the Burrup, several engraved rocks in the "Museum Compound" were examined regarding their acidity (as measured with a surface pH electrode), the water-soluble minerals on the rock surfaces and the microbiological activity. Samples of the rock surface were swabbed with sterile culture material and placed into prepared phials. The biological material was stored at zero degrees before being taken to laboratories in Perth (Department of Agriculture) for characterisation. Other reference measurements were conducted on Gidley and Dolphin Islands in the Dampier Archipelago to act as reference points away from industrial activities associated with the Woodside gas plant and iron ore shipping out of Dampier ports.

Analysis of the solution chemistry collected between 2003 and 2004 provided strong indications of the causal link between the amount of nitrate on the rocks and the level of microbiological activity. This in turn indicated that the acidic metabolites from the organisms were significantly contributing to the overall acidification of the rock surfaces and mobilisation of key minerals containing both iron and manganese, as well as copper and nickel. In the light of this background information, it was decided to conduct solution sampling on the rock surfaces on the six CSIRO approved sites within the 2 km radius of the Pilbara Nitrates plant. The rock irrigation data was done in conjunction with surface measurements of the pH and chloride ion activity. The wash solutions were analysed for sulphate, sulphite, nitrate and nitrite ions, as well as for oxalate, of which there was none. The electrical conductivity of the wash solutions was also measured as a guide to the overall nature of the soluble minerals and salts that were mobilised during the five minutes of sample collection.

Field work was conducted on the six monitoring stations around the Yara plant in August 2019 and at an additional site 4 which is close to the Withnell Bay road near the Woodside flare tower, as shown in Figure 2. This report includes commentary on the interpretation of the colour measurements from the Konica Minolta Chromameter. The sites are part of the CSIRO colour and mineralogy monitoring of the Burrup that has been undergoing continuous evaluation for the past 14 years. In addition to the spectrophotometric work a series of pH, chloride and redox potential readings were taken directly on the rocks adjacent to the CSIRO monitoring points. In order to quantify the relationship between the surface chemistry, as measured by the contact with the flat surface pH and chloride electrodes, standard volumes of distilled water were used to temporarily irrigate (wash) the rocks, to collect the water-soluble metal ions and all discernible anions (chloride, nitrate, nitrite, oxalate, and sulphate). The refrigerated samples were stored off site until they were transported by air to the Bentley based laboratories of the ChemCentre for independent NATA accredited chemical analyses.

This report examines in detail the solution chemistry and provides a synthesis on the historical data relating to two sets of solution and surface pH measurements conducted in 14-15 years before the present work. The referenced sites of interest to Yara included granophyre at the Burrup Road (5), the

Water Tanks (6) and Yara West (21) sites, while gabbro rocks were found on sites at Deep Gorge (7), Yara North East (22) and Yara East (23). All these sites lie within a 2 km radius of the present operational sites of the ammonia plant and the Technical Ammonium Nitrate (TAN) site. The additional site that was chemically assessed was number 4 and an adjacent rock site 4a some five metres closer to the Withnell Bay road, adjacent to the Woodside plant about two hundred metres from the flare tower.

Measurement of the rock surface pH and chloride concentration

The pH and chloride ion measurements taken on rocks adjacent to the CSIRO reference engraved sites so that the colour reference rocks would be kept in a "pristine state". The pH data was recorded using a flat surface pH electrode which had been calibrated each morning using standard pH buffers at pH 4 and pH 7 before the field measurements commenced. The pH meter was temperature compensated using a thermocouple connected to the TPS pH meter (Aqua pH/ORP/^{o}C)) and the glass electrode was a VWR model no W7567287. Readings of the surface pH were standardised by recording the values after an elapsed interval of one minute. If the surface was more responsive and the pH reading stabilised in 40 seconds, then that value was recorded and keeping the probe in position did not alter the steady value that had been noted. Owing to the porous nature of the rock substrate prolonged equilibration times can result in pH values that are not reflective of the local microenvironment. A small amount of water is needed to keep the bulb wet and the solution in contact with the internal reference electrode. The electrical circuit of the pH electrode is completed through connecting the internal Ag/AgCl reference electrode through two fine wicks which are situated at 180° to each other on either side of the glass membrane and held in place by the soft plastic ring fitting inside the 12-mm external diameter solid epoxy body. The chloride ion activity was measured using a TPS WP-90 ion-pH-mV-^{o}C meter coupled with an Orion Thermo 1609-186881 chloride ion specific electrode. The rocks were wetted with two drops (0.08 ml) of a 0.05 molar sodium nitrate solution to provide an electrolyte to stabilise the liquid junction between the sensing head and the rock surface. Stable readings of the chloride activity were obtained within a minute. The electrode was calibrated daily with a 1,000 and a 100-ppm chloride reference solution before any field measurements were made.

Figure 2: Map of reference sites with mean 2019 pH values noted on the map.

Analysis of sea borne salts on the rocks

The amounts of surface chloride detected on the rock surfaces provide direct evidence of the impact of the marine environment and indicate that salt weathering of rocks, with extensive dehydration and rehydration cycles apparently playing a significant role in the local environment. The wash solutions from the rock surfaces showed up a range of ions commonly associated with sea water, namely Na^+, K^+, Mg^{2+}, Ca^{2+}, Cl^- and SO_4^{2-}. Analysis of the way in which the concentrations varied across the Burrup was consistent with known weather patterns of prevailing winds and proximity to the sea. When the wash concentrations of sulphate are plotted as a function of the chloride, most of the data follow a linear relation that reflects the common ratios of the anions that are found in seawater. Data from the most recent irrigation data obtained in August 2019 is shown in Table 1. Significant differences from the normal ratios found in seawater are found on the rock surfaces in the Burrup.

The microenvironment of the rocks was assessed through a combination of surface chloride (Orion Thermo combination Cl electrode) and surface pH (WVR flat electrode) measurements on the rock surfaces. The first round of measurements was made using a 0.05 M $NaNO_3$ solution in distilled water electrolyte was used for chloride measurements and the pH was recorded after equilibration with two to three drops (0.04-0.06 ml) of distilled water on the rock surface. The Chemistry Centre of WA determined the soluble nitrate, nitrite, sulphate, chloride, oxalate concentrations on the rock surfaces by ion chromatography from distilled water washings collected from the rock surfaces and standardized to a 200 cm^2 area. Metal ions in the wash solutions were determined by inductively coupled plasma–mass spectrometric (ICP–MS) methods. This study is based on an initial survey in June 2003 (winter) of relocated engraved rocks which was then extended in August 2003 (spring) to include several sites located at a distance from known emission sources was concluded in February 2004 (summer) with repeated measurements on the Burrup. Data obtained for the 2019 measurements for cations measurements were made on 200 ml samples and anions in 100 ml sample bottles collected over an area of approximately 500 cm^2.

Table 1: Ratio of salts in sea water and in the rock washings around the Yara plant

Solution ratios	Sea	Site 4 Gabbro	Site 4a Gabbro	Site 5 Grano.	Site 6 Grano.	Site 7 Gabbro	Site 21 Grano.	Site 22 Gabbro	Site 23 Gabbro
Cl^-/Na^+	1.8	1.1	1.0	3.1	1.3	3.9	2.8	1.6	1.0
Cl^-/SO_4^{2-}	7.1	2.3	1.3	2.8	2.1	2.3	4.3	5.3	1.9
Cl^-/Ca^{2+}	47	4.5	3.8	13.6	2.4	6.8	23.4	4.2	2.1
Ca^{2+}/K^+	1	0.7	2.4	2.8	2.3	4.2	2.7	1.0	3.0
Ca^{2+}/Ba^{2+}	8,000	222	240	149	538	403	385	357	900
Mg^{2+}/Ca^{2+}	3.1		0.33	0.43	0.00	0.36	0.80	0.00	0.28
Na^+/K^+	27	2.7	9.0	12.2	4.3	7.3	22.2	2.6	6.3

A major difference between the site 4 data on the Cl^-/SO_4^{2-} ratio was observed in the 2019 washing as the ratio had increased from 0.7 in 2018 to 2.3 while the values for sites 5,6, 7 and sites 21- 23 were essentially the same. This implies that something has changed on the surface of the reference rock, with a significant drop in the amount of sulphate activity in 2019. The adjacent rock site 4a has much the same chloride to sulphate ratio as the reference rock 4 had in 2018. The adjacent rock is only five metres closer to the Withnell Bay road, as shown in Figure 2. It was also noted that site 4 was the only one of the seven sites measured for surface pH that had a more alkaline value than in 2018. The behaviour of the CSIRO reference rock number 4 is anomalous for its chemistry and the pH are markedly different to that of the adjacent rock 4a which is, as previously noted, only 5 metres away. A possible explanation for this apparently confusing situation is that the rock was subjected to an

extremely localised watering event that brought about a significant drop in acidity that had been previously recorded in 2018 and in 2017.

When the electrical conductivity to pH ratio is plotted, as shown in Figure 3, there are some strong indications as to the nature of the anomalous event at site 4. For four sites (no 5, 6, 21 and 22) there is a direct increase in electrical conductivity (E.C.) with increasing pH and this is where the acidity, or increasing alkalinity, as associated with an increase in the surface chloride readings. For these four sites the electrical conductivity is given by Equation 1,

$$E.C. = 65 \text{ pH } -302 ....(1)$$

With an R^2 value of 0.9929 there is a very high degree of confidence that the relationship is valid. For surface salt levels being so low as to give zero electrical conductivity, the pH would be 4.64, as seen at the crossing point for the linear regression line described by Equation 1. Inspection of the graphical plot shows that site 4, for its pH value, is very low in soluble mineral species and has a conductivity of only 0.5 mS/m while the rock 5 metres away had a conductivity of 3mS/m. This mysterious behaviour can be explained if an extremely localised washing event took place on rock 4 site that did not cover the adjacent rock site 4a, whose solution chemistry was previously reported to Yara by WS Fish Consulting and HCS in first quarter of 2019.
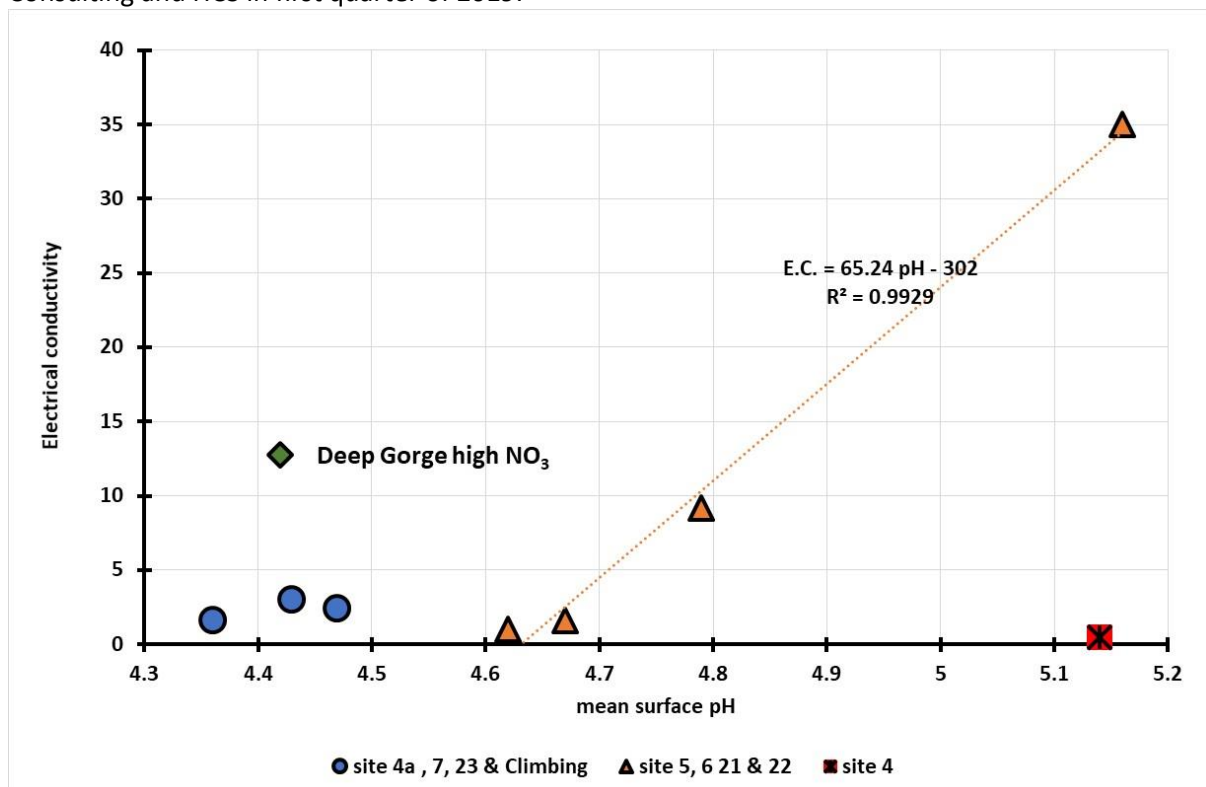
Figure 3: Plot of the electrical conductivity of the wash solutions vs mean surface pH

It is interesting to note that site 21 had again the highest electrical conductivity of 35 mS/m which is consistent with it having a very high chloride wash solution concentration of 82 ppm compared with Deep Gorge site 7 having the next highest chloride value of 17 ppm and an E.C. value of 12.7 mS/metre. The mean pH at site 4 a (Figure 2) was 4.4 while at site 4 it was 5.1, with the 0.7 difference in pH being equivalent to a fall of five times in acidity. The low salt content and the high pH are consistent with a highly localised influx of water onto the surface of the rock. Contact with the rangers at the Murujuga Aboriginal Corporation confirmed that there had been no reports of a highly localised rain event at site 4 which could have accounted for the changed conditions. The Deep Gorge site 7 has been highlighted in a green diamond shape in Figure 3 to show that it has a much higher than expected electrical conductivity which is consistent with a high nitrate ion concentration.

Analysis of cation stoichiometry from salt spray deposits on the rocks

In determining the significance of the ratio of Cl^-/SO_4^{2-} it is important to remember that for sites with a lower ratio, such as those at 4, 4a, 5, 6, 7 and 23, which had a mean value 2.1 ± 0.5, it means that there is a greater amount of sulphate ions present than would otherwise be expected for chlorides coming from deposition of sea salt spray. The sites which have elevated sulphate levels includes those close to the Witness Bay Road and those at elevated positions which can catch SO_x associated with emissions from ships loading iron ore. Thus, the Burrup Road West, the Water tanks, Deep Gorge and Burrup East all had increased sulphate concentrations. This is contrasted with sites 21 (Yara West) and site 22, Yara NE, and the rock below the Climbing Man had a mean ratio of 4.7 ± 0.5. It is useful that there is a statistically significant difference between the two groups of data as it assists in the modelling of the dispersal of airborne gases.

An additional discriminating ratio is that for chloride to calcium salts. Sites 4, 4a, 6, 7, 22 & 23 had a lower Cl^-/Ca^{2+} ratios with a mean of 3.4±1.1 were found for while the Climbing Man site and sites 5 & 21 had a mean ratio of 15.8±6.8. The lower ratios are due to more calcium containing minerals being found on those sites while the Climbing Man site, along with site 5 and 23 are granophyre sites. The much higher calcium content of the gabbro rock crust, 10.9±1.9% CaO, compared with the granophyre crust of 1.4±0.8 % CaO, is reflected in the relative amounts of chloride to calcium in the wash solutions (Ramanaidou and Fonteneau, 2017). Thus, the ratio of Cl^-/Ca^{2+l} is a good identification indicator as to whether the underlying geology of the rocks is either gabbro (low ratios) or granophyre (high ratios). In addition, the CSIRO analysis of the weathered crusts on granophyre rocks had 3.7 % Na_2O while the gabbro rocks had 1.9%, so some of the elevated sodium levels may be associated with a specific weathering pattern.

Six of the sites (4a, 5, 6, 7, 21 & 23) have varying Ca^{2+}/K^+ ratios which are all significantly greater than that found in seawater at a mean value of 2.9 ± 0.6 which indicates that the potassium is being mobilised from minerals found in weathering products such as clays on the rock crusts. This is a similar result for many of the sites as found in 2018. The surface chemistry at site 4, 22 and Climbing Man reflect that of normal sea water with a mean ratio of 0.7 ± 0.3, which is experimentally indistinguishable from normal seawater.

Most of the sites had a common ratio of Ca^{2+}/Ba^{2+} of 418 ± 219, which is very similar to that observed in 2018. All values are significantly depressed from the ratio of 8,000 for sea water and this is simply due to the solubilisation of barium containing minerals in the weathered crusts on both the gabbro and granophyre rocks. The only exception was found on Site 5, the Burrup Road West site which had a Ca/Ba ratio of 149. Additional studies will be needed to determine the nature of the extra barium in the rock surface, but the Ramanaidou and Fonteneau study reported significant local variations in the geology of the rock crusts.

Analysis of rainwater pH and nitrate at Yara monitoring stations

Data from the air monitoring sites at site 5 (Burrup Road West) shows that, apart from an event on the 29[th of] March in 2016 when the NO_3^- spiked at 0.24 ppm. or three times the average, the background level of nitrates has remained relatively constant at 0.082 ± 0.032 ppm over the last 4½ years. Considering that for the last two years the TAN plant has been closed for maintenance and operational reasons, it is likely that the prevailing NO_x concentrations are not associated with production facilities operated by Yara Pilbara Nitrates. The graphical representation of the data from the Burrup Road monitoring site is shown in Figure 4. However, it is noted that the concentration of ammonia and the conjugate acidic form of ammonium ions has shown a steady increase from levels of around

0.1 ppm to 0.2 ppm during three measurements in 2019, which suggests that the wind is driving potential emissions of ammonia to the monitoring site on Burrup Road West.
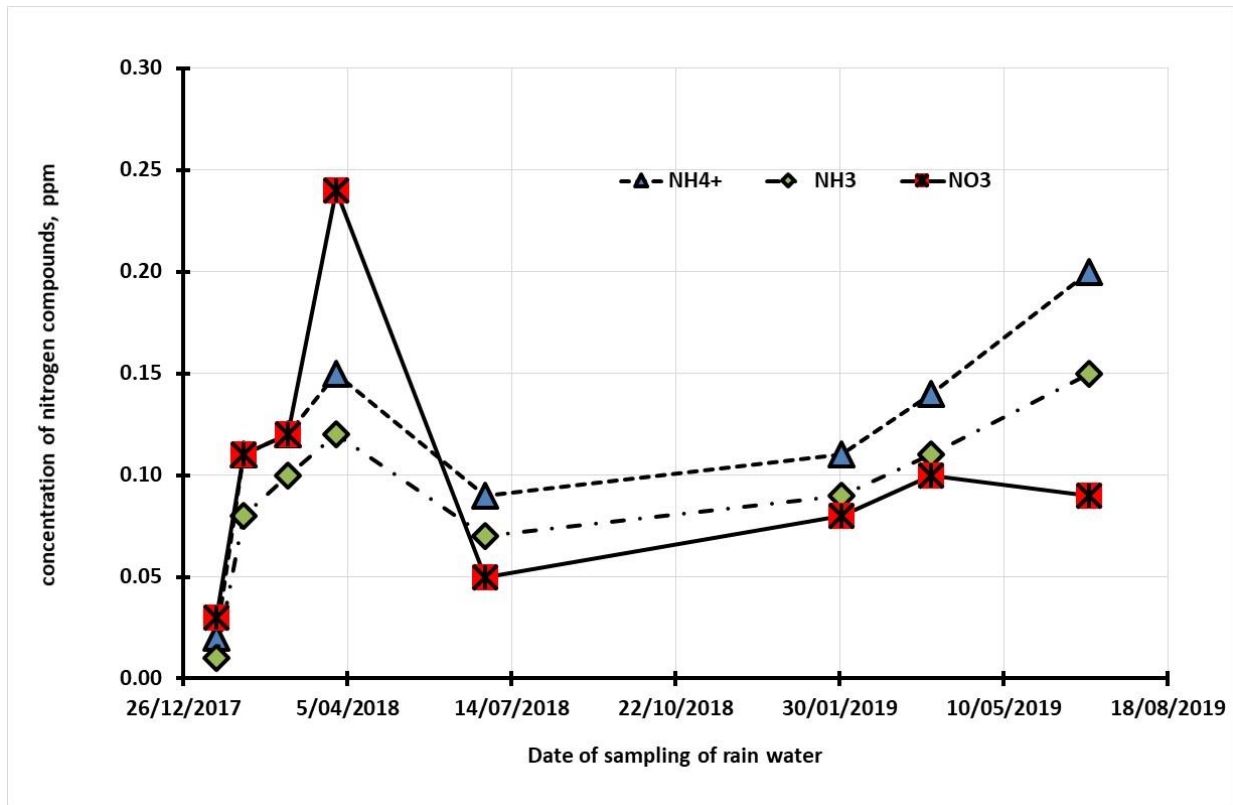
Figure 4: Distribution of nitrogen species in rainwater from no 5, Burrup Road West.

Analysis of the pH of the collected rainwater at the Burrup Road West site (5) shows that there is a direct relationship between the solution pH of the rainwater and the amount of soluble nitrate in solution, as given by the regression equation 2 viz.,

$$pH_{\text{rainwater site 5}} = 7.0\ (0.1) - 3.5\ (0.5)\ [NO_3] \dots\dots\dots\dots\dots\dots\dots\dots(2)$$

The values in parenthesis are the errors associated with the slope and the intercept; given that the R^2 value for Equation 2 is high at 0.9529 a high degree of confidence can be placed in the validity of the data. Thus, as the amount of nitrate in the rainwater increases there is a strong and steady decline in the pH, i.e., the acidity of the rainwater is strongly associated with the adsorption of NO_x from the background chemistry of the local environment. This data is very valuable in that it shows the direct relationship of acidity of the rainwater with the nitrate concentration in an inherently sterile condition i.e., without the complications of microflora and the minerals on the weathered rock surfaces. For the Water Tanks (site 6) there was also a linear decrease in pH with increasing nitrate concentration but the R^2 value was much lower at 0.657 and so Equation 3 had a much higher standard deviation associated with the slope and the intercept values, and a much lower apparent sensitivity to the amount of nitrate.

$$pH_{\text{rainwater site 6}} = 6.6\ (0.5) - 1.7\ (0.1)\ [NO_3] \dots\dots\dots\dots\dots\dots\dots\dots(3)$$

The most encouraging note regarding the dependence of the pH of the rainwater at sites 5 and 6 is that the intercept values, i.e., at zero nitrate concentration, is neutral at a pH of 7.0. There was insufficient data on nitrate and pH recorded at the Deep Gorge weather station to allow for any detailed analysis. Regardless of the lack of rainfall at Deep Gorge and the associated monitoring reports, there is sufficient monitoring data at the Water Tanks site 6 and the Burrup Road West site to establish that even in the sterile environment of the monitoring stations there is a direct link with the acidity and the nitrate levels.

Interpretation of solution chemistry and cation mobilisation

Because the concentrations of cations in the wash solutions are low, it is more convenient to use a logarithmic value, expressed as pM, in the same format as pH represents the hydrogen ion activity. Thus, for a metal ion in solution the pM^{n+} = $-\log_{10}[M^{n+}]$ where the metal ion concentration is expressed in units of mole/litre or M. Higher pM values mean less metal ion activity. When mineralisation dissolution (rock corrosion) occurs, minerals from the weathering rock crusts are dissolved. These reactions involve neutralisation of either oxides or hydroxides of the metal ions. When metal hydroxides are mobilized by acid dissolution the generic dissolution reaction can be written in the form show in Equation (4),

$$M(OH)_n + n\ H^+ \longrightarrow Mn^{n+} + n\ H_2O \dots\dots\dots(4)$$

In equation 4 the n value is the oxidation state of the metal, typically 2 and 3 for iron and mixtures of 2, 3, 4 etc. for manganese. The concentration of the metal ions is derived from the general equilibrium constant for the dissolution of a metal hydroxide into the component elements. In this fashion it can be seen that $K_{sp} = [OH^-]^n \times [M^{n+}]$, is mathematically the same if we rewrite the expression using the reciprocal values i.e.

$$^1/K_{sp} = \{^1/_{[OH^-]^n}\} \times \{^1/_{[M^{n+}].}\} \dots\dots\dots(5)$$

Since the logarithm of $\{^1/_x\}$ is pX, then equation 5 can be expressed by the formula

$$pK_{sp} = n\ p[OH] + pM_{OH} \dots\dots\dots(6)$$

By definition, $p[OH] = pK_w - pH$ which can be substituted into equation 6 then rearranged to give equation no 7, remembering that the self-ionisation constant of water, pK_w has a value of 14.

$$pM_{\text{hydroxides}} = pK_{sp} + n(pH-14) \dots\dots\dots(7)$$

Thus, for plots of the pM values for metal ions the intercept at zero pH is equal to (pK_{sp} -14 n). For metal oxides of the general formula M_xO_y dissolving to give metal ions and water, the concentration of the metal is given by Equation 8,

$$pM_{\text{oxides}} = \ ^1/x\ \{pK_{sp}\} + 2\{y/x\}\ pH \dots\dots\dots(8)$$

When the pM values are plotted as a function of pH it is theoretically possible to determine if the dissolution process involves a hydroxide, which has a slope of n for the pM vs. pH plot. If the product dissolving is a mixed valency oxide, the slope of the pM vs. pH plot is $2^y/_x$, if the soluble ion is an un-complexed free metal ion.

Mobilisation of barium and calcium

Calcium solubility from 2003-2020

The most significant difference in the behaviour observed at the beginning of the monitoring program is that for the February 2004 data there was a change of mechanism of solubilisation of calcium as the slope of the p [Ca] vs pH plots changed from one (Equation 9) to two in 2004 (see Table 2). The most likely mechanism is that for a 1:1 reaction it is the dissolution of calcium carbonate to form a soluble bicarbonate complex,

$$CaCO_3 + H^+ \rightarrow Ca(HCO_3)^+ \dots\dots\dots(9)$$
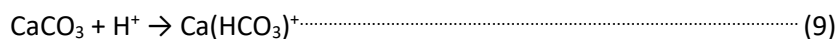
This is the reaction that dominates the solution processes for the 2003 and the 2017 conditions. Owing to the changed microenvironmental conditions the mechanism changed to a 1:2 reaction for February 2004 in which the calcium carbonate would have dissolved fully as the disassociated bicarbonate, as shown in Equation 10.,

$$CaCO_3 + 2\ H^+ \rightarrow Ca^{2+} + H_2CO_3 \dots\dots\dots(10)$$

The most likely reason for the change in mechanism is due to the increasing acidity of the local environment, as the mean pH changed by 0.7 or an increase in acidity by a factor of five, as seen in Table 2 below. For calcium minerals, the slope in both November 2017 and September 2018 is the same as originally observed in August 2003 but it was greater in August 2019 at a statistically significant level (the differences over 16 years being greater than the sum of the standard deviations). The mean pH of the measured sites in 2019 was more acidic at pH 4.6±0.3 than the other Burrup sites measured in 2003 when the pH was 5.0±0,5.

Table 2: Solution properties of calcium and barium washings on the Burrup rocks

Date	mean pH	mean p[Ca]	mean p[Ba]	slope p[Ca]/pH	slope p[Ba]/pH
August '03	5.0 ± 0.5	3.6 ±0.4	6.6 ± 0.2	1.0 ± 0.1	0.4±0.2
February '04	4.3 ± 0.5	4.1 ± 0.6	7.2 ± 0.4	2.0 ± 0.2	2.0
November '17	5.7 ± 0.5	2.0 ± 0.6	5.2 ± 0.3	1.3 ± 0.3	0.5±0.1
Sept. '18	5.5 ± 0.8	3.3 ± 0.2	7.9 ± 3.2	1.3 ± 0.5	0.2 ± 0.1
August '19	4.6 ± 0.3	4.4 ±0.6	7.5 ± 6.3	1.5 ± 0.2	2.4 ± 0.7

This comparison is not strictly valid as it did not cover the same seven sites as in 2017-2019. However, when the data from the three years of monitoring of the Yara and the Woodside (no 4) site there is a definite increase in the mean acidity, and this is reflected in the slope, or the number of protons involved in mobilisation of calcium minerals from the rock surface. The data presented in Table 2 is shown graphically in Figure 5 where there is a clear correlation between the increasing acidity of the sites and the number of protons involved in the mobilisation of calcium ions.

The impact of the release of ammonia, which acts as a pH buffer on the rocks, is shown by the two points from 2017 and 2018 which lie to the right of the regression line shown in Figure 5 and equation 11,

$$\text{Slope p } [Ca]/pH_{seasonal} = 8.07 - 1.4 \text{ pH} \dots\dots\dots\dots\dots\dots\dots(11)$$

It is now readily apparent that the solubility of calcium on the rock surfaces is directly affected by the mean acidity of the environment.
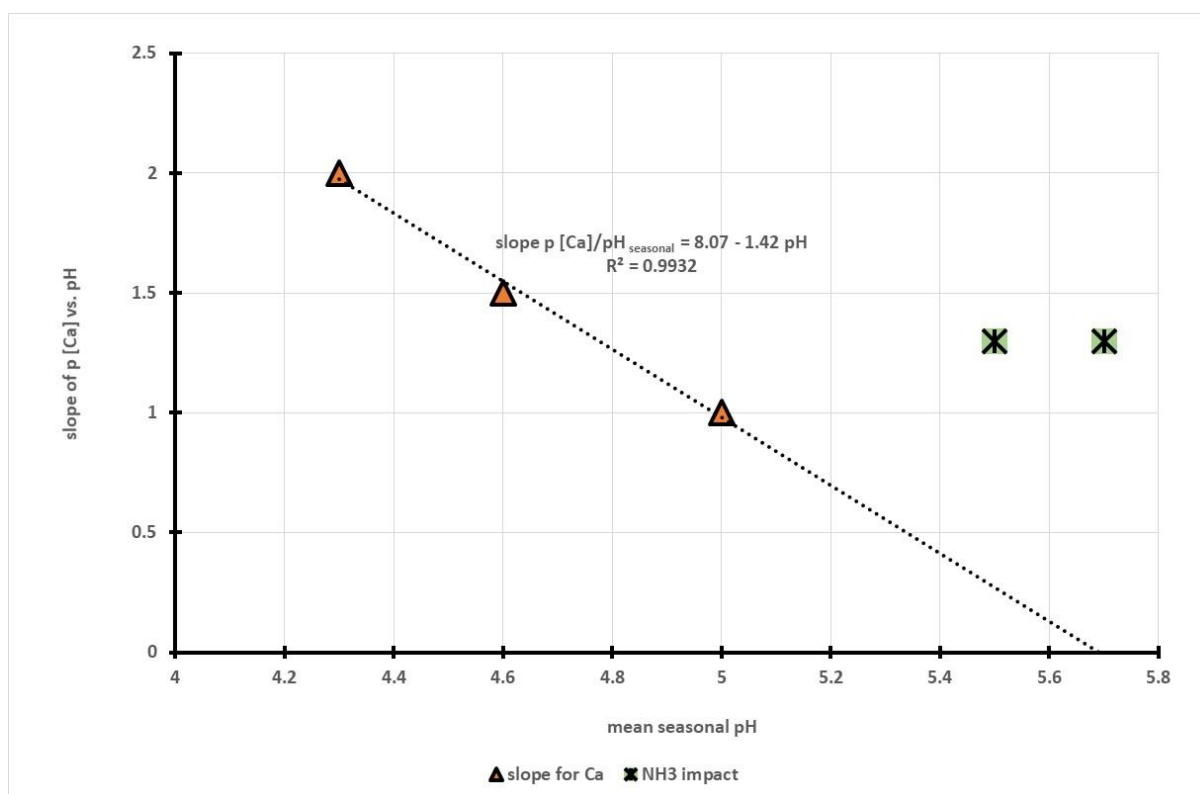
Figure 5: Plot of slope of pM vs. pH vs. seasonal mean pH across the Burrup sites.

From the sensitivity of the dependence of the solubility on the mean pH for calcium minerals (Figure 5 and Equation 11) it can be seen that the data from 2017 and 2018 are significantly more alkaline by between a factor of 5 (delta pH 0.7) to 8 times (delta pH of 0.9) and the presence of ammonia and

ammonium ions has changed the surface chemistry. Such changes are clearly reversible as the slope dependence on pH returned to "normal" for the data collected in 2019.

Solubility of barium between 2003 and 2019

The chemical analysis done by CSIRO on the mineralogy of the rock crusts' weathered zones did not show up any significant amounts of barium, so it is considered likely that the presence of varying amounts of this heavy alkaline earth metal came from the sea. The chemistry of the barium minerals was considered a likely candidate to see if there was any systematic change in the rock chemistry from the time of the original measurements made in 2003 and the present round of data collected in 2019. Plots of the $p[Ba^{2+}]$ versus pH conformed to the equation 12, viz.,

$$p[Ba^{2+}] = -3.3\,(3.3) + 2.4\,(0.7)\,pH \dots\dots\dots(12)$$

For this relationship the R^2 value was 0.79 so there is a reasonable degree of fit for the linear regression and the associated errors in the intercept of ±3.3 and of ± 0.7 in the pH give a strong indication that the mobilisation of barium is consistent with the following reaction (Equation 13) viz.,

$$BaO + 2\,H^+ \rightarrow Ba^{2+} + H_2O \dots\dots\dots(13)$$

Figure 6: Sulphate distribution map across the 2019 monitoring sites

The same slope is found for the dissolution of barium hydroxide but the most likely form of barium in the weathered crusts on the gabbro and granophyre rocks is the barium oxide. Regardless of the precise form that the barium is therein present, it means that as the pH falls there is a regular increase

in the solubility of barium ions into the wash solution, but it is still essentially a mineral associated with low solubility. The pK_s of $BaSO_4$ is 9.6 and the mean ionic product of the barium and sulphate solutions in the rock washings was 13.4 ± 1.0 which means that there is no combination of barium and sulphate concentration on the rock surfaces that will result in precipitation of $BaSO_4$ as the mean ionic product is $10^{3.8}$ times less than the solubility product. When the sulphate distributions are shown as a function of location of the measuring points (Figure 6) it can be seen that there is an almost fifty-fold increase in SO_4^{2-} concentration between site 22 (Yara NE) and site 21 (Yara W) that can be closely correlated with winds coming in from the iron ore loading facilities and accumulating at the high points on site 21 and other high areas such as Burrup Road West (site 5) and Deep Gorge (site 7).

When the corresponding analyses are conducted on the solubility of barium ions, as a function of the mean seasonal acidity (pH $_{seasonal}$) the slope of sensitivity by which p [Ba] changes with pH is given by equation 14

$$\text{Slope p [Ba]/pH}_{seasonal} = 8.5 - 1.6 \text{ pH} \dots\dots\dots\dots\dots\dots(14)$$

The line of best fit was for the 2003, 2004 and 2019 seasons but the regression had errors of ± (2.6) in the intercept and ± (0.5) in the pH dependence and so it is seen that both equations have essentially the same pH dependence, but the intercept values are significantly different. Inspection of equation 14 and equation 11 show that both barium and calcium have similar pH sensitivity to their mobilisation.

Mobilisation of transition metal cations from the rock surfaces

Analysis of the wash solutions collected in August 2019 showed that, contrary to the insolubility of iron in the ammonia affected rock surfaces in 2018, there was measurable mobilisation of iron minerals from all the rock surfaces with the mean p[Fe] being 6.2 ± 0.2, as shown in Table 3 which lists the transition metal ions in order of decreasing solubility as you move down the table. The next most soluble metal to iron was its neighbour in the Periodic Table, manganese, at a mean pM_{Mn} of 6.9 ± 0.5 which is just statistically significantly different from the iron levels and very similar to the small amounts of zinc with a mean pM_{Zn} of 7.2 ± 0.3. There was only one site that showed any measurable chromium and that was the Deep Gorge site (7) which, as seen in Figure 2, had a significantly more acidic microenvironment which was equal to site 4a by the gas plant as being the most acidic location of the test sites.

Table 3: Summary of solubility dependence of metals at monitoring points

Element	Mean pM	Standard deviation	pM vs. pH slope
Iron	6.18	0.21	4.24 +0.38 pH
Aluminium	6.69	0.40	4.39 + 0.52 pH
Manganese	6.91	0.48	-4.87 + 2.57 pH
Zinc	7.15	0.31	-0.22 +1.65 pH
Chromium	7.94	one point	one point
Cobalt	8.32	0.21	4.46 + 0.84 pH
Vanadium	8.35	0.26	3.11 + 1.10 pH
Copper	8.88	0.19	-0.76 + 2.1 pH

In terms of metal dissolution reactions, it is common to interpret an equilibrium metal ion concentration of 10^{-6} M or pM^{n+} of 6.0 as being essentially as "no corrosion" and so the only metal ion that just falls into that category is iron ions at a mean pM $_{Fe}$ of 6.2 ± 0.2 (Pourbaix 1974). While there is discernible mobilisation of the metal ions, given the high sensitivity of the analytical methods used at the Chemistry Centre of WA, it cannot be said that there is active mineral dissolution at the sites that were examined. For copper, vanadium, cobalt and chromium the pM values between 8.9 and 8.0 represent insignificant mobilisation of minerals containing these metal ions. For zinc there is an order

of magnitude higher concentration, which follows the general trend in solubility of transition metal complexes. The mobilisation of manganese is within the same range as zinc and both are significantly lower than the amount of iron, the dominant mineral, which is to be expected.

When the metal ion solubilities (Table 3) are all plotted as a function of pH there are interesting trends in the way in which the various transition metal ions respond to changes in the pH. The increased acidity across the monitoring sites (Figure 6) has resulted in iron being the most abundant of the metal ions present in the wash solutions with a mean pM_{Fe} of 6.18 ± 0.21. From the data shown in Table 3 aluminium was the second most soluble cation, mean pM_{Al} 6.69± 0.40 which is consistent with the presence of alumino-silicates being major weathering products of the gabbro and granophyre rocks in the Burrup.
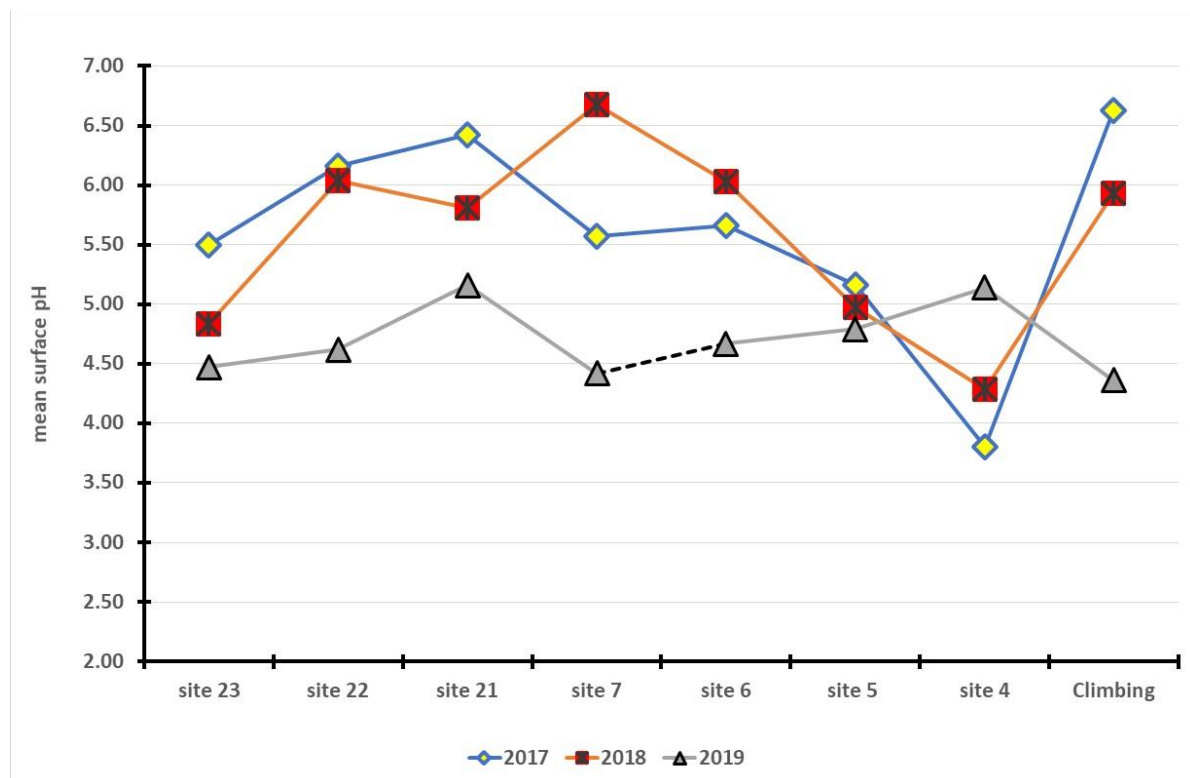
Figure 7: Plot of the mean pH for eight monitoring points between 2017-2019

Inspection of the data in Table 3 illustrates the complexity of the dissolution of manganese species from the solid phase is more complex because the only stable ionic species in the pH range of 4.0-5.5 is the Mn^{2+} ion. Redox processes that are commonly facilitated by fungi that reduce Mn(IV) species to Mn^{2+} ions (Gadd 2004). There is a direct increase in the manganese ions in the wash solution with increasing acidity of the rock surfaces. The solution chemistry of manganese is very complex, with solid phases of Mn^{2+} being MnO and $Mn(OH)_2$, for Mn^{3+} there is Mn_2O_3 and for the mixed valence of Mn_3O_4, which is a mixture. like its iron analogue magnetite, of one Mn^{2+} and two Mn^{3+} ions. In addition, there are equilibria involving the precipitation of MnO_2 as in equation 17.

Interpretation of the pH effects on iron and manganese mobilisation

Previously published work by MacLeod (2005) and MacLeod et. al. (2017, 2018) has shown that at the pH values recorded in 2003 and 2004 (Appendix IV) there was measurable mobilisation of iron and manganese containing minerals. Analysis of the wash solutions from the early data sets has shown up significant concentrations of aluminium, iron, manganese, nickel, copper and some zinc and lead from the parent rock crusts. Because the mineralogy of the highly weathered gabbro and granophyre is

characterized by a series of mixed amorphous iron—manganese oxides, in the form of desert varnish, iron(III) oxy-hydroxides and weathered minerals such as smectite, kaolinite, illite and mica (Clark 2004) it is not unexpected to find mobilization of metallic cations under the acidic conditions. A review of metal ion solubility in terms of the pH of the microenvironment is instructive as it exposes the underlying chemistry and the complex web of interactions that exist between the surface acidity and the mobilisation of minerals within the surfaces, across both the engravings and the background surfaces.

It is instructive at this point to consider the way in which the mean pH of the Yara inspection sites has changed over the past three years, since it is the acidity of the rock surfaces that drives issues of colour change and mobilisation of minerals from the rock crusts. The mean pH recorded at the seven sites is shown in Figure 2 and the trends for the three years of monitoring for Yara Pilbara Nitrates is shown in Figure 7. Other than site 4, the CSIRO Reference point near the Withnell Bay road, all the other measurements were more acidic than in 2018. It has been previously noted that site 4 had anomalously low electrical conductivity for its pH, it had abnormally low sulphate levels (Figure 6) which all point towards the site having been subject to a remarkably localised rainfall or washing event.

It is instructive to look back at the more acidic surfaces in the 2003 spring and the February 2004 summer measurements since both seasons gave data which was amenable to analysis of plots of pM_{Fe} vs. pH. Thus, the plots for iron showed that for both seasons the p[Fe] vs. pH plots have an average slope of +1.98 ± 0.06 pH which confirms the following mechanism (Equation 15):
$$Fe_2O_3 + 4\ H^+ \rightarrow 2\ Fe(OH)^{2+} + H_2O \ \dots\dots\dots\dots\dots\dots\dots\dots\dots\dots(15)$$
The Pourbaix diagram for iron in the range of pH observed on the rock surfaces shows that the $Fe(OH)_2^+$ and the $Fe(OH)^{2+}$ ions are the dominant form of soluble iron(III) under oxidizing conditions (Pourbaix 1974). The pH data from all the five seasons of measurements is shown in Appendix IV. Similar plots indicate that copper is mobilized by dissolution reactions involving two protons per metal ion as is the case for nickel.

Using washing solution data for the mobilisation of aluminium allows similar plots for the solubility of aluminium with surface pH to be determined. For the Burrup rocks examined 15 years ago the aluminium mobilisation graphs had an average slope of 1.4±0.2 pH, which is consistent with the dissolution of kaolinite ($Al_2Si_2O_5(OH)_4$) to give the $Al(OH)_2^+$ ion and $AlSi_2O_5^+$, as shown in Equation 16.
$$Al_2Si_2O_5(OH)_4 + 3H^+ \rightarrow Al(OH)^{2+} + AlSi_2O_5^+ + 3\ H_2O \ \dots\dots\dots\dots\dots\dots(16)$$
The data from August 2019 showed that the pM_{Al} slope against pH was given by Equation 17,
$$pM_{Al} = 4.39 + 0.5\ pH \ \dots\dots\dots\dots\dots\dots\dots\dots\dots\dots\dots\dots(17)$$
A possible reaction is the partial dissolution of kaolinite, according to equation 18,
$$Al_2Si_2O_5(OH)_4 + H^+ \rightarrow Al(OH)^{2+} + Al(OH)Si_2O_5 + H_2O \ \dots\dots\dots\dots\dots(18)$$
which would account for the 0.5 pH slope of the solubility plot as a function of pH. The 2019 mean pM_{Al} value was 6.69±0.40 across sites 4a (near the Woodside plant), site 7 and site 21. The mean pH for these three sites in 2019 was 4.7±0.4 which shows that the aluminium surface minerals are quite sensitive to changes in the acidity. Kaolinite has been identified as one of the aluminium containing minerals on the Burrup rocks along with feldspar, chlorite, mica, smectite and some gibbsite (Clark 2004) and it was a major mineral identified in the CSIRO Accelerated Weathering experiments (CSIRO 2016). It is not unexpected for aluminium ions to have been mobilized under the very mild sample collection regime that was used.
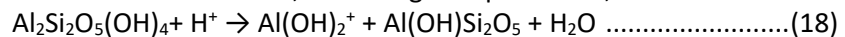
A summary of the data from the redox potentials and the pH recorded on the seven sites in Table 5 which gives the mean redox potential, standard deviation of the same and the Pourbaix slope in mV per pH and the redox potential at a pH of zero (obtained by extrapolation of the linear regression to the intercept value on the voltage axis). The value of conducting the Pourbaix analyses and fitting

regression equations to the data is that it provides a unique insight into the competing equilibria on the rock surfaces and gives an understanding of the vast array of redox reactions that may occur which have the potential for bacteria, yeasts, moulds and fungi to utilise the suite of oxidation and reduction reactions to provide them with the energy they need for effective colonisation and metabolism. It is not surprising that most of the identified redox reactions on the rocks are reflections of the multi-valent state of manganese.

The main issue to note is that the Deep Gorge site was significantly more acidic in 2019 than in 2018 and so it is to be expected that the reactions controlling the mobilisation of manganese would be different to that of the previous year, when high ammonia concentrations in rain water samples recorded at the weather station at the foot of the small hill on which site 7 is located, may have impacted on the buffering of the rock surface. The concentration of manganese in the rock irrigation measurements done in August 2019 had a maximum of 5.8×10^{-7} M or a pMn of 6.24 at the Deep Gorge (site 7). Previously, it had been noted that there was considerable value in being able to plot the redox potential of the soluble metal ions on a rock art site as a function of the surface pH. The most responsive site for mobilisation of manganese is shown in Figure 8, which is the Pourbaix diagram for site 7 at Deep Gorge.

Inspection of the slopes in the Pourbaix diagram in Figure 8 shows that there is just one mechanism controlling the precipitation of solid phases and dissolution of the same. By way of contrast in 2018 there were two oxidation and reduction reactions with slopes of 256 mV, involving oxidation of Mn^{2+} ions to Mn_3O_4, and 120 mV per pH involving Mn^{2+} being oxidized to MnO_4^{2-}. The 2019 mechanism is given by equation 21 and it similarly involves oxidation of Mn^{2+} to MnO_2,

$$Mn(OH)^+ + H_2O \rightarrow Mn(OH)_2^{2+} + H^+ + 2e^- \quad \text{...................................... (19)}$$
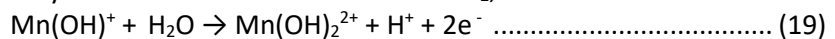
The slope of lines Pourbaix $_{01 \& 02}$ are the same at 0.028(0.008) and 0.031(0.008) respectively and this agrees with the theoretical slope of 0.029 V/pH associated with equation no 19. The Deep Gorge site had the maximum NO_3^- concentration of 2.1 ppm and a mean pH of 4.4 which gave a pMn of 6.5 which is very similar to the other high manganese concentration at site 4a of pM 6.1 at a mean pH of 4.7±0.4 and a soluble nitrate concentration of 0.99 ppm. The same Pourbaix slope and associated mechanism shown in Equation 19 was also reported at site 4a and site 21.

When the manganese solution data was plotted as a function of surface pH the regression analysis confirms that the likely dissolution reaction is shown in equation 20 for sites 6, 21 and 22 viz.,

$$MnO + H^+ \rightarrow Mn(OH)^+ \quad \text{.. (20)}$$

There was significant scatter of the data, with a low R^2 of 0.64, and so the pM vs. pH slope was 1.24 ± 0.93 which could also easily represent the mobilisation of manganese oxide to manganous ions, as shown in equation 21 viz.

$$MnO + 2 H^+ \rightarrow Mn^{2+} + H_2O \quad \text{... (21)}$$

At the pH and E_h range of the rocks examined in 2019 it is highly likely that the Mn(II) ions are present as a combination of Mn^{2+} and $Mn(OH)^+$ ions, as shown in Equations 20 and 21.

In Table 5 there is a summary of the data from the Pourbaix diagrams from the eight sites that were examined in full in 2019. What is readily apparent is the differences in the electrochemistry observed at site 4, where the mobilisation of iron was the electrochemical process dominating the site, which, as previously noted, has been characterised by abnormally low electrical conductivity when compared with the relatively alkaline pH of the rock surface. Sites 4a, five metres north of site 4, and site 7 at Deep Gorge and site 21, the closest monitoring point to the Yara ammonia plant, all had the 30±3 mV slope which is consistent with one proton per two electrons involved in the oxidation-reduction reaction shown in Equation 19.
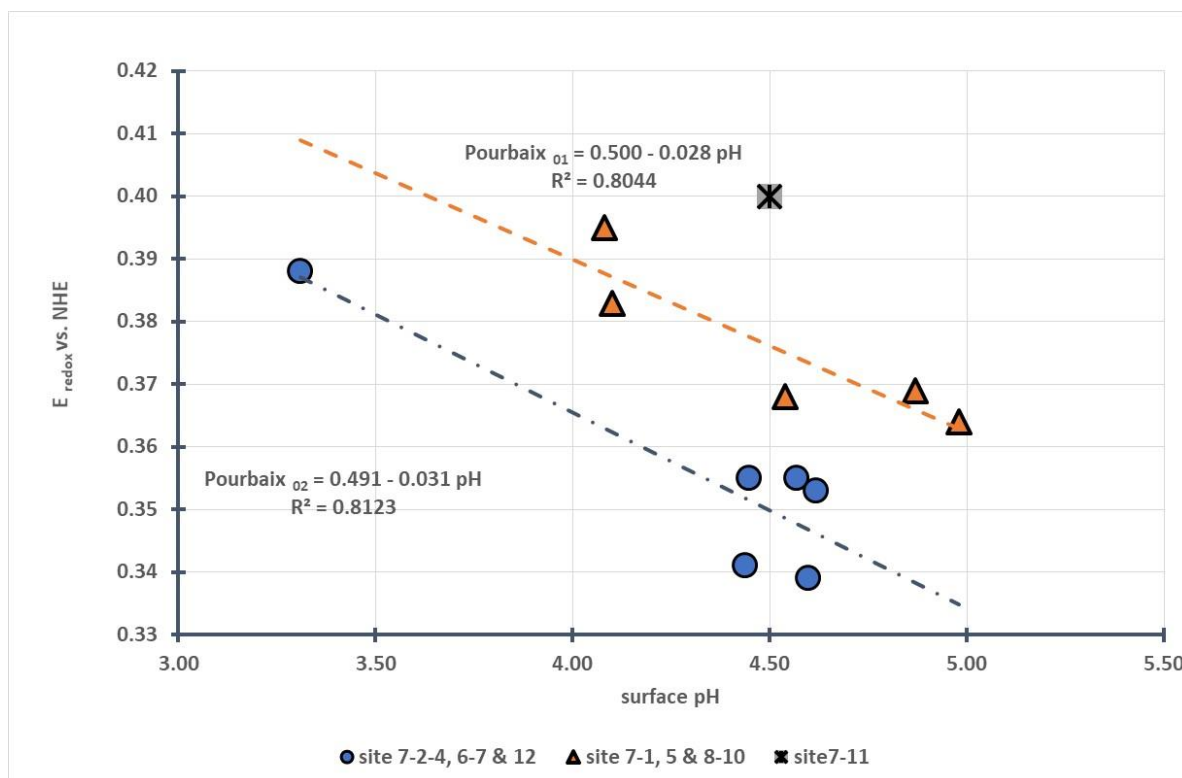
Figure 8: Pourbaix plot for site 7 at Deep Gorge, August 2019

In order of decreasing sensitivity of the slope of the Pourbaix diagrams to pH, the probable reactions with mobilisation of manganese minerals goes from the slope for 4 protons per electron is -236 mV/pH as in Equation 23, through two protons per electron as in Equation 24, -118 mV/pH. The last reaction involving one proton and two electrons has been previously described in Equation 19. The 1:1 ratio was found with Equation 25 which is simply the iron (III)/(II) redox reaction.
[c] Theoretical slope for 1 proton per electron is -59 mV/pH as in equation 25

$$Mn_3O_4 + 8\ H^+ + 2e^- \rightarrow 3Mn^{2+} + 4\ H_2O \dots\dots\dots\dots\dots\dots\dots (23)$$
$$MnO_2 + 4\ H + 2e^- \rightarrow Mn^{2+} + 2\ H_2O \dots\dots\dots\dots\dots\dots\dots (24)$$
$$Fe^{2+} \rightarrow Fe^{3+} + e^- \dots\dots\dots\dots\dots\dots\dots\dots\dots\dots\dots (25)$$
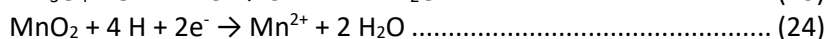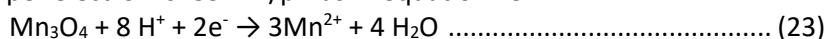
Table 4: Analysis of Pourbaix slopes at seven monitoring sites from 2019

Site	E_h at pH zero, V	Slope of plot E_h/pH, V	E_h error ± volts	Slope error ±, V	R^2	E^0 voltage & redox couple
4a	0.559	-0.033	0.016	0.003	0.9679	E^0 0.564
7	0.500	-0.028	0.036	0.008	0.8014	$Mn(OH)^+ + H_2O \rightarrow$
21	0.586	-0.034	0.032	0.006	0.9545	$Mn(OH)_2^{2+} + H^+ + 2e$
4	0.784	-0.072	0.110	0.021	0.8507	E^0 0.771 $Fe^2 \rightarrow Fe^{3+} + e^{-\ +}$
6	0.935	-0.114	0.148	0.032	0.9285	E^0 1.104
23	0.940	-0.116	0.059	0.012	0.9649	$Mn^{2+} + 2\ H_2O \rightarrow MnO_2 + 4\ H^+ + 2e^-$
5	1.412	-0.214	0.413	0.087	0.5997	E^0 1.480
22	1.319	-0.199	0.099	0.021	0.9567	$3Mn^{2+} + 4\ H_2O \rightarrow Mn_3O_4 + 8\ H^+ + 2e^-$

Voltages corrected to NHE by adding calibrated voltage of 0.202 volts for the Ag/AgCl electrode

It has been noted that for sites 4a, 7 and 21 there is the common oxidation of Mn^{2+} to MnO_2 with the standard slope of 30 mV/pH. For site 4 the slope is that of one electron per pH and the voltage is typical of the Fe^{3+}/Fe^{2+} redox couple and so this site proves to be the exception to the rule, but the reasons for this have already been mentioned in terms of the site having experienced a highly localised rainfall or water irrigation event that removed acidity found on the adjacent rock and resulted in exceptionally low electrical conductivity of the solution, compared with the pH of the site.

Sites 6 and 23 have a common mechanism of two protons per electron in the oxidation reaction with a slope of 118 mV per pH and a mean E^0 of 0.938 ± 0.004 volts. This is consistent with the following oxidation of manganous ions to manganese dioxide,

$$Mn^{2+} + 2\ H_2O \rightarrow MnO_2 + 4\ H^+ + 2\ e^- \ \text{...} (23)$$
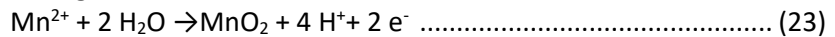
Sites 5 and 22 have a slope consistent with the oxidation of Mn^{2+} to Mn_3O_4 which is described by equation 24.

$$3\ Mn^{2+} + 4\ H_2O \rightarrow Mn_3O_4 + 8\ H^+ + 2e^- \ \text{...} (24)$$
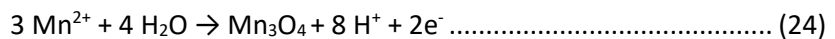
Inspection of the distribution of the pH measurements on the adjacent rock surface to site 7 (the rear of the engraved rock) showed up the localised variations that can occur when the measurement point picks up a spot of high microbiological activity. All the other eleven points had a mean pH of 4.52 ± 0.27 which makes the spot with the pH of 3.31 more than 4.5 times greater difference than the standard deviation so it is clearly highly significantly more acidic.
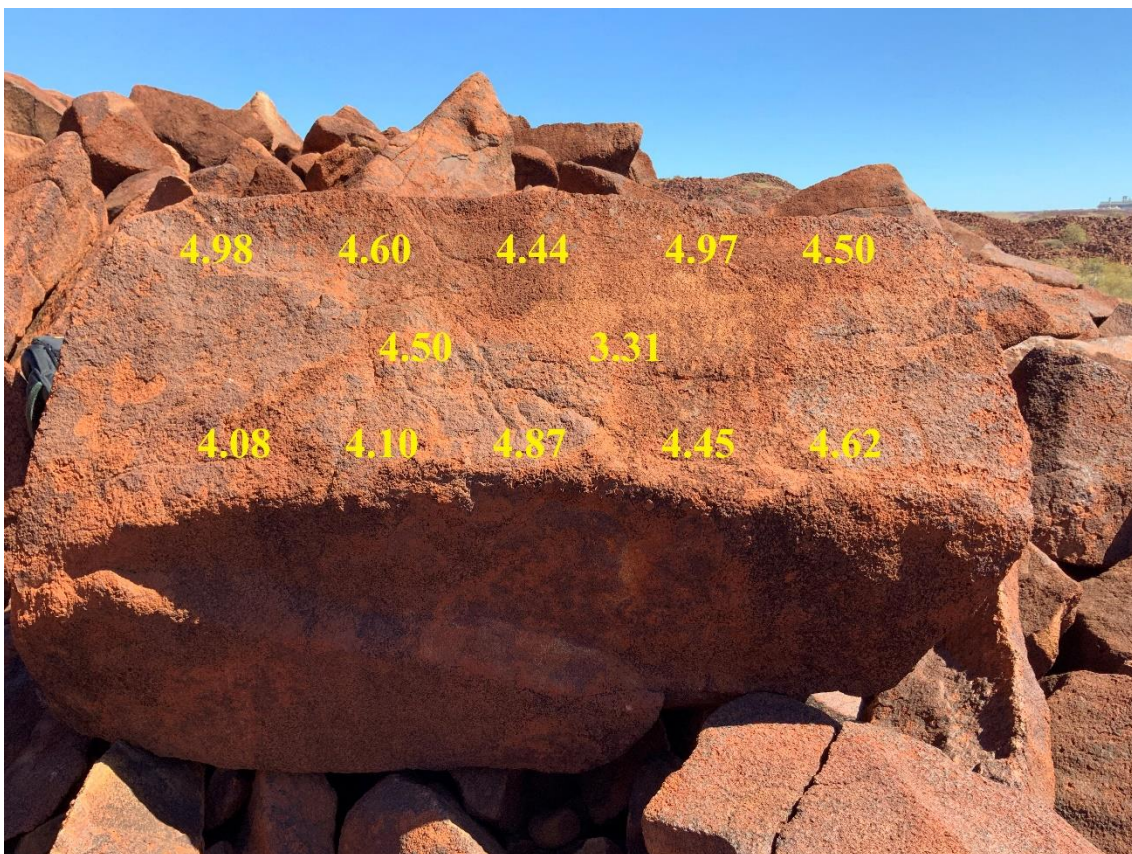
Figure 9: Deep Gorge site 7 with pH data recorded onto the image, September 2018

The general trend over the past year appears to be associated with most sites showing an increase in acidity compared with the September 2018 values when there was no measurable iron in the washing solutions. The mean pM $_{metal\ ion}$ values and the standard deviations are shown in Table 4. For the 2003-2004 data the slope of the pM vs. pH plots for iron had a slope of 2.0, which is consistent with the dissolution of iron (III) oxyhydroxide, FeOOH viz.,

$$FeO(OH) + 2\,H^+ \rightarrow Fe(OH)^{2+} + H_2O \qquad\qquad (18)$$

The 2017 November data showed that there was a slope of 0.3 pH per pM i.e., there is a completely different dissolution mechanism in the present (2007) rock data around the Yara compound compared with the 2003-2004 measurements. The lack of acidity on the rocks has kept iron minerals in an insoluble condition during the 2018 season of measurements. The detailed examination by CSIRO of the parent and weathered rock surfaces of the gabbro and granophyre rocks in the Burrup has provided an exhaustive list of the minerals that are present in the mineral crusts on the gabbro and granophyre rocks (Ramanaidou et.al. 2017). Iron containing minerals that do not follow simple stoichiometry include actinolite, $Ca_2(Mg, Fe)_5Si_8O_{22}(OH)_2$, augite, $(Ca, Mg, Fe)_2(Si, Al)_2O_6$ and chlorite $(Mg, Al, Fe, Li, Mn, Ni)_{4-6}(Si, Al, B, Fe)_4O_{10}(OH, O)_8$ which are all found on the Burrup rocks (idem 2017). The accelerated acid ageing study showed that chlorite appeared to be one of the first minerals to dissolve. It is important to conduct additional studies on the Yara sites in 2019 to ensure that the September 2018 data are not an anomaly, which should be able to be discerned through detailed analyses as discussed above. The only monitored site that had any boron in the washing solution was site 7 (Deep Gorge) at the minor level of $9x\,10^{-3}$ ppm or 8.3×10^{-7} M or a pM_B value of 6.08

One of the main factors affecting the rocks appears to be associated with the six massive rainfall events, due to cyclonic activity, in the intervening 13-years. The rainfall events are summarised in Table 4. The main difference between the six Yara sites and their pH values is that since the 2003-2004 measurements is that it appears that there has been a significant alkaline shift from a mean pH of 4.78 ± 0.27 in February 2003 to 5.69 ± 0.51 in November 2017. The shift of just over one pH unit means that the six sites are on average ten times less acidic that the other rocks in the region which were sampled by solution washing. Although the rain event in June 2018 was less intense than in previous years the mean surface pH for the September data was 5.52 ± 0.84, which is statistically the same as the mean data in the previous year.

Table 5: Major cyclonic rainfall (mm) events in the Burrup 2003-2017

02 March 2004	10 Jan. 2006	25 June 2013	31 Dec. 2013	06 May 2014	09 Feb. 2017	06 June 2018
190.8	212.4	209.4	112.8	107.4	210.6	62.4

During the period between the measurements in September 2018 and August 2019 a total of only 107 mm of rain fell but no single rain event was greater than 13 mm, which appears to be insufficient to provide a "temporary wash" solution for the rock surfaces. As previously note the mean pH for all the recorded sites in 2019 was 4.61 ± 0.25, except for the anomalous values for site 4, which is not statistically significantly different to the mean value in 2018 due to the high standard deviation of the data. However, there is a measurable difference between this current year of 2019 and the data collected in September 2018.

Despite apparent simple changes to the solubility of iron and manganese compounds with pH, the absence of a common dissolution mechanism across the three seasons of measurements makes it difficult to interpret the data. The large standard deviation in the p Fe values (±2.6) for August 2003 measurements makes it impossible to tell if there is any real difference between this data and the material sampled in February 2004. The lower standard deviation of the Feb 2004 and the Nov 2017 data on iron solubility provides evidence that the solubility of the iron minerals decreases with increasing pH, despite the apparent change of mechanism. Manganese compounds are more soluble at neutral pH than their iron analogues are reflected in the 2018 data from the Burrup rock art washings, where no soluble iron was detected. The reasons for this lie in the ability of acidic metabolites to complex the cations found in the weathered crusts. The mean p Mn values show an average of 50 times lower solubility in 2018 than in 2017, pMn 6.8 for 2018 compared with 5.0 in

November 2017, as seen in Table 6. This observation is supported by data from Krauskopf (1957) who found that Fe compounds are less soluble than corresponding Mn compounds under naturally occurring Eh-pH conditions.

Table 6: Mean pH and solubility of iron and manganese minerals from rock irrigation

Period	Mean pH	Mean p Fe	mean p Mn	Slope p Fe/pH	slope p Mn/pH
August 2003	4.97 ± 0.48	6.01 ± 2.60	7.17 ± 0.45	2.0 ± 0.1	0.9 ± 0.4
February 2004*	4.78 ± 0.27	6.34 ± 0.44	7.31 ± 0.35	2.0 ± 0.1	2.1 ± 0.1
November '17	5.69 ± 0.51	6.80 ± 0.15	5.03 ± 0.35	0.3	1.1 ± 0.1
September '18	5.52 ± 0.84	Nil soluble	6.79 ± 0.35	Not applicable	1.2 ± 0.9
August ' 19	4.62 ± 0.26	6.18 ± 0.40	6.91 ± 0.48	0.4	2.3 ± 0.4

* the mean pH is determined for the points that were used in the regression analyses.

Solubilisation of Mn and Fe compounds in rock varnish can lead to removal of important compounds required to bind clay minerals to form the hard, outer layer of the varnish and to bind it to rock inner surfaces. A predominant Mn compound in rock varnish is birnessite, which has hexagonal structured sheets with binding clay minerals $\{(Na_{0.3}Ca_{0.1}K_{0.1})(Mn^{4+},Mn^{3+})_2O_4·1.5H_2O\}$. Lefkowitz et al. (2013) demonstrated that birnessite sheets were disrupted when pH was < 7.0. Under mildly acidic conditions observed in the Burrup the varnish would become thinner and softer with removal of these manganese compounds.

Mobilisation of boron from parent rocks and crusts

The presence of measurable amounts of boron in the wash solutions seemed to vary with the surface pH values recorded in both the 2003 and 2004 measurements. To discriminate between the boron coming from seawater, where it is a minor component at 4.6 ppm compared with chloride at 18,980 it was decided to plot the chloride to boron ratio as a function of the mean surface pH values. The data recorded in the first set of washing solutions from August 2003 showed some interesting patterns. What became clear was that normal Cl/B ratio in seawater of 4,130 was massively lower in the washings from all the Burrup rock art sites, where the maximum value was 143 on rock 938 in the "museum compound". This supported the view that boron containing minerals were being dissolved leading to much lower chloride to boron ratio from that expected from wind borne sea salts. As the mean rock surface pH fell the ratio also fell, which supports the data from accelerated weathering conducted by CSIRO (Ramanaidou et.al. 2017). The only site in 2019 with boron found in the washing solution was site 7 (Deep Gorge) where the ChemCentre analyses gave a $^{Cl}/_{B}$ ratio of 1889, and this data does not follow any of the previously reported correlations between the chloride to boron ratios found in the previous studies.

Anions in wash solutions

Oxalates:

Analyses from the five field trips showed that only two reference rocks in the collection of the Western Australian Museum had measurable amounts of oxalate ions, $C_2O_4^{2-}$, which were 1.8 mg/l from Enderby Island (B7477) and 0.7 mg/l from Happy Valley (B2494) in the Burrup. These rocks were collected at a time before there was any industrial activity on the Burrup. The washing samples analysed for oxalate were from June and August 2003, February 2004, November 2017, September 2018 and August 2019. In none of these washing solutions was any oxalates found. Oxalates are major biodeterioration of pigments in the Kimberley region where the monsoonal climate has characteristic wet and dry periods. By comparison the arid climate of the Burrup is less amenable to a wide range of bacteria and plants which produce oxalates as their metabolites. Based on this information, oxalate does not appear to have a significant present role in biodeterioration of the rock art in the Burrup.

Chlorides:

The amounts of surface chloride detected on the rock surfaces provide direct evidence of the impact of the marine environment and indicates that salt weathering of rocks, with extensive dehydration and rehydration cycles, play a significant role in the local environment. The wash solutions from the rock surfaces showed up a range of ions commonly associated with sea water, namely Na^+, K^+, Mg^{2+}, Ca^{2+}, Ba^{2+}, B^{3+}, SO_4^{2-} and Cl^-. Analysis of the way in which the concentrations varied across the Burrup was possible as the February 2004 data included several remote sites such as Gidley and Dolphin Islands in the Dampier Archipelago (MacLeod 2005). The deposition of sea salt on the rock surfaces means that the carbonate and bicarbonate ions will tend to act as buffers and minimize any changes in the surface acidity resulting from a combination of microbiological and chemical reactions on the surfaces.

The initial monitoring conducted in 2003 and 2004 involved direct measurement of the surface pH and the surface chloride ion concentrations. In addition, the washing of the rock surfaces in August 2003 and February 2004 provided data on the solution concentrations of chloride ions. All the data was then assessed through linear regression analyses and the results are summarised in Table 8, which showed that the pH increased with increasing chloride ion activity. This buffering reaction is demonstrated by the relation between the pH and chloride concentration on the rocks as shown in Equation 25,

$$pH_{mean} = a + b\,[Cl^-] \quad\text{...(25)}$$

The 2003-2004 linear regression analyses showed that there was a common slope of the pH vs [Cl] plots but they had different intercepts, as shown in Table 8. The manner in which this slope changed during the measurements in 2019 is illustrated in Figure 8 below.
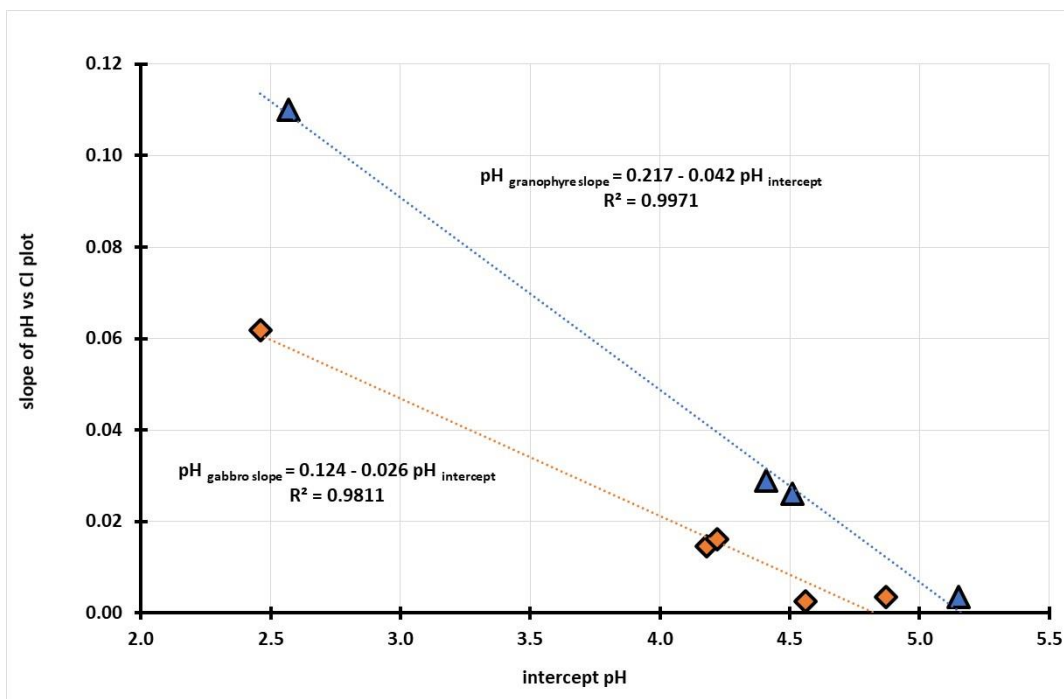
Figure 10: Plot of the slope of the pH vs. [Cl] graph as a function of intercept pH.

The intercept values relate to their primary geology of the underlying rocks and the impact of factors such as the amount of nitrate on the rock surfaces, which is discussed in the following section of this report. Each site had a variable value of the slope *b* so when the data is plotted from the way in which the slope changed with chloride, there was a clear trend in behaviour in which the gabbro sites showed significantly less sensitivity to the chloride ion concentration as shown in Equation 26 and for granophyre in Equation 27.

$$^{2019}\text{pH slope } b_{\text{ mean gabbro}} = +0.124 - 0.026\ \text{pH}_{\text{intercept}} \quad\text{.........................(26)}$$
$$^{2019}\text{pH slope } b_{\text{ mean granophyre}} = +0.217 - 0.042\ \text{pH}_{\text{intercept}} \quad\text{.....................(27)}$$

This is an important observation as it confirms that the underlying chemistry of the gabbro rocks is indeed different to the granophyre sites.

It is likely that one of the reasons why there was a much more readily discernible trend in the data in 2019 is that all the sites had become more acidic and the localised impact of the accidental loss of ammonia or other industrial emissions in 2018, was essentially neutralised. For the 2019 data there was a complex relationship between the mean pH and the amount of chloride ions present on the surface. For the four sites consisting of 4a, 7, 21 and 22 the mean pH steadily increased with the chloride ion, as shown in Equation 28. It is noted that the intercept at zero chloride was 4.37, compared with 4.90 the year before, which indicates that these four sites have become more acidic,

$$^{2019}\text{pH }_{\text{mean}} = 4.37 + 0.0083\ [\text{Cl}]_{\text{surface}} \quad\text{...(28)}$$

There was a very high R^2 value for this regression equation, 0.9972 so there is a very good agreement with a linear response model. It is also noted that apart from the lower intercept value the slope of the mean pH on the alkaline sea salt (source of the chlorides) was at least ten times less than in the previous year where the slope was 0.093 pH/ppm chloride.
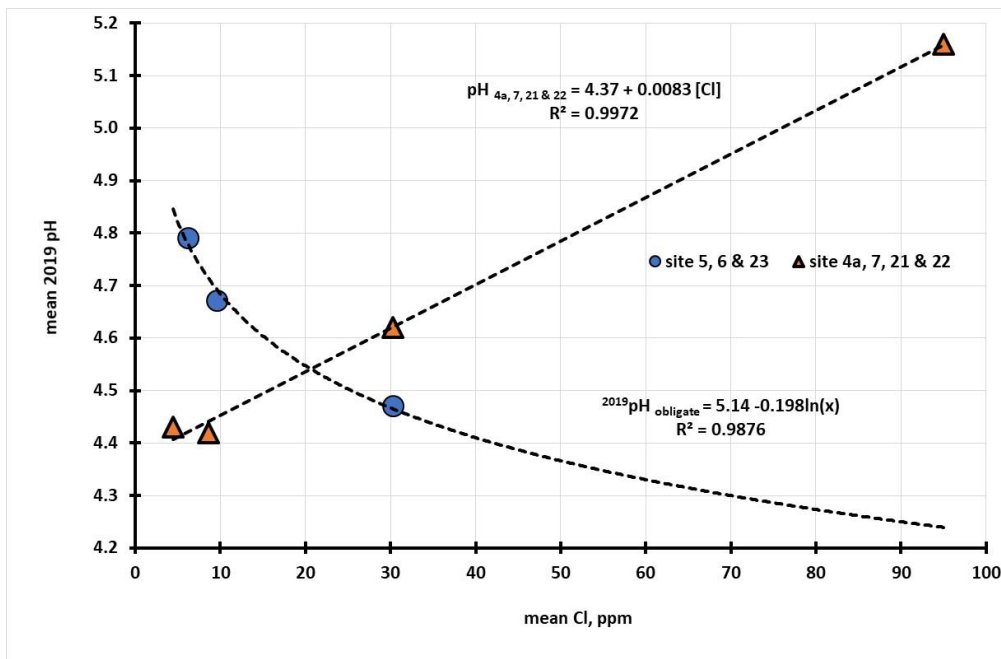
Figure 11: Plot of the mean pH against the mean [Cl] for 2019 measurements

For sites 5 at Burrup Road West, site 6 the Water Tanks and site 23 (Yara East) there was increasing acidity with increasing salt levels, which is similar to the trends in some locations in 2018 and 2017 which would indicate that the microflora were in control of the acidity which went against the trend seen in Equation 28 for the sites 4a, 7, 21 and 22. Analysis of the pH and chloride data for the increasing acidity with increasing salinity gave Equation 29, with a logarithmic dependence on pH, viz

$$^{2019}\text{pH mean} = 5.14 - 0.46\ \log\,[\text{Cl}] \quad\text{..(29)}$$

There was a good fit for these three sites, with an R^2 for the linear pH vs. log [Cl] analysis of 0.9876. If such microorganisms are present, then their metabolites will be acidic and overcome the buffering effect of the increased amount of sea salt deposition. In order to bring improved understanding of the complex microflora controlling the rate of biodeterioration in the Burrup, it would be advisable to consult with the team from Murdoch University who conducted genomic studies on some of the sites examined as part of the compliance reporting.

The data in Table 8 covers all the sets of measurements of rocks in the Burrup and in the Dampier, Archipelago shows that the build-up of sea salt deposits on the rocks does have a measurable impact on the way the rocks respond to changes in the chemical environment. From the data presented in Table 6 there appears to have been a systematic decrease in the slopes of the pH vs. [Cl] graphs between 2002 and 2017, as shown in Figure 7 and equation 24 viz.,

$$\text{slope } \{^{pH}/_{Cl}\} = 0.0725 - 0.0121 \text{ pH} \dots\dots\dots\dots\dots\dots\dots\dots\dots\dots\dots\dots\dots\dots(24)$$

This relationship confirms that all the pH and chloride data are closely linked and that, in the absence of other factors, the ability of the rocks to minimise the response to the development of an acidic microenvironment is largely controlled by the amount of salt deposition. Inspection of the data in Table 7 shows that the solution washing concentration of chloride is very similar to the surface readings at sites 4, 5 and 6 and that the mean values recorded in 2018 are much lower than those in 2017 so it is not surprising that the trend shown in Figure 10 was not continued and that the median surface pH was the same, within one standard deviation, as the value in 2017 but the sensitivity of the surface pH to chloride activity is significantly different. It is pleasantly reassuring that when the same mean acidity, within the range of less than one standard deviation, is reported then the same mean slope of the sensitivity of the pH slope to the chloride ion activity is observed. Thus, the mean slope for 2019 is the same as in 2004 because they have the same mean pH (see Figure 10).

Table 7: Analysis of the relationship between chloride and mean pH

Date	mean Cl ppm	Intercept, a	Slope, b	R^2
June 2003 (winter)	38 ± 40	3.4 ± 0.6	0.030 ±0.004	0.98
August 2003 (spring)	34 ± 31	3.4 ± 0.8	0.033 ± 0.003	0.98
February 2004 (summer)	21 ± 15	4.1 ± 0.6	0.023 ± 0.001	0.98
November 2017				
Site 5: Burrup Road West	32 ± 28	5.0 ± 0.9	0.008 ± 0.001	0.95
Site 6: Water tanks	191 ± 97	5.4	0.001	0.96
Site 7: Deep Gorge	22 ± 12	5.0	0.026	0.77
Site 21 Yara west	125 ± 44	5.8	0.006	0.64
Site 22: Yara north east	373 ± 24	5.3	0.009	0.70
Site 23: Yara east	13 ± 17	5.5	0.021	0.77
September 2018				
Site 4 Withnell Bay Road	2.2 ± 2.1	3.0	2.7	0.93
Site 5: Burrup Road West	4.1 ± 3.4	4.5	0.22	0.45
Site 6: Water tanks	2.3 ± 3.2	6.1	0.13	0.01
Site 7: Deep Gorge	19 ± 8	6.0	0.03	0.99
Site 21 Yara west	20 ± 13	5.0	0.12	0.94
Site 22: Yara north east	10 ± 11	5.5	0.03	0.34
Site 23: Yara east	30 ± 17	3.9	0.02	0.96
August 2019				
Site 4a Withnell Bay Road	4.9 ± 2.0	4.75	0.092	0.96
Climbing Man site	14.4 ± 0.2	4.27	0.020	0.93
Site 5: Burrup Road West	6.3 ± 2.5	4.51	0.026	0.98
Site 6: Water tanks	9.7 ± 6.3	4.41	0.029	0.94
Site 7: Deep Gorge	8.6 ± 3.8	2.57	0.110	0.99
Site 21 Yara west	95 ± 70	4.87	0.004	0.91
Site 22: Yara north east	30 ± 5	4.18	0.015	0.98
Site 23: Yara east	30 ± 10	2.46	0.015	0.97

Further studies to determine the precise nature of the interactions are needed and it should be noted that the solution washings were taken on rocks adjacent to the chloride and pH testing sites, other than in site 7 which had sufficient flat areas on which to place the collection device and to irrigate the

areas that had been measured for pH and for chloride. Future work is naturally constrained by the geology and the aspects of the rocks on each site location. When choosing the surfaces for pH and chloride measurements a significant factor is the choice of rocks with a similar aspect and orientation to the CSIRO reference sites. Many of these rocks have near vertical surfaces and this makes it impractical to recover samples of enough volume to allow for efficient chemical analysis of the surface wash solutions.

During the 2019 data gathering and the subsequent analyses it was noted that the Deep Gorge site (no 7) and the Withnell Bay Road site (no 4a) had much higher apparent sensitivity of the slope than was typically observed with other sites. Site 7 had the highest nitrate concentration in the washing solution at 2.1 ppm and site 4 had a value of approximately 1.0 ppm, compared with the mean value of 1.0 ± 0.3 ppm. In addition, site 7 had many data points that showed increasing acidity with increasing chlorinity, which supports the supposition that one some sites chloride obligate bacteria are active. It was also noted that site 4a had a set of pH and chloride measurements which showed increasing acidity with chlorinity, and this accounts for the anomalous slope observed on this site, in the same fashion as for site 7.

Chloride distribution patterns across the rock surfaces

During the 2019 field measurements the distances across the rock surfaces and the distance down the rock faces were recorded to see if there was any common pattern emerging from the way in which the chloride ions were distributed across the rocks. For all the sites, other than the massive near vertical site no 23 at Yara East, all the other rocks followed a parabolic plot and as such it was possible to obtain the turning point of the relationship from the first order differential of the quadratic equations.
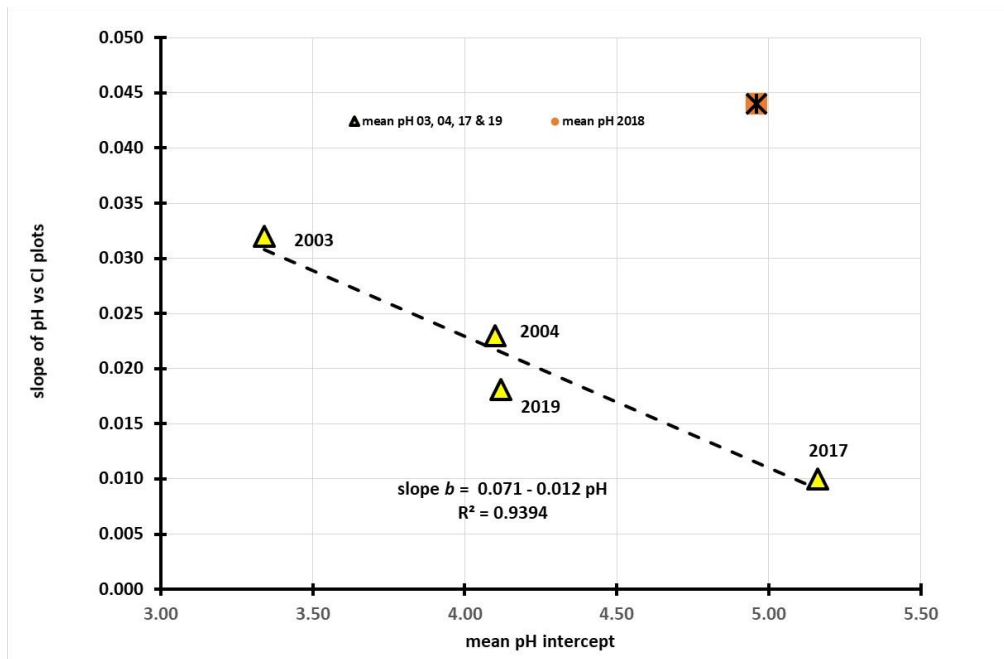
Figure 12 : Sensitivity of pH vs [Cl] plots versus the mean pH $_{intercept}$ at zero chloride

For site 4, which appears to have experienced a highly localised rainfall or other irrigation event, the equations showed that the minimum chloride concentration was found at a distance of between 13 and 41 cm below the line of the first chloride measurements, which were always running from left to right across the leading edge of the rock. This data, along with pH and E_h may provide useful modelling tools for the modes of deposition of air borne chemicals. For the massive site 23 rock the chloride distribution was the inverse and so it reached a maximum (rather than a minimum) chloride concentration 30 cm below the first line of measurements. In this case the modelling indicates that

chlorides were migrating downwards from a primary deposition line and migrating upwards on the gabbro rock. In the cases of the other rocks (except no 4) there appears to be an evaporative concentration of chlorides at the upper and lower surfaces of the exposed rocks.

If there were to be an extension of the CSIRO modelling studies it might be instructive to look at adsorption models of sea salts and other airborne particulates and gases since the data in Figure 11 shows that there is a real difference in the underlying acidity of the granophyre and the gabbro rocks. For the same equivalent chloride concentration, the rougher surface of the gabbro rock was between twice (delta pH 0.33 at 100 ppm chloride) to around 20 times more alkaline than the granophyre rock surfaces, and this will relate to the underlying nature of the weathered crusts and the amount of oxide minerals that are mobilised. This issue has been previously discussed in the commentary on the ratios of sodium to calcium in the washing solutions that were obtained by surface irrigation methods and wet solution chemistry analyses conducted by the ChemCentre of WA.
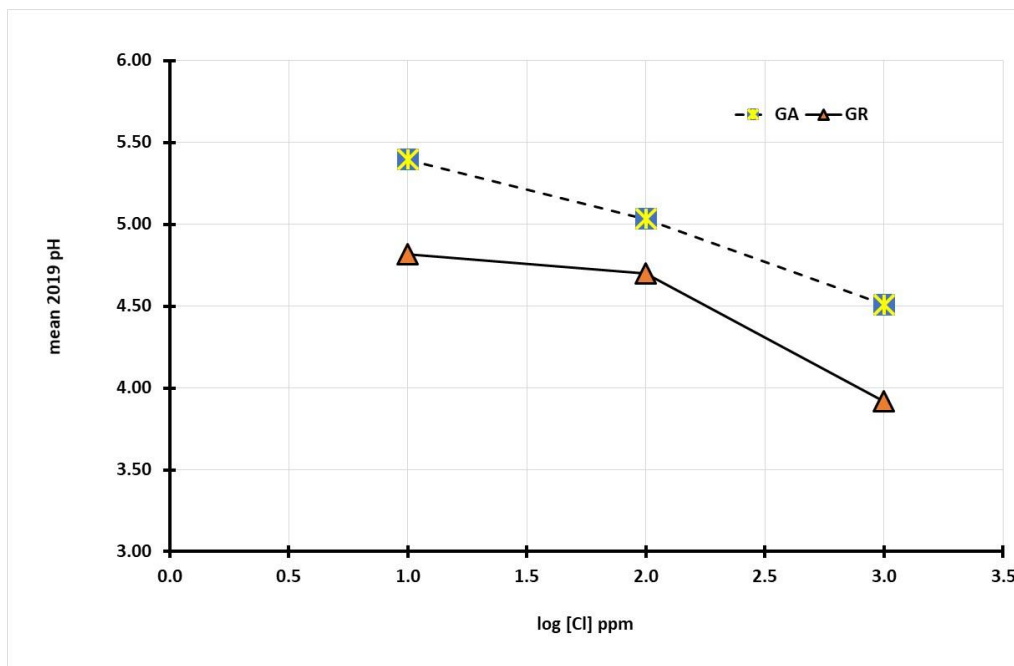
Figure 13 : Sensitivity of rock type to mean pH with log [Cl] for the six Yara sites

Nitrates:

Previous studies in 2003 and 2004 had focused on the acidity and the concentration of nitrate ions, since there was very strong data supporting the inference that nitrate ions were stimulating the overall microbiological activity on the rocks. Since bacterial and fungal metabolites are often acidic it was decided to check to see if there was a correlation with the number of bacteria and the nitrate levels. Data published in 2005 by MacLeod demonstrated that the logarithm of the number of bacteria was directly related to the decreasing pH, thus the amount of nitrate ions, from both natural and human sources, was likely to be a key determinant in the overall rates of weathering of the rock surfaces in the Burrup. Owing to the contrasting nature of the engraved and background areas there was concern about the long-term impact of such accelerated ageing on the rock surfaces. Surface pH values as low as 3.5 were recorded on rocks near the Climbing Man panels adjacent to the Woodside operational flare tower (site 4 and 4a) servicing trains 1-4, as Pluto had not yet been constructed let alone become operational. As part of the February 2004 data collection, samples of rock pH, chloride and nitrate ions were collected on rock engraving sites at Gidley and Dolphin Islands in the Dampier Archipelago, in the belief that these remote sites would be low in nitrates, owing to their distance from apparent point sources on the coastal lands associated with industrial developments. A summary of the relevant

data is shown below in Table 8, which lists the mean nitrate for 2003, 2004, 2017, 2018 and 2019 as well as the range of the maximum to the minimum values that were recorded.

Table 8: Nitrate concentration ranges across Burrup, ppm

Date	Maximum	Minimum	Mean ppm
August 2003	19, Withnell Bay	1.5, at Burrup SW 1–2	6.3 ± 5.1
February 2004	9.2, rock 938	1.3, Deep Gorge	4.5 ± 3.7
November 2017	1.8, site 21	0.10, site 5	0.6 ± 0.7
September 2018	1.4, site 7	0.19, site 22	0.7 ± 0.4
August 2019	2.1, site 7	0.15, Climbing Man	0.7 ±0.6

Although the nitrate concentration was essentially the same in August 2003 and February 2004, the slope of the pH vs $[NO_3]$ $_{ppm}$, as seen in Table 9, was diminished by over 40%. This is roughly in line with the 30% reduction in the mean nitrate concentration between the two sets of measurements. The data in Table 10 shows that common intercept pH values, at zero nitrate, at 5.69 for the 2003 and 2004 analyses. The common intercept value shows that the same chemical mechanism is controlling the response of the rocks in those two seasons of measurements. It should be noted that with the R^2 value of 0.97 the 2003 intercept value of 5.33 value is within experimental line fitting error the same as the 5.44 from rocks in the museum compound that was noted in February 2004. Of concern were the lower pH $_{intercept}$ values of 4.95 and 4.66 for sites that included rocks in the museum compound as well as those at the Climbing Man, Deep Gorges and Withnell Bay sites.

In the 16-years since the February 2003 data was collected, there were six cyclonic rain events, as listed in Table 6, which deposited between 63-212 mm of rain in the region in a 24-hour period. These periods of inundation of the rock surfaces is likely to be the underlying reason for the big drop in the nitrate ion concentration found in the rock washings in November 2017. There was a 62.4 mm rainfall event on 6th June 2018 which would have caused significant washing of the rocks in the test areas. As previously noted, there have been no major rainfall events in the 11 months between the 2018 and 2019 measurements being conducted.

Table 9: Dependence of pH on the nitrate concentration found in wash solutions

Date	pH $_{zero NO3}$	Slope pH/[NO3]	R^2
August 2003	5.69, Climbing man, Deep Gorge & Compound	-0.14	0.92
		-0.14	0.97
	5.33, Burrup SW, King Bay & Compound		
February 2004	5.69, Withnell & Compound	-0.08	0.91
	5.44, Compound	-0.08	0.99
	4.95, Withnell & Compound	-0.07	0.66
	4.66, Deep Gorge & Climbing Man	-0.08	0.78
November 2017	6.18, Sites 5,6,7, 21, 22 & 23	+0.94 log [NO3]	0.99
September 2018	3.14 all sites other than 22	non-linear	0.86
August 2019	4.41$_{min}$, sites 5, 21 & 22	+0.39	0.97
	3.76$_{min}$, sites Climbing Man, 7 & 23	-0.22	0.87
	4.60 $_{median}$, sites CM, 6, 7, 22 & 23	-0.04 (0.02)	0.43
	5.56 $_{median}$, sites 4a, 5 & 21	-1.13(0.59)	0.79

The five-fold fall in nitrate concentration since typical 2003 & 2004 values would have been expected to reduce the impact of the biological activity due to the nitrate concentration but other factors appear to have weighed heavily in bringing about a change in acidification. It has been noted that the mean chloride ion concentration on the Yara sites is approximately 30 times saltier in

November 2017 than the rocks that were sampled in February 2003. A plot of the 2019 data of pH against nitrate concentration shows up interesting variations on the simpler plots of 15-16 years ago. For sites 5, 21 and 22, which are relatively close to potential emissions of ammonia from the plant, there is an increase in the pH as the nitrate levels increase from above 0.15 to 0.57 ppm and like in the 2018 year, this may be due to the localised adsorption of industrial emissions including ammonia from the production facility, as shown in Figure 12. The alkaline nature of ammonia brings about partial sequestration of the acidity from metabolites, through the formation of the NH_4^+ ion. The site 6 data, the Water Tanks, are the closest to the plant and so there are clearly counteracting sources of acidity to bring this pH towards levels somewhat commensurate with the solution nitrate levels. It is possible that acidity from other sources is working to overcome the likely buffering impact of the ammonia or NO_x vapours. However, the low amount of sulphate, 0.8 ppm, precludes any significant contribution from SO_x.
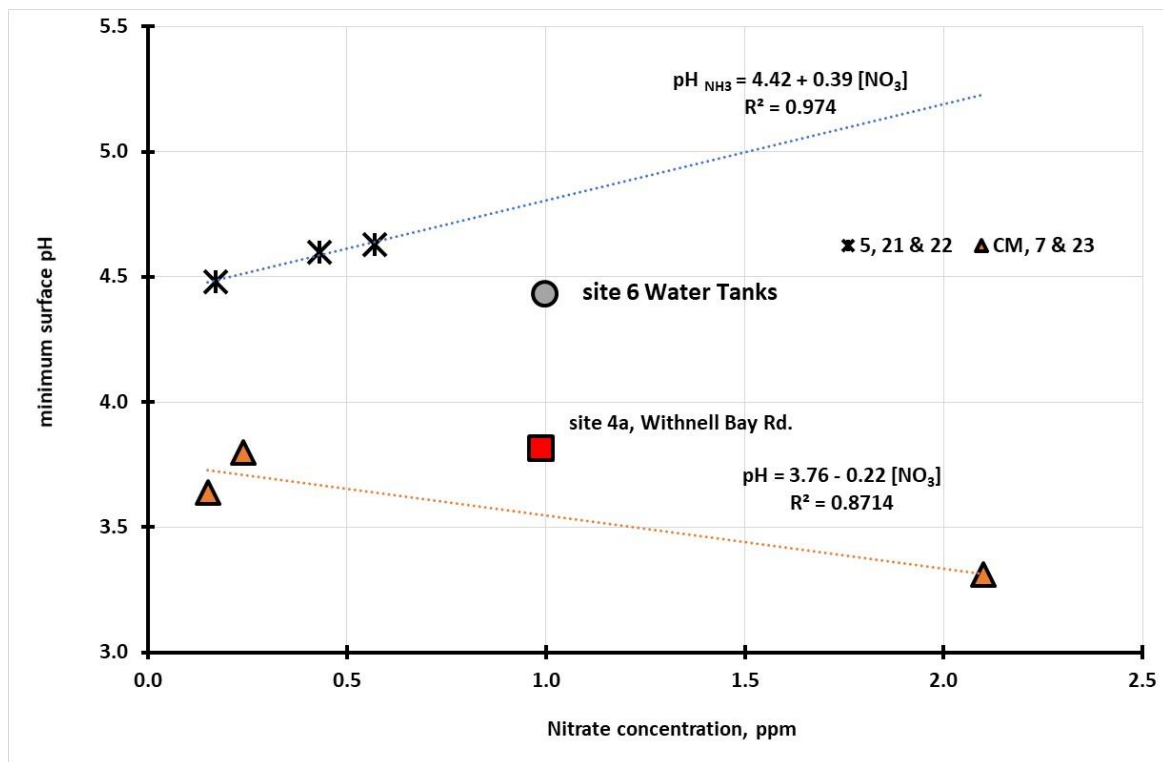
Figure 14: Plot of minimum pH vs. nitrate concentration in the rock washings

When the median [2019]pH values are plotted, instead of the minimum values shown in Figure 12, a different picture emerges. When the data from sites 6, 7, 22, 23 and Climbing Man sites are plotted as a function of nitrate (ppm) the scatter fits Equation 25, with the errors noted in parenthesis. With a low R^2 of 0.43 it is noted that the errors are large.

$$^{2019}pH_{median} = 4.61\ (0.02) - 0.035\ (0.022)\ [NO_3] \dots\dots\dots\dots\dots\dots\dots\dots(25)$$

Thus, Equation 25 covers the falling pH with increasing nitrate for five of the seven sites and the slopes and intercept values are similar to those reported in Table 10 for February 2004. In addition to this relationship the median pH for sites 4a (close to the old flare tower), site 5 (close to Pluto flare tower) and site 21 is given by Equation 26,

$$^{2019-2}pH_{median} = 5.56\ (0.41) - 1.13\ (0.59)\ [NO_3] \dots\dots\dots\dots\dots\dots\dots(26)$$

Comparison of Equations 25 and 26 show a much stronger dependence of the median pH on nitrate concentration for the 4a, 5 and 21 sites. The reason for these different sensitivities is not currently known. However, it is important that continued monitoring and assessment of the sensitivity of the rocks to soluble nitrate is further investigated.

A possible explanation for this behaviour is that to bring about an overall increase in the acidity of the rock surfaces a significantly higher than 1 ppm nitrate needs to be present to provide the bacteria, yeasts moulds and fungi with enough nutrient to overcome the inhibition that the high salt content of the rock surface appears to be providing. Additional monitoring needs to be done on the Yara sites and sites that were previously addressed in the 2003-2004 field work need to be sampled at the same time to see if the Yara sites represent a niche microenvironment or if the overall conditions in the Burrup have changed. It is most unlikely that the latter is the case since independent measurements of many of the previous sites in June 2017 (MacLeod 2017b) has shown increasing acidification of sites near the Climbing Man in the same gully. Rocks from the relocated museum compound were found to have more alkaline pH than in 2003 when they had been thoroughly scrubbed to remove all the paint residues when their "registration numbers" were chemically removed. In an instance when the number had failed to be removed the pH of the rock had fallen i.e. it showed increasing signs of acidification.

Sulphate

The distribution of sulphate in the washings is shown graphically in Figure 6 and is tabulated for Burrup sites in Table 10, which reports the data from the August 2003 and February 2004 rinses, along with the most recent data on the Yara sites from November 2017, September 2018 and most recently from August 2019.

Table 10: Range of sulphate ions in the wash solutions on Burrup and Yara sites

Date	Maximum	Minimum	Mean [SO_4^{2-}] ± SD ppm
August 2003	66.7 Rock 938	1.2 Burrup SW2	9.8 ± 14.2
February 2004	26.1 Rock 938	0.8, Deep Gorge, site 7	4.9 ± 5.5
November 2017	9.8, site 23	1.5, site 22	5.2 ± 3.0
September 2018	2.2, site 6	0.3, site 22	1.2 ± 0.7
August 2019	19.1, site 21	0.4 site 4a, site 22	4.5 ± 6.4

The 2019 sulphate values are much the same as in February 2004 and the mean pH is very similar the data from 15 years ago. The data shows that there has been essentially no change in the amount of sulphate present in the 2017 compared with the 2004 readings, other than the maximum value for 2004 was nearly three times that observed in 2017 at the Yara sites. The highest values reported were found on rock 938 in 2003 at the "museum compound" which lay inland from the Climbing Man gully and was located behind the hills from the Woodside gas production facility. In August 2003 the pH was 4.8 ± 0.4 and in February 2004 it was 4.9 ± 0.6 which makes them statistically the same i.e., there was no correlation between the wash solution sulphate concentration and the underlying acidity. It has been previously noted that the pH of the rock surfaces is significantly affected by the chloride levels, coming from the sea salts, so it is instructive to see how the $^{Cl}/_{SO4}$ ratios vary across the Burrup in the different periods of measurement (Table 11).

Table 11: Ratios of chloride to sulphate ions in the wash solutions from Burrup rocks.

Date	Cl^-/SO_4^{2-} mean	Cl^-/SO_4^{2-} high	Cl^-/SO_4^{2-} low	Cl^-/SO_4^{2-} sea
August 2003	5.7 ± 5.4	6 sites @ 11.8 ± 6.6 Climbing Man, off museum site rock 162,	14 sites @ 3.1 ± 1.2 Dampier, King Bay, Deep Gorge	7.1
February 2004	21 ± 15	14 sites @ 9.9 ± 5.1	27 sites @ 4.3 ± 1.2	7.1

		Climbing Man, off museum site, Rock 3	Gidley & Dolphin Islands, Dampier, Rocks 86, 162, 938,	
November 2017	1.1 ± 0.3	site 22, 2.2	site 7, 0.7	7.1
September 2018	2.8 ± 1.8	site 22 Yara NE 6.0	site 4 Woodside 0.7	7.1
August 2019	3.0 ± 1.3	4.7 ± 0.5, sites 21, 22 & Climbing Man	2.1 ± 0.5, sites 4, 4a, 5, 6, 7, 23	7.1

Despite the large standard deviations of the mean values for 2003 and 2004 data the high ratios of Cl^- : SO_4^{2-} do reflect the expected amount of sulphate present in the individual rock washings when compared with the chloride ratios found in seawater. From the numbers of sites sampled, roughly one-third of the rocks had the expected chloride to sulphate ratio. For the ratios that are significantly lower than those found in normal seawater, this implies that there is additional sulphate present in the rock surface washings i.e. sulphate is not coming from the sea. For the Yara monitoring sites there is a one third lower Cl^-: SO_4^{2-} ratio which means that additional sulphate is coming from sources other than the sea. These sources are altering the surface chemistry of the sites. It is likely that deposition of SO_x is affecting 66% of the Burrup rock art sites and that this impact is felt even on remote sites such as Gidley and Dolphin Islands.
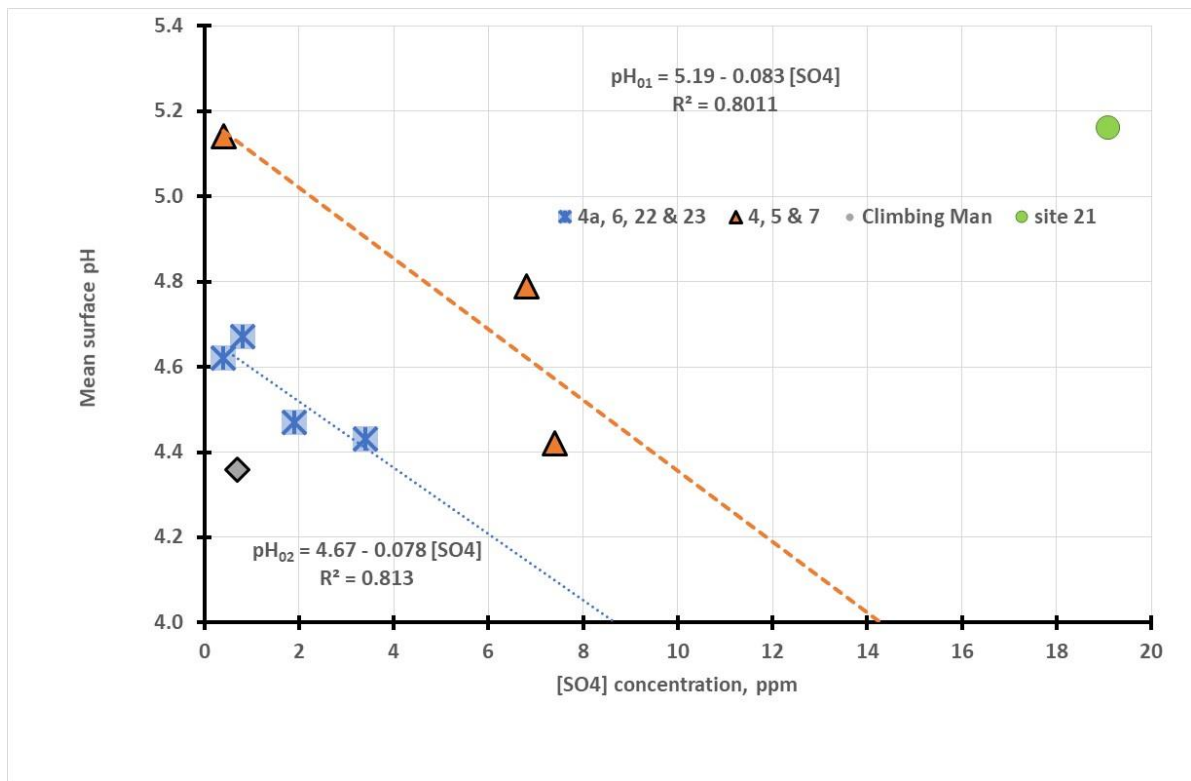
Figure 15: Plot of mean [2019] pH against the sulphate (ppm) concentration.

However, it is noted that in the 2019 data site 4a, near the Woodside flare tower, had the lowest ratio of chloride to sulphate at 1.3, which is consistent with the deposition of SO_x from the combustion products of the flared gases. The exposed position of site 22 at Yara NE gave a near normal ratio of 5.3, compared with 7.1 for seawater. The relationships between the amount of sulphate in the wash solutions and the mean surface pH is shown in Figure 13 and is described by Equations 27 and 28.

For equation 27, which links the sites no 4, 5 and 7, the R^2 value is 0.80 and so the errors in the slope and intercept are relatively large and are reported as the values in parenthesis.

$$^{2019-01}pH_{mean} = 5.19 \ (0.24) - 0.083 \ (0.041) \ [SO_4] \quad\quad\text{.............................(27)}$$

The sensitivity of the pH to sulphate concentration of both sets of regression lines is experimentally the same so the underlying acidity of the sites separates out the groupings of the specific test regimes. The R^2 for Equation 28 was 0.81, the same as for equation 27.

$$^{2019\text{-}02}pH_{mean} = 4.67\,(0.05) - 0.078\,(0.026)\,[SO_4]\dots\dots\dots\dots\dots\dots(28)$$

The data points covered by Equation 28 included the surrogate site at site 4 (4a), site 6 (Water tanks), site 22 (Yara NW) and site 23 (Yara East). The outlying point was observed at site 21 which has elevated chloride and associated sulphate due to the accumulation of sea salts on the nearby reference rock.

Comparison of pH between 2017, 2018 and 2019

A summary of the differences between the three seasons of measurements is found in Table 12 and in Figure 7, which is repeated below to facilitate discussion. For site 23 although the mean pH has fallen between the three seasons of measurements, the result for each comparative data set is not statistically significant. For site 22 the 2018 results were indistinguishable from 2017 (not significantly different when looking at the combination of the standard deviations compared with the difference in the mean values of acidity. However, the differences between 2018 and 2019 with an increase in acidity of pH 1.42 is significantly different. This site has the smallest geometric surface area of the reference rocks. For site 21, the closest to the Yara plant, there was no significant difference between the 2018 and 2017, or the 2019 and 2018 data. This NO and NO response is the same for Site 23, Site 21, and sites 4 and 5. For the Deep Gorge site 7 there was significant increase in alkalinity between 2017 and 2018 (delta pH 1.11) which made the increase in acidity in 2019 even more dramatic to a pH change of 2.26 between the 2018 and the 2019 data sets. For the Climbing Man site, not one of the CSIRO reference sites but one that is culturally extremely significant to the community represented by the Murujuga Aboriginal Corporation, there was a statistically significant increase in alkalinity between 2017 and 2018 and a statistically significant increase in acidity between 2018 and 2019.

Table 12: Changes in mean surface pH between Nov 2017 and September 2018

Location	2017 mean pH	2017 std dev	2018 mean pH	2018 std dev	2019 mean pH	2019 std dev	Δ pH '18-17	Δ pH '19–'18
site 23	5.50	0.62	4.83	0.64	4.47	0.28	-0.67	- 0.36
site 22	6.16	0.48	6.04	0.57	4.62	0.10	-0.12	- 1.42
site 21	6.43	0.45	5.81	0.65	5.16	0.30	-0.62	- 0.65
site 7	5.57	0.42	6.68	0.39	4.42	0.44	+1.11	- 2.26
site 6	5.66	0.70	6.03	0.54	4.67	0.18	0.37	- 1.36
site 5	5.17	0.60	4.98	0.43	4.79	0.17	-0.10	- 0.19
site 4	3.81	0.52	5.52	0.92	5.14	0.14	+ 1.71	+ 0.86
Site 4a	3.86	0.46	4.28	0.59	4.43	0.35	+ 0.42	+ 0.15
Climbing Man	3.85	0.15	5.81	0.39	4.36	0.50	+ 1.96	- 1.45

There is no consistent pattern of changing pH differences that relates directly to the underlying geology, as to whether the sites were granophyre or gabbro. Inspection of the data in Figure 7 (below) shows how the spread of data for each site, as reflected in the standard deviations of the mean, effectively obliterates the significance of the changes between 2017 and 2018 for sites 23, 22, 21, 6, 5 and 4. The only sites with statistically significant changes in the same time period were sites 7 at Deep Gorge and the Climbing Man site, both of which had significant alkaline shifts. For the Deep Gorge site, we know from analysis of rainwater from the adjacent monitoring station provided by Yara that the increase in alkalinity may have been associated with adsorption of ammonia emissions from the Yara site. Given that the Climbing Man site is close to Site 4 it is most reasonable to assume that there was localised rainfall in that area between the November 2017 and September 2018

measurements, as the increase in pH associated with intense rainfall is similar to those geographically linked locations. A cyclonic rainfall event that covers this period is listed in Table 5.
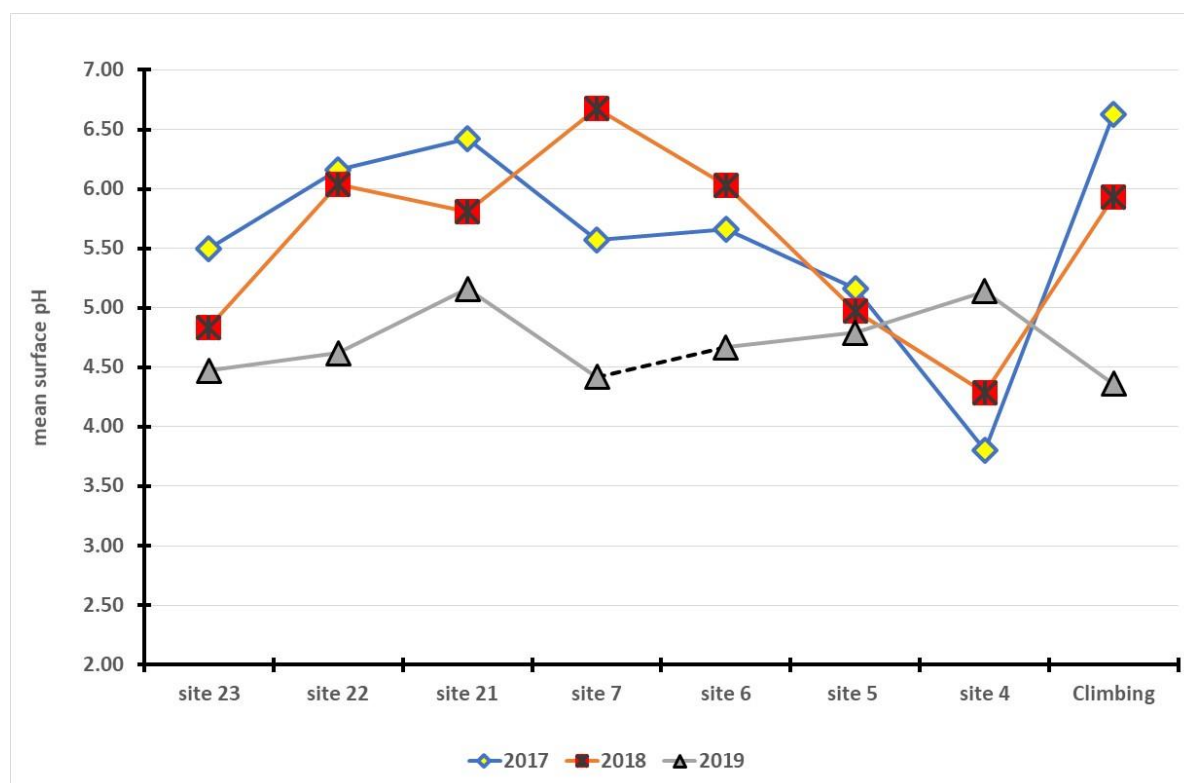
Figure 7: Plot of the mean pH for eight monitoring points between 2017-2019

When reviewing the plot of the mean pH for the three seasons of measurements it is readily apparent that site 22, 7, 6 and Climbing Man have undergone a significant increase in the underlying acidity of the rock surfaces. It is important to keep monitoring this data and to continue to seek solutions for any systematic increase in the acidity.

Summary of the surface pH, chloride & redox at Yara sites

It should be noted that in the 2017 measurements on the Yara test sites only the surface pH and chloride ion activities were recorded. The utilisation of redox data on the Burrup rocks was not developed until July 2017 and was not adopted until after peer review had confirmed it was a viable indicator of chemical activity on the rock surfaces. For this section of the report, the statistical analysis of the distribution of pH, chloride and redox potentials for each of the sites is discussed in turn.

Site 23

Inspection of the data in Table 13 for the three seasons at site 23, Yara East, shows a regular fall in the mean pH but this is not matched by the median pH where it can be seen that there was effectively no change in the pH_{median} value between 2019 and 2018. The amount of sea salt deposited on the reference rock remained essentially constant and all the measures of change assessed for the redox potential indicated a lowered voltage, which seems to be counterintuitive to the changes in the mean pH. It was noted that the minimum pH for 2019 at 3.8 was lower than 4.2 value for 2018 but the differences are not statistically significant. The site is exposed to any winds blowing in from Hearson's Cove.

Table 13: Statistical analysis of pH, chloride and E_h readings on site 23, Yara East

	2019 pH	2018 pH	2017 pH	2019 Cl	2018 Cl	2017 Cl	2019 E vs. NHE	2018 E vs NHE
Mean	4.47	4.83	5.50	30.4	29.6	18.5	0.397	0.484
Std. Error	0.08	0.18	0.20	2.8	4.6	5.5	0.006	0.004
Median	4.60	4.63	5.65	30.0	25.0	11.5	0.395	0.488
Mode	4.62	4.63	#N/A	32.0	#N/A	6	0.395	0.489
Std. dev.	0.28	0.64	0.62	9.7	17.2	17.4	0.019	0.016
Range	0.9	2.15	1.97	40	53.7	50.5	0.064	0.068
Minimum	3.8	4.16	4.42	16	11.5	4.5	0.361	0.440
Maximum	4.7	6.31	6.39	56	65.2	55	0.425	0.508

Site 22

Known as site 22 the reference rock lies high on top of a hill on a ridge running towards the coast. During the 2019 on site measurements the wind was gusting strongly, with estimates of speeds up to 70 km per hour, which tended to knock the assessment team off their feet. The location is to the North East of the Pilbara nitrates plant and the mean pH for 2019 is significantly lower than it was in the two previous years. This chloride concentration on the site in 2019 is essentially the same as it was in 2017 so the change in acidity (a decrease in pH of 1.54 between 2017 and 2019 cannot be due to changes in acidity due to chloride obligate bacteria). The mean redox potential of sites 23 and 22 is very similar which is not surprising since they are both gabbro rocks, but both are lower than in the previous year which indicates that the redox couple controlling the voltage has changed.

Table 14: Statistical analysis of pH, chloride and E_h readings on site 22, Yara East

	2019 pH	2018 pH	2017 pH	2019 Cl	2018 Cl	2017 Cl	2019 E_h vs NHE	2018 E vs AgCl
Mean	4.62	6.04	6.16	30.3	10.2	33.3	0.382	0.492
Std. Error	0.03	0.17	0.15	1.4	3.4	7.7	0.005	0.004
Median	4.61	5.82	6.42	30.0	8.5	26.3	0.387	0.495
Mode	4.55	n.a.	6.42	33.0	n.a.	n.a.	0.388	0.491
Std. dev.	0.10	0.57	0.48	4.9	11.2	24.3	0.018	0.012
Range	0.37	2.01	1.3	18.0	40	82.5	0.059	0.044
Minimum	4.48	5.3	5.3	21	1.4	14.5	0.348	0.458
Maximum	4.85	7.3	6.6	39	41	97	0.407	0.502

Site 21

For Site 21 (Yara West) there is an apparent systematic fall in the mean pH from 2017 through 2018 to 2019, however the large standard deviation of the 2018 data means that there is no statistically significant difference between the successive years. However, there is a continuing fall (increase in acidity) in the pH for the minimum value from 5.8 in 2017, to 4.9 in 2018 to 4.6 in 2019, which follows the trend in the mean values. The chloride readings in 2019 were much higher than in 2018 but had a significantly larger range of 225 ppm with the maximum 2019 value being 250 ppm. The very exposed position of the flat rock on top of the hill meant that like site 22 the research team was nearly blown over by the very strong winds that only abated once we had come down from the top of the hill into the plain. Lower chlorides are associated with a reduced buffering capacity to resist the acidification

due to metabolic activity of the microflora and this site may have increased acidity due to the activity of chloride obligate bacteria.

Table 15: Statistical analysis of pH, chloride and E_h readings on site 21, Yara West

	2019 pH	2018 pH	2017 pH	2019 Cl	2018 Cl	2017 Cl	2019 E_h vs. NHE	2018 Eh vs. NHE
Mean	5.16	5.81	6.43	95	20	143	0.369	0.487
Std. Error	0.09	0.18	0.14	20	4	14	0.005	0.204
Median	5.21	5.70	6.44	68	21	136	0.369	0.489
Mode	5.21	n.a.	5.98	25	n.a.	214	n.a.	0.484
Std. dev.	0.30	0.65	0.45	70	13	44	0.018	0.209
Range	0.97	2.1	1.5	225	46	126	0.066	0.229
Minimum	4.60	4.9	5.8	25	1	88	0.340	0.472
Maximum	5.6	6.9	7.3	250	47	214	0.406	0.499

Site 7 Deep Gorge

The acidity on this site had significantly increased since the alkaline spike in 2018 by the time the measurements were taken in 2019 , some 11 months later. The 2018 data had a mean pH was 6.7 ± 0.4 which is much more alkaline than the mean value in 2017 of 5.6 ± 0.4 but the reduction in acidity in 2018 is not due to increases chloride content on the surface, as the 2018 values are the same as those recorded in 2017. The monitoring station adjacent to Site 7 showed that in 2018 there was a significant amount of ammonia and ammonium ions found in the local rainwater. Adsorption of ammonia vapour from the Yara site may have been the reason for a surge in alkalinity i.e., loss in surface acidity.

It is interesting to note that on this gabbro rock the mean redox potential in 2019 was significantly lower by 59 mV than those observed on the sites 21, 22 and 23 where the mean value was 0.488 ± 0.004 volts vs. NHE. It is also noted that with the change in the mean pH from 6.7 ± 0.4 to 4.4 ± 0.4 in 2019 also brought about a change in the Pourbaix diagram. In 2018 the dominant electrochemical process involved the formation of significant amounts of the manganese equivalent of magnetite, namely Mn_3O_4 while for the 2019 measurements the slope had changed to 29 mV per pH unit and that the dominant mechanism was controlled by Equation 19 viz.,

$$Mn(OH)^+ + H_2O \rightarrow Mn(OH)_2^{2+} + H^+ + 2e^- \quad\text{.......................................(19)}$$
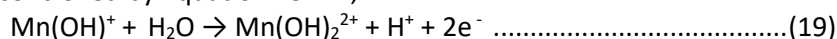
The dramatic change in apparent decay mechanism on the rock surface as the mean pH shifted by 2.3 or 200 times is not unexpected as it is well known that dissolution of manganese minerals and the associated deposition reactions with formation of different insoluble minerals is very sensitive to changes in the prevailing pH.

Table 16: Statistical analysis of pH, chloride and E_h readings on site 7, Deep Gorge

	2019 pH	2018 pH	2017 pH	2019 Cl ppm	2018 Cl ppm	2017 Cl ppm	2019 E_h vs. NHE	2018 E_h vs. NHE
Mean	4.42	6.68	5.57	8.6	18.6	21.5	0.368	0.429
Std. Error	0.13	0.12	0.11	1.1	2.5	3.7	0.006	0.008
Median	4.52	6.67	5.53	7.2	17.3	24.0	0.366	0.432
Mode	n.a.	7.02	5.90	6.9	#N/A	30.0	0.355	0.432
Std. dev.	0.44	0.39	0.42	3.8	7.8	11.7	0.020	0.025

Range	1.67	1.14	1.49	13	28.8	27.8	0.061	0.082
Minimum	3.31	6.06	4.92	4.3	8.2	7.2	0.339	0.380
Maximum	4.98	7.20	6.41	17.3	37.0	35.0	0.400	0.462

Site 6: The Water Tanks

The rock immediately adjacent to site 6 was systematically assessed for surface pH, chloride and redox potential in both 2019 and 2018 and both pH and chloride in 2017. The pH data collected in 2019 was statistically significantly more acidic than when the site was assessed in 2018 when the mean pH was 5.9 ± 0.7. The 2018 pH was not statistically different to the 2017 value of 5.7 ± 0.2. Although cyclonic rain before the 2018 measurements had reduced the mean chloride from 191 to 2.3 ppm this dramatic fall in chloride does not account for the small increase in the mean pH in 2018, since lower chloride means less buffering of the rock surface by the alkaline nature of sea salts. The mean redox voltage in 2019 was 0.391 ± 0.017 volt compared with 0.396 ± 0.020 which is the lowest voltage of all the seven sites examined, but it did confirm that the chemical environment was the same as the previous year. The 2019 Pourbaix diagram had a slope of 120 mV per pH and so the most likely reaction is seen in Equation 24 viz.,

$$MnO_2 + 4 H + 2e^- \rightarrow Mn^{2+} + 2 H_2O \dots\dots\dots\dots\dots (24)$$

Where the oxidation of soluble manganous ions leads to the precipitation of insoluble Mn (IV) species in the form of manganese dioxide.

Table 17: Statistical analysis of the pH, chloride and E_h readings in 2019 at site 6, water tanks

	2019 pH	2018 pH	2017 pH	2019 Cl	2018 Cl	2017 Cl	2019 E_h vs NHE	2018 E_h vs NHE
Mean	4.67	5.85	5.66	9.7	2.3	190.8	0.391	0.396
Std. Error	0.05	0.19	0.07	1.8	0.9	48.6	0.005	0.006
Median	4.64	6.11	5.76	8.5	1.2	164.5	0.390	0.403
Mode	4.59	4.70	5.85	n.a.	#N/A	#N/A	n.a.	0.403
Std. dev.	0.18	0.70	0.22	6.3	3.2	97.3	0.017	0.020
Range	0.58	1.7	0.57	21	11.3	218	0.050	0.068
Minimum	4.43	4.7	5.28	3	0.3	108	0.369	0.358
Maximum	5.01	6.4	5.85	24	11.6	326	0.419	0.426

Site 5: Burrup Road west

The mean pH for 2019 is not statistically significantly different to that of the mean pH of the 2018 and 2017 readings. The range of pH data in 2019 is much less than in the other seasons of measurement at 0.2 pH compared with 1.7in 2017. There is no systematic difference between the minimum pH between the three seasons of measurements and the slightly more alkaline value of mean pH in 2017 is likely due to a higher salt content deposited on the rock surfaces. It was noted that in 2019 the range of E_h was 131 mV compared with 32 mV the previous year which does indicate that despite the apparent homogeneity of the pH data in 2019 there is a lot of difference in the way in which the electrochemical nature of the surface is expressed at the platinum electrode. The dark patches of rock surface on this site are due to the formation of Mn_3O_4, the manganese equivalent of magnetite. This insoluble purple black mineral is formed when soluble Mn^{2+} ions are oxidized in the reverse reaction of Equation 23 shown below.

$$Mn_3O_4 + 8 H^+ + 2e^- \longleftrightarrow 3Mn^{2+} + 4 H_2O \dots\dots\dots\dots(23)$$
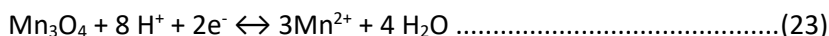
It needs to be remembered that all the redox reactions listed in the discussions on the interpretation of the E_h and pH data are in fact reversible electrode reactions and so need to be considered as

dynamic equilibria. Thus, minerals that form in one year can at least be partially or completely dissolved between one year and the next, which explains to a large extent the apparent variability of the colour measurements on the rock surfaces.

Table 18: Statistical analysis of the pH, chloride and E_h readings in 2019 at site 5, Burrup Road

	2019 pH	2018 pH	2017 pH	2019 Cl	2018 Cl	2017 Cl	2019 E_h vs NHE	2018 E_h vs NHE
Mean	4.79	4.98	5.17	6.3	4.1	31.7	0.391	0.467
Std. Error	0.05	0.12	0.18	0.8	1.0	8.6	0.011	0.003
Median	4.72	5.02	5.17	5.8	3.1	24.0	0.394	0.466
Mode	4.72	4.87	n.a.	4.6	n.a.	n.a.	0.377	0.458
Std. dev.	0.17	0.43	0.60	2.5	3.5	28.5	0.038	0.011
Range	0.49	1.61	1.68	8.6	12.8	101.8	0.131	0.032
Minimum	4.63	3.97	4.36	4.4	1.2	4.2	0.318	0.453
Maximum	5.12	5.58	5.17	13	14	106.0	0.449	0.485

Non Yara sites: CSIRO Site 4: Climbing Man gully near flare tower

The CSIRO reference rock no 4 is located close to the Withnell Bay Road some 250 metres up the gully from the roadway. The surface pH, chloride and E_h data was collected in the same manner as the other sites. The rock is large, and 15 sets of measurements were taken beginning at the upper left-hand side and moving in five steps across before moving down the rock face to the left and then stepping down to keep up a zig-zag sampling patter. The site is about 75° to the vertical.

Table 19: Statistical analysis of the pH, chloride and E_h readings in 2019 at site 4

	2019 pH	2018 pH	2019 Cl ppm	2018 Cl ppm	2019 E_h vs NHE	2018 E_h vs NHE
Mean	4.43	5.52	4.4	2.2	0.392	0.485
Std. Error	0.10	0.24	0.5	0.5	0.004	0.003
Median	4.48	5.34	3.8	1.4	0.389	0.485
Mode	4.48	5.34	2.8	1.5	0.376	0.480
Std. dev.	0.35	0.92	1.9	2.1	0.015	0.011
Range	1.12	2.90	5.9	6.6	0.037	0.046
Minimum	3.83	4.38	2.6	0.5	0.375	0.467
Maximum	4.95	7.28	8.5	7	0.412	0.513

This site generated quite complex pH and chloride data, which is best illustrated in Figure 16. Some areas of the site 4a showed a decrease in the pH with increasing chloride while others showed the opposite trend. The decreasing pH with increasing chloride is an indicator of the activity of chloride obligate bacteria (Equation 29) and the intercept value for Equation 29 is typical of the natural acidity of gabbro and granophyre rocks that have been extensively weathered. Those parts of the rock that showed increased alkalinity with increased chlorinity were "sterile" areas that were responding to the greater concentration of alkaline sea salt evaporites, as shown in Equation 30.

$$^{Cl\ obligate}pH_{site\ 4a} = 5.23 - 0.19\ [Cl] \dots\dots\dots\dots\dots\dots\dots\dots\dots\dots\dots\dots(29)$$

$$^{Cl\ sea\ salt}pH_{site\ 4a} = 3.48 + 0.12\ [Cl] \dots\dots\dots\dots\dots\dots\dots\dots\dots\dots\dots\dots(30)$$

The linear regression for Equation 30 is characterised by a very high R^2 value of 0.991 while the corresponding value for Equation 29 is 0.627. When the statistical analysis is done on the regression

Equation 29, the error in the intercept is ± 0.29 and in the slope, it is ± 0.08, which makes the slope statistically indistinguishable from the slope of Equation 30, but it is just opposite in polarity. The pH readings across the top of the rock surface and then back along the second line towards the left are described by Equation 29 while the upper left pH point and the bottom row, where the sea salt spray would naturally accumulate and evaporation result in increased chlorides, it is that section of the rock which is controlled by the accumulation of sea salts – see Figure 16.
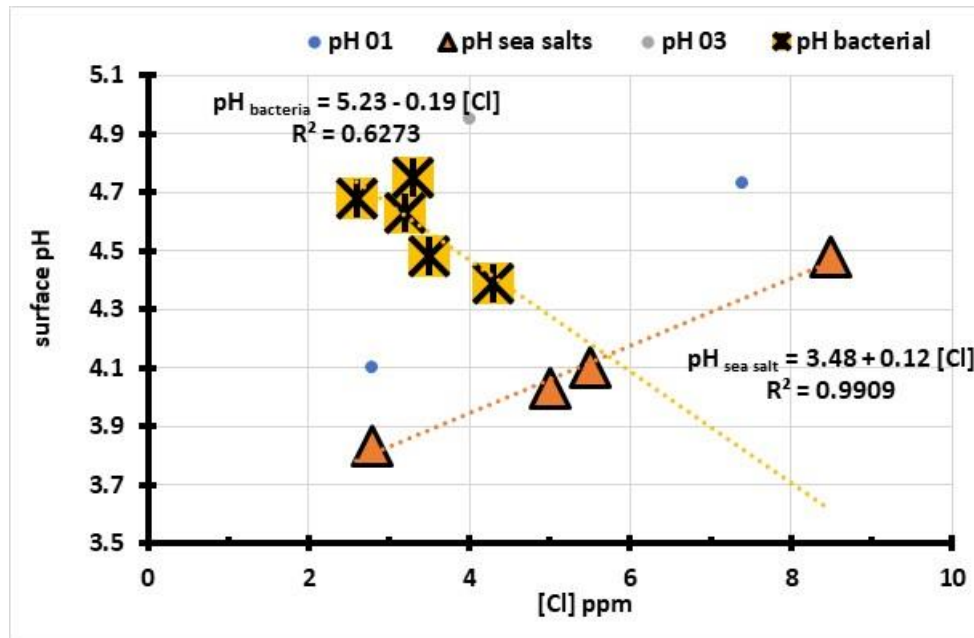
Figure 16: Site 4a pH vs. surface chloride near the Withnell Bay North road.

In order to gain a better understanding of the complex set of inter-relationships between microbiological and electrochemically controlled reactions on the rock surfaces, it was instructive to look at how the E_h varied across the surfaces of reference rock 4a. The data is shown below in Figure 17 where the voltage is seen to have two different responses to chlorinity.
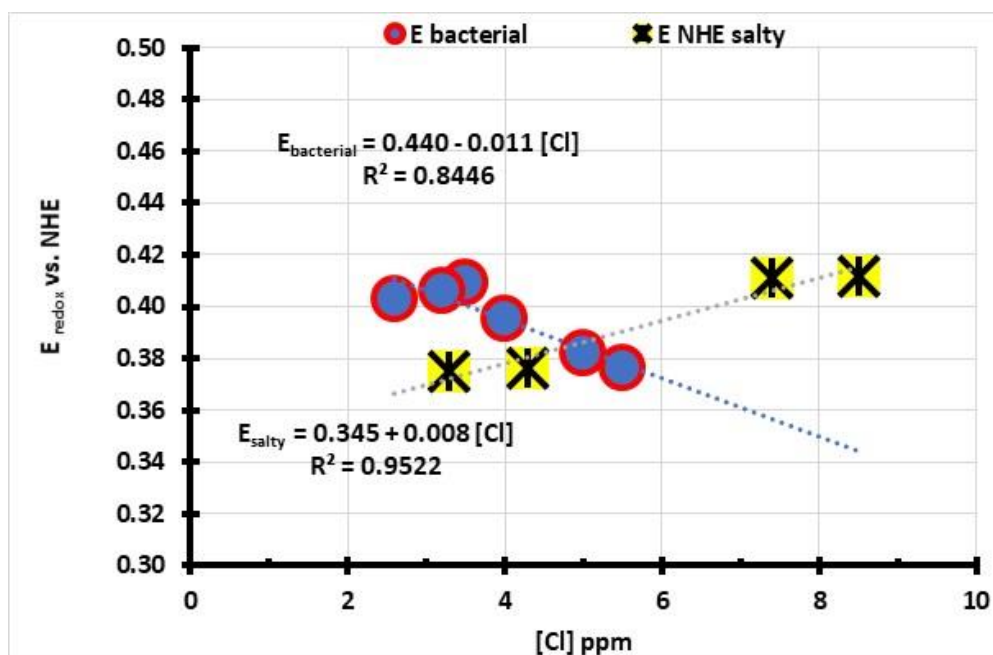
Figure 17: Plot of the 2019 redox voltage at site 4a near the Withnell Bay Road north.

The slope for the chloride obligate bacterially controlled E_h is -0.011 ± 0.002 volts/ppm and the slope of the "salty" E_h is +0.008 ± 0.001 volts/ppm so they are equal and opposite in sign. This similarity in slopes of the E_h and the pH with chloride ion concentration shows that the processes are closely linked. Just as the metabolites of bacteria produce more acid with increased chloride concentration the acidic metabolites appear to be complexing the manganese ions and so the redox potential is being lowered in response to chloride ions. For the sections of the rock where there is an increase in pH with sea salt concentration and there is a corresponding increase in the redox potential this is in response to the improved activity of manganous ions (Mn^{2+}) as weak chloride complexes over the lowered activity associated with the partially hydrolysed Mn (II) species viz., $Mn(OH)^+$ which dominates in the observed pH range. This dual nature of the rock surfaces was also observed on the same rock in the previous year in the September 2019 readings. This explanation is supported by the observation that in the most acidic parts of the rock surface where the mean pH was 4.2 ± 0.3 the mean E_h was essentially invariant at 0.378 ± 0.003 volts vs. NHE which is due to there being no $Mn(OH)^+$ species found in this pH range. Thus for the less acidic parts of the site, with a mean pH of 4.6 ± 0.2 it was possible for the monohydroxy species to be formed and the subsequent oxidation to Mn^{4+} ions, in the form of $Mn(OH)_2^{2+}$ which gave the Pourbaix slope of one proton per two electrons or − 30 mV per pH.

Comparison of Yara and Climbing Man gully sites in August 2019

In reviewing the mean pH of the rock surfaces in 2019, 2018 and 2017 the only significant change is that the Deep Gorge site 7 became more alkaline and then significantly more acidic, as shown in Figure 18 which records the changes in pH over the three years of monitoring. The change in pH from the initial (base line) records in 2017 and those in 2018 and 2019 are listed on the *y* axis and the sites are recorded below.
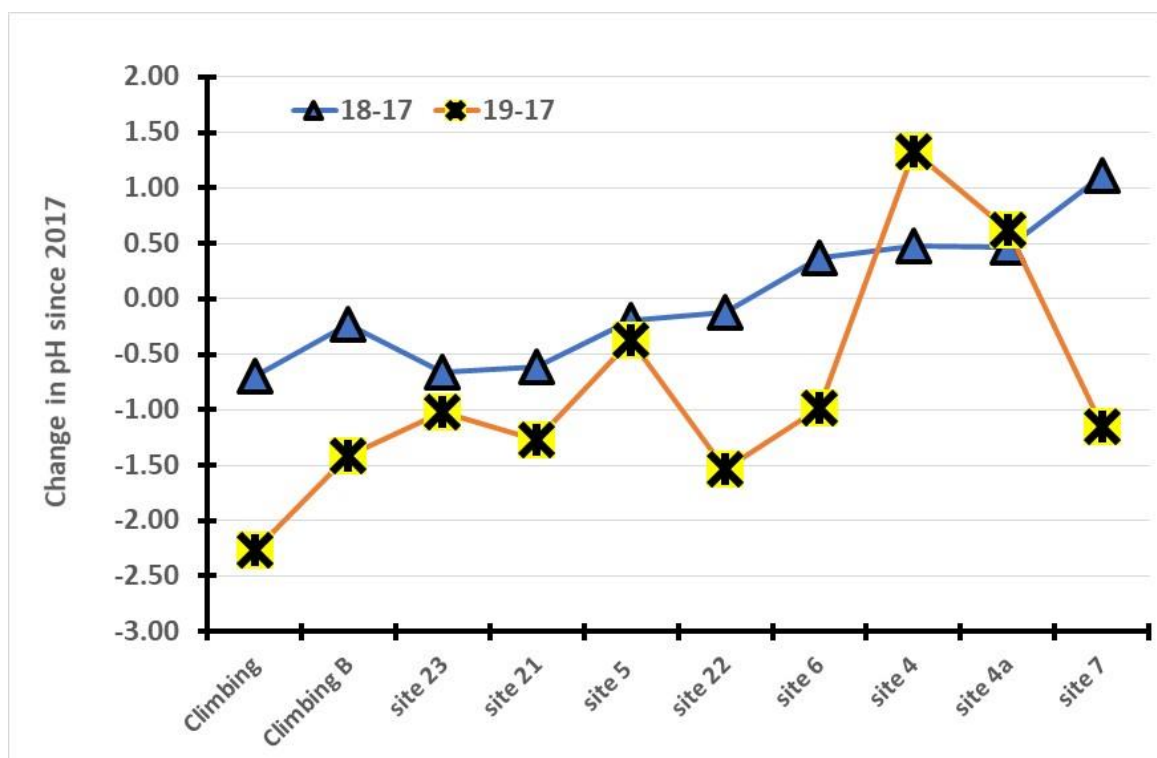
Figure 18: Plot of the differences in pH between 2017 and subsequent years.

In reviewing the data associated with Figure 18, the *Climbing* site is the actual engravings of the Climbing Man itself and *Climbing B* is the 30º upward facing massive slab rock that lies below and

approximately 1.5 metres to the left of the main image. The initial pH fall of 0.7 in the first data set was increased to 2.27 in 2019 which represents a major increase in acidity. The smaller increases of acidity of 0.23 and 1.42 over the same time interval reflects differences in the aspect of the rocks and in their localised geology but it is clearly seen that, in terms of inherent preservation environment, the Climbing Man site has deteriorated over the past three years. For the Yara East (site 23) the change of increased acidity between 2019 and 2018 is within the variation that is found on the rock itself and so is not statistically significant. For Site 21 on top of the hill near the Yara plant it is apparent that there is an increased acidity in 2019 compared with 2018, with an approximate doubling of the pH change of -0.62 to -1.27 for the 2019 measurements. For site 5, Burrup Road West, there is no significant difference between 2019 and 2018 data points but both are more acidic than they were in 2017. For site 22 lying on top of the ridge at Yara NW the fall in pH from -0.12 to -1.54 is a significant increase in acidity and the water tanks (Site 6) had moved from a more alkaline shift of 0.37 pH in 2018 to -0.99 in 2019 which is the same as the increased acidity noted at Site 22. For the CSIRO reference rock at site 4, the nature of what appears to have been an extremely localised rainfall event had been previously discussed but the shift of pH 1.33 in the alkaline direction goes against all the other site measurements which were either much the same pH in 2019 as in 2018 or were more acidic. The adjacent site 4a had the same mean acidity in 2019 as in 2018. The largest change in pH is reserved for the Deep Gorge site (no 7) where the delta pH went from +1.1 to -1.2 or a swing of 2.3 or an increased acidity of 200 times. It is readily apparent that the key sites for checking for changes in the surface chemistry and colour change are those associated with site 7, site 6 and site 22.

Redox potentials and the impact of chloride ion activity

The impact of chloride on the alkalinisation of sites, through deposition of sea salt spray and its subsequent evaporation, has been dealt with in detail and the evidence of chloride obligate bacterial acidification was demonstrated at site 4a where it affected not only the pH but there was a concomitant effect on the redox chemistry of the rock surfaces, through the changes brought about by the alteration of the surface acidity. When all the data on the chloride dependence of the redox potential it is apparent that there is a second order effect of the chloride on the voltage, for when the slopes of the plots of the E_h values against chloride is plotted as a function of the mean ^0E_h of the sites the slope falls as the redox potential at zero chloride ion rises, as shown in Figure 19.
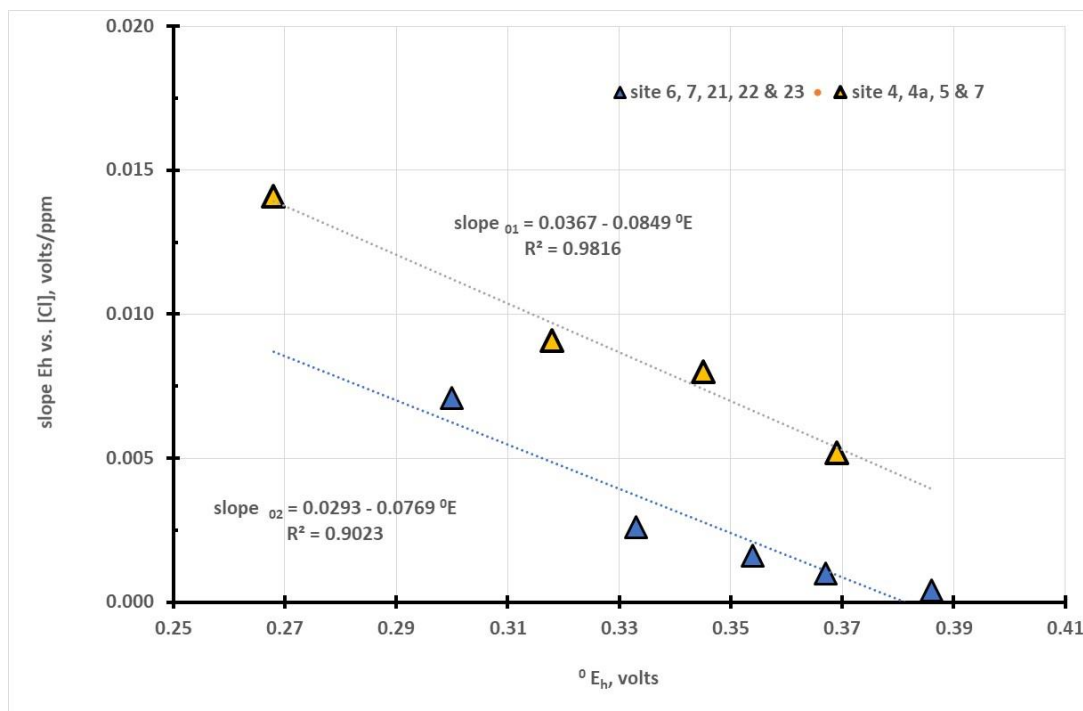
Statistical analysis of the two linear regression equations shown in Figure 19 show that the slopes of Equations 31 (0.0849 ± 0.0082) and Equation 32 (0.0779 ± 0.0146) are the same but that the intercepts of slope $_{01}$ at 0.037± 0.003 and slope $_{02}$ at 0.029 ± 0.005 are just statistically significantly different.

$$Slope_{01} = 0.0367(0.0027) - 0.0895 (0.0082)\ ^0E_h \dots\dots\dots\dots\dots\dots(31)$$
$$Slope_{02} = 0.0293(0.0051) - 0.0769 (0.0146)\ ^0E_h \dots\dots\dots\dots\dots\dots(32)$$

The sites that are grouped together by equations 31 and those collected in equation 32 are a mixture of gabbro and granophyre rocks so the differences in the response of the redox potential to chloride ion activity remains to be determined. For Equation 31 the prediction is that the redox potential becomes independent on chloride at a voltage o 0.410 volts and that for Equation 32 the voltage is much lower at +0.381 volts vs. NHE. The R^2 value for Equation 31 was 0.982 and for Equation 32 it was 0.870, which is why the slope and the intercept errors were higher.

When the slopes in Equation 31 are plotted against the mean pH of the same sites there was a strong correlation that gave rise to Equation 33 with an R^2 of 0.921, viz.

$$Slope_{01} = 0.28 (0.06) - 0.055 (0.011)\ pH_{mean} \dots\dots\dots\dots\dots\dots\dots(33)$$

For the sites covered by Equation 32 a much better fit was obtained when the slopes were plotted against the median pH as the R^2 value went from 0.754 for the mean pH to 0.903 for the median pH, as shown in Equation 34, I

$$Slope_{02} = 0.25(0.04) - 0.053 (0.008)\ pH_{median} \dots\dots\dots\dots\dots\dots\dots(34)$$

Since the values of the slopes are constant that means that there is a direct relationship between the mean pH for sites 4, 5, 6 and 21 and the ^0E_h values, so the connection is clearly related to the distribution of hydroxy species of the electrochemically active ions present on the rock surfaces. While the intercepts in Equations 31 and 32 are different they are within experimental error of each other so with the slopes of the relationships being the same, all the sites are showing a common mechanism which shows that the chloride independent E_h is directly controlled by the pH, which in turn determines the amount of hydroxy species such as $Mn(OH)^+$ which are present on the rock surfaces.

Colour measurements

Colour measurements were conducted on sites 4, 5, 6, 7, 21, 22 and 23 using the Konica-Minolta Chromameter (KMC) were made with an average of 20 independent measurements on the background and engraved surfaces at the four designated reference points. The details of the colour measurements made in 2019 have been compared with those made in 2018 and in 2017. The recommendation from Bruce Ford, of Microfading Australia, is that our sampling protocol should change as dust particles on the rock surface cause light scatter and do not allow an accurate assessment of the real colour. Colour measurements on inhomogeneous surfaces is fraught with difficulty but by rigidly applying "no change to the surface" as the sampling protocol there is little to be gained and much to be lost. In future years, a light brushing of the rock surfaces is likely to lead to improved reproducibility and the chance of being able to discern colour change.

The initial analysis of the colour differences was conducted using the methodology outlined in the CSIRO September 2008 Report (Burrup Peninsula Aboriginal Petroglyphs: Colour Change and Spectral Mineralogy 2004–2007 D. Lau, E. Ramanaidou , S. Furman , A. Hacket , M. Caccetta , M. Wells & B. McDonald). This involved using the CIE standard formula for colour difference by taking the square root of the differences between the L, a and b values recorded by the Konica Minolta Chromameter. The formula used for determining the colour difference was as noted below in Equation 35,

$$delta\ E_{97} = \{(L_b-L_e)^2 + (a_b-a_e)^2 + (b_b-b_e)^2\}^{\frac{1}{2}} \dots\dots\dots\dots\dots\dots(35)$$

In Equation 35 the subscripts after the L, a and b values relate to the *b* for the background and *e* for the engraved surfaces. Unlike the 2017 measurements there was much less dust on the rock surfaces,

and this is likely due to the heavy rainfall that took place in June 2018. However, some sites were dustier than others. Owing to uncertainties associated with the assessment of the colour difference readings on each of the six sites, both the original data and the calculated delta E values were reviewed by Bruce Ford of www.microfading.com since there have been major revisions by colour conservators regarding the evaluation of what are statistically reliable measurement of colour differences. Using the criterion that the MCDMt (total mean colour distance from the mean)/Delta E > 0.5 the sites were assessed for colour difference between the background and the engraved areas as being compliant or not.

It is noted that when the contrast between the $L^*a^*b^*$ is made between the background and the engraved areas on each measurement point and in each location, the authors erred on the side of caution and accepted that a just significant difference could, in the first instance, be regarded as being significant. For site 5 at Burrup Road the data points 5-1, 5-2 and 5-4 were all significantly different in contrast and all were still clearly showing differences from 2017 through to 2019. However, site 5-3 was not significantly different between background and engraving in 2018 but returned to "normality" in 2019 so the "cormorant" image on the rock can be regarded as being readily discernible. For site 6, the Water tanks near the Yara plant, the differences between the engraved and background areas are more problematic with site 6-1 being discernible in 2017 and 2019 but not in 2018. Sites 6-2 and 6-3 did not meet the difference criteria at any of the three annual sets of measurements and site 4 was only discernibly different in 2017, so for 2019 it is only spot 6-1 that is of any use for monitoring.

The site at Deep Gorge, site 7, had clear differences for all four spots in 2017, but only spot 3 was statistically discernible in 2018 and 2019 while spot 2 changed from No to Yes in 2019, which is perhaps due to the greater acidity associated with the readings across the large rock. For site 21, on top of the hill at Yara West, which is less than 1 km from the plant, spot 1, 3 and 4 were a Yes for discernment in 2017 through to 2019, while spot 2 changed from a No to a yes in 2018 and 2019 so this is a good site for assessment of the colour changes with changing microenvironmental conditions. For site 22, the Yara North East location, the first spot lost its discernment in 2018-2019 and spot 2 changed from Yes to No to Yes over the three-year interval. Spot 3 was OK in 2017 - 2019 but had lost its colour contrast in 2019. Spot 4 gave clear colour discernment throughout the period of review between 2017 and 2019.

Table 20: 2019 Colour differences *b-e* for each site compared with 2018 & 2017
Data highlighted in yellow have colour differences that deems them not to be significant.

site	ΔE00 2017	ΔE00 2018	ΔE00 2019	MCDM/ΔE00 2017	MCDM/ΔE00 2018	MCDMt/ΔE00 2019	Signif. 2017	Signif. 2018	Signif. 2019
S5 spot1	5.83	5.31	4.84	0.19	0.18	0.20	y	y	y
S5 spot2	6.70	5.81	6.66	0.12	0.25	0.20	y	y	y
S5 spot3	7.61	4.81	9.86	0.12	0.63	0.15	y	n	y
S5 spot4	4.15	6.45	5.78	0.12	0.15	0.18	y	y	y
S6 spot1	1.51	2.04	1.91	0.41	0.44	0.61	n	~	y
S6 spot2	1.02	2.15	0.88	0.98	0.53	2.23	n	n	n
S6 spot3	1.86	2.80	1.54	0.40	0.45	1.43	~	~	n
S6 spot4	3.10	2.33	1.83	0.26	0.51	0.78	y	n	n
S7 spot1	6.75	2.51	3.56	0.19	1.26	0.71	y	n	n
S7 spot2	3.01	2.47	3.30	0.19	1.04	0.53	y	n	~
S7 spot3	3.84	5.67	5.14	0.10	0.33	0.52	y	y	~
S7 spot4	4.60	5.50	4.40	0.13	0.40	0.66	y	~	n

site											
S21 spot1	5.34	7.99	4.62	0.08	0.99	0.28	y	y	y
S21 spot2	3.00	3.86	5.44	0.60	0.84	0.23	n	~	y
S21 spot3	5.23	4.15	3.97	0.13	0.28	0.23	y	y	y
S21 spot4	3.88	6.63	5.53	0.30	0.23	0.36	y	y	y
S22 spot1	6.63	2.56	1.02	0.05	0.99	1.20	y	n	n
S22 spot2	2.43	1.16	2.80	0.24	0.84	0.40	y	n	y
S22 spot3	4.61	3.12	2.71	0.23	0.28	1.04	y	y	n
S22 spot4	3.91	3.98	5.32	0.17	0.23	0.32	y	y	y
S23 spot1	2.17	3.47	3.32	0.34	0.50	0.49	y	~	m
S23 spot2	2.52	4.31	1.34	0.32	0.29	1.13	y	y	n
S23 spot3	6.97	3.48	1.05	0.13	0.39	1.78	y	y	n
S23 spot4	2.65	3.28	4.65	0.44	0.34	0.31	~	y	y
S4 spot 1			3.56			0.29			y
S 4 spot 2			1.91			0.83			n
S 4 spot 3			1.60			0.53			~
S 4 spot 4			1.04			1.65			n

Table 21: Comparison of delta E values between 2017, 2018 and 2019

site	ΔE change 2017–2018	MCDM (t)	MCDM (t)/ΔE	Sig.	ΔE change 2017–2019	MCDM (t)	MCDM (t)/ΔE	Sig.	ΔE change 2018 - 2019	MCDM (t)	MCDM (t)/ΔE	Sig.
S5 spot1	0.52	1.45	2.79	n	0.99	1.45	1.47	n	0.47	1.36	2.89	n
S5 spot2	0.89	1.66	1.86	n	0.04	1.57	39.20	n	-0.85	2.00	2.35	n
S5 spot3	2.80	3.19	1.14	n	-2.25	1.74	0.77	n	-5.05	3.38	0.67	n
S5 spot4	-2.30	1.08	0.47	y	-1.63	1.16	0.71	n	0.67	1.42	2.12	n
S6 spot1	-0.53	1.10	2.06	n	-0.40	1.32	3.30	n	0.13	1.47	10.90	n
S6 spot2	-1.13	1.52	1.34	n	0.14	2.21	15.93	n	1.27	2.28	1.79	n
S6 spot3	-0.94	1.46	1.56	n	0.32	2.33	7.29	n	1.26	2.54	2.02	n
S6 spot4	0.77	1.44	1.87	n	1.27	1.65	1.30	n	0.50	1.85	3.71	n
S7 spot1	4.24	3.44	0.81	n	3.19	2.84	0.89	n	-1.05	4.06	3.88	n
S7 spot2	0.54	2.62	4.82	n	-0.29	1.83	6.31	n	-0.83	3.10	3.71	n
S7 spot3	-1.83	1.91	1.05	n	-1.30	2.69	2.07	n	0.53	3.25	6.16	n
S7 spot4	-0.90	2.27	2.52	n	0.20	2.99	14.95	n	1.10	3.66	3.33	n
S21 spot1	-2.65	2.56	0.97	n	0.72	1.34	1.86	n	3.37	2.83	0.84	n
S21 spot2	-0.86	2.04	2.37	n	-2.44	2.18	0.89	n	-1.58	1.57	1.00	n
S21 spot3	1.08	1.12	1.03	n	1.26	1.14	0.91	n	0.18	1.27	7.10	n
S21 spot4	-2.75	1.49	0.54	n	-1.65	2.32	1.40	n	1.10	2.21	2.00	n
S22 spot1	4.07	2.55	0.63	n	5.61	1.26	0.23	n	1.54	2.81	1.82	n
S22 spot2	1.27	1.14	0.89	n	-0.37	1.26	3.40	n	-1.64	1.47	0.90	n

S22 spot3	**1.49**	1.39	0.93	n	**1.90**	3.02	1.59	n	**0.41**	2.95	7.19	**n**
S22 spot4	**-0.07**	1.13	17.09	n	**-1.41**	1.82	1.29	n	**-1.34**	1.94	1.44	**n**
S23 spot1	**-1.30**	1.88	1.44	n	**-1.15**	1.80	1.56	n	**0.15**	2.38	15.71	n
S23 spot2	**-1.79**	1.49	0.83	n	**1.18**	1.71	1.45	n	**2.97**	1.96	0.66	n
S23 spot3	**3.49**	1.62	0.46	y	**5.92**	2.08	0.35	y	**2.43**	2.31	0.95	n
S23 spot4	**-0.63**	1.62	2.55	n	**-2.00**	1.83	0.92	n	**-1.37**	1.81	1.33	n
S4 spot 1									-3.56	1.04	0.29	y
S 4 spot 2									-1.91	1.58	0.83	n
S 4 spot 3									-1.60	0.85	0.53	~
S 4 spot 4									-1.04	1.72	1.65	n

The data from site 23, Yara East, had spot 1 remained discernible through the three seasons, spot 2 & 3 went from Yes, to Yes to No while spot 4 was no good in 2017 but became better in 2018 and 2019, which correlates with an increase in acidity. When all the data in Table 21 are reviewed it is clear (highlighted in yellow) that only site 5, spot 4 for 2017-2019 showed a real difference in colour and that Site 23 spot 3 had real colour differences in 2017-2018 and again in 2019-2017. Finally, there was a real colour difference at Site 4 spot 1 between the 2018 and 2019 measurements.

When the mean colour changes for the sites, where there was real discernment of the differences between the engraving and the background material, there was a clear relationship between the mean surface pH and the colour difference, as shown in Figure 20. There was one relationship, given by Equation 36, which showed that the colour differences were directly related to the mean pH of the site and so with less acidity the differences become increasingly difficult to discern.

$$\text{Delta E (background -engraving)} = 64 - 13\, pH \dots\dots\dots\dots\dots\dots\dots(36)$$

The regression analysis with an R^2 of 0.8998 gave an error of ± 14 in the intercept and a slope error of ± 3.1 which makes the two slopes (-11 and -13 pH experimentally the same).
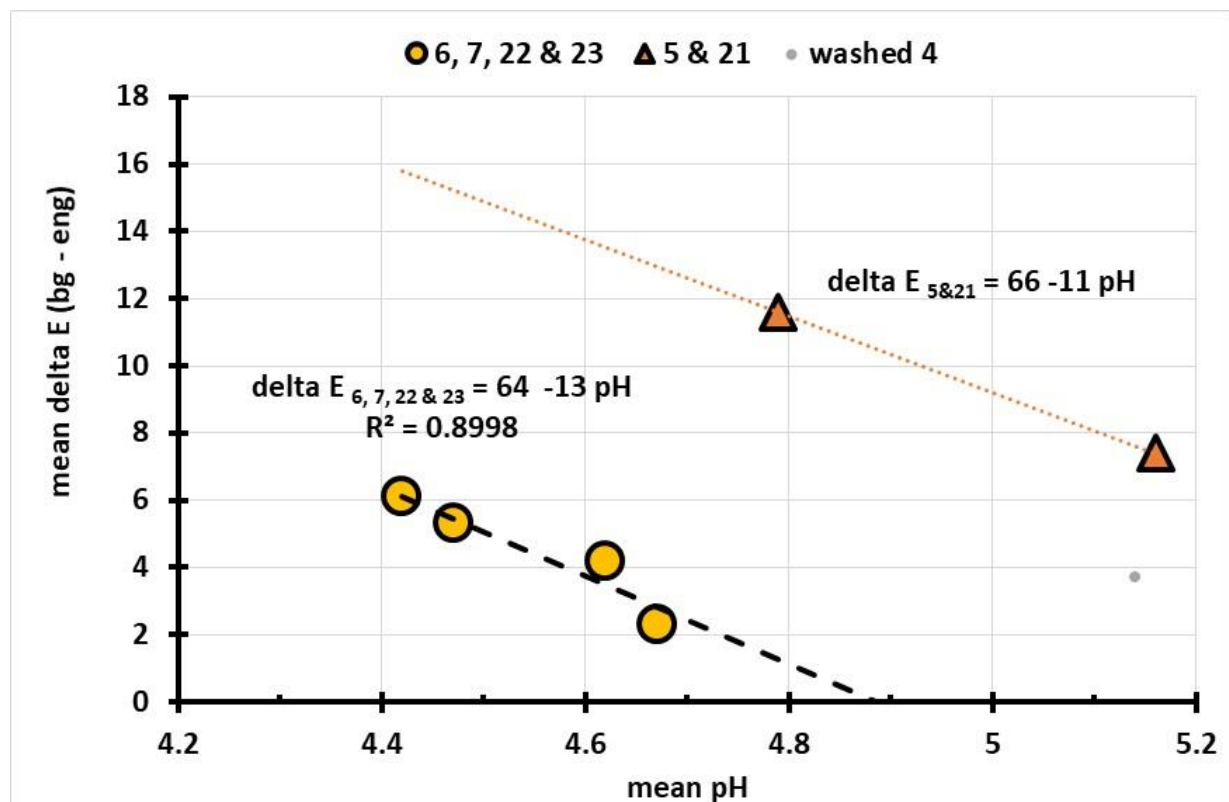
Figure 20: Plot of delta E (background – engraving) vs. mean pH values in 2019.

In essence it can be stated that the way in which at times the colour differences are real and then they "disappear" is entirely consistent with the CSIRO reports. From our three years of detailed examination of the rock surfaces it is apparent that a complex series of mineral formation and dissolution reactions take place at the rock surface. The main determinant of the mobilisation and the precipitation reactions is the availability of moisture (water) and the ambient acidity. There are clear indications that the amount of colour contrast is dependent on the nitrate ion concentration which in turn affects microbiological metabolic rates and the formation of acidic metabolites.

All the colour measurements from 2019 (median values of the 20 measurements on each point on each spot on each site) are summarised in Appendix X. In this tabular form it becomes clear as to why some of the measurements have to be rejected as the moving of the sensing head 20 times to a different spot over the rough rock surfaces meant that at times the engraving was lost or the background merged into the engraved area. These issues represent inherent weaknesses in the original colour method. The sites under concern were site 4 spot 3 and spot 4, site 6 spot 2, site 22 spot 1 and site 23 spots 2 and 3.

Conclusion

The analysis of the relationship between the pH and the amount of metal ions reporting to the wash solutions enabled the mechanisms controlling the release of manganese containing minerals to the wash solutions to be determined. From a combination of the Pourbaix diagrams and the regression analyses of the voltages extrapolated to zero pH, the formal redox voltages of the electroactive species could be obtained. In all but one site, the dominant minerals were manganese related materials. The only site where the redox potential involved iron was on site 4, the large goanna site near the Withnell Bay Road north, which had redox potentials associated with the activity of the Fe^{3+}/Fe^{2+} couple. The redox data combined with the pH has confirmed that manganese exists in a range of oxidation states on the rock surface and this will be a controlling factor in the rock patination. The re-examination of the data obtained from the previous studies indicates that this change of mechanism for the release of manganese ions into the wash appears to be subtly controlled by the alkalinity associated with increased salt deposits.

Analysis of the relationships between the surface pH and the ions associated with wind borne sea salts has shown that it is most likely that calcium is reporting to solution through the formation of a mixture of calcium carbonate dissolving to produce either free Ca^{2+} ions or the soluble calcium bicarbonate. Increasing chloride ion concentration is an indicator of increasing deposition of sea salts on the rock surfaces. One major effect of the increased salts is that it produces a buffering effect and appears to be inhibiting the activity of micro-organisms associated with the metabolism of nitrogen (nitrate) containing species found on the rock surfaces. Owing to the lack of rain there is a limited amount of data obtained from the three monitoring stations but the information shows that during the last 12 months there has been no NO_x spike in airborne contamination and that the amount of nitrogen oxides in the environment is constant, which is consistent with it coming from other industries in the local area of the Burrup. The impact of seven major cyclonic downpours between February 2003 and March 2017 has been previously reported and these events, combined with changes in local industries changing to ceramic lined burners for power sources, has significantly reduced the amount of soluble nitrate being biologically available. There has been either a steady mean pH at the sites, such as at Yara East (no 23) and Burrup Road West (no 5) and significant acidification at sites 22, 21, 7, 6 and the Climbing Man. The odd one out was site 4 which went more alkaline with a delta pH of 0.86 or seven times less acidic.

For the six sites examined in and around the Yara facility there is a decreased amount of sulphate ions than cannot be explained by the increased presence of sea salts. The mean sulphate in 2017 was 5.2 ± 3.0 which decreased to a value of 1.2 ± 0.7 ppm in 2018 and it was 4.5 ± 6.4 ppm in 2019. The maximum concentration was 19 ppm on top of site 21 and other high-value sulphate wash sites included Deep Gorge at 7.4 and 6.8 ppm at site 5 at Burrup Road west. These three sites are aligned with the NW direction which indicates that the extra source of sulphate is associated with the export trade of the iron ore shipments. The impact of the extra sulphate burden on the rocks is not known at present but polyvalent anions increase the amount of localised precipitation of minerals through the common ion effect.

The response of the rock surface pH to soluble nitrates in the washings was complex. For sites 5 (Burrup Road West), 21 (Burrup West) and site 22 (Yara NE) the pH of the rocks increased with nitrates and this is believed to be due to ammonia absorption controlling the pH (making it more alkaline and so neutralising the effect of microbiological activity). For the Climbing Man and sites 7 (Deep Gorge) and site 23 (Yara East) there was a linear decrease in the pH (increasing acidity) with increasing nitrate concentration in the surface washings. For the Climbing Man site, the pH fell by almost 1.6 compared with the values in 2018. A similar significant change in pH of 1.15 for the Deep Gorge site happened between 2018 and 2019 while the change at Yara East was less dramatic at a fall of 0.36 or 2.3 times more acidic. Given that the airborne nitrate concentration remains much the same over the past three

years the increasing acidity on several sites is dominated by the lack of rain to "re-set" the acidity clock. Given the lack of industrial activity from the TAN plant by Pilbara Fertilisers over the past year there is little evidence to support the supposition that Yara operations has had any negative impact on the rock surfaces.

REFERENCES

Arthur, I, 2004, Report on the identification of yeasts and moulds from rocks in the Burrup, Mycology, Department of Health Laboratories, Western Australia, Unpublished report, 1-6.

Burford, E P, Fomina, M and Gadd, G M, 2003, Fungal involvement in bioweathering and biotransformation of rocks and minerals, *Mineralogical Magazine* 67 (6), 1127–1155.

Clark, R, 2004, Identification of surface minerals in weathered rocks from the Burrup peninsula, unpublished report to the Burrup Rock Art Monitoring Scientific Committee, November 2004, 1–18.

Gadd, G M, 2004, 'Mycotransformation of organic and inorganic substrates', *Mycologist* 18 (2), 60–70.

Lau, D, Ramanaidou E., Furman, S., Hacket A., Caccetta M., Wells M., McDonald B., 2008, *Burrup Peninsula Aboriginal Petroglyphs: Colour Change and Spectral Mineralogy 2004–2007*, CSIRO Materials Science and Engineering, Clayton, Victoria, Australia, 1-44.

King, J, 2003, Report on the identification of bacteria, yeasts, moulds and fungi in the Burrup, unpublished report, Department of Agriculture, Perth, Western Australia.

MacLeod, I D, 2003, A micro-environmental study of rocks on the Burrup: effects of water and nutrients on pH and microflora, unpublished report, Western Australian Museum, 1–66.

MacLeod, I.D., 2017, Report to the Murujuga Aboriginal Corporation; Impact of industrial emissions on the pH and Eh of engraved rock art on the Burrup peninsula", Unpublished report of Heritage Conservation Solutions, pp 1-17.

MacLeod, I.D., and Fish, W.S., 2018, Surface chemistry of Burrup Rock art at the Yara monitoring sites, Unpublished report for Yara Pilbara Nitrates, pp 1-58.

Markley T., Wells M., Ramanaidou E., Lau D. and Alexander D., 2015, Burrup Peninsula Aboriginal Petroglyphs: Colour Change & Spectral Mineralogy 2004–2014, CSIRO report, EP1410003 October 2015, 1-189.

North, N A, 1982, Corrosion products on marine iron, *Studies in Conservation* 27, 75–83.

Pourbaix, M., 1974, *Atlas of electrochemical equilibria in aqueous solutions,* National Association of Corrosion Engineers, Houston, Texas USA pp 1-644.

Ramanaidou E., Walton G. and Winchester D., 2017, Extreme Weathering Experiments on the Burrup Peninsula / Murujuga Weathered gabbros and granophyres, EP172193 May 2017, 1-62.

APPENDIX I: MacLeod publications on rock art conservation

Refereed journal articles

Haydock, P. & MacLeod, I.D. (1987) "The use of micro-meteorological studies as an aid to the conservation of aboriginal rock art". *ICOM Committee for Conservation*, Sydney, September 1987, p 1149-1153.

MacLeod, I.D. (1991) "Microclimate modelling in old museum buildings". *Historic Environment-Conservation in Context: Artefact and Place,* 8(1&2), p 37-41

Ford, B., MacLeod, I.D., and Haydock, P., (1994) "Rock art pigments from the Kimberley region of Western Australia: identification of the minerals and conversion mechanisms", *Studies in Conservation* 39, p 57-69.

MacLeod, I.D., Haydock, P., Tulloch, D. & Ford, B. (1995) "Effects of microbiological activity on the conservation of aboriginal rock art" *AICCM Bulletin* 21(1), 3-10

MacLeod, I.D., Haydock, P & Charton, E., (1996) "Avian guano and its effects on the preservation of rock paintings" *Preservation of Rock Art 1995 AURA Occasional Papers 9*, Ed. Andrew Thorn & Jacques Brunet p 60-64.

MacLeod, I.D., Haydock P. and Ford, B. (1997) "Conservation Management of West Kimberley Rock Art: Microclimate studies and Decay Mechanisms" *Kimberley Society Occasional Paper No 1. Aboriginal Rock Art of the Kimberley* Ed K.F. Kenneally, M.R. Lewis., M. Donaldson and C. Clement, Kimberley Society Inc, Perth, Western Australia. pp 65-69.

MacLeod, I.D., (2000) "Rock art conservation and management: the past, present and future options", *Reviews in Conservation,* 1, pp 32-45.

MacLeod, I.D., and Haydock, P., (2002) "Microclimate modelling for prediction of environmental conditions within rock art shelters", Preprints for ICOM-CC Triennial Meeting, Rio de Janeiro, Brazil September 2002, Vol II, 571-577.

MacLeod, I.D. (2005) "The effects of moisture, micronutrient supplies and microbiological activity on the surface pH of rocks in the Burrup peninsula", Preprints for ICOM-CC Triennial Meeting, Den Haag, The Netherlands, September 2005, Vol II 386-393

Black, J., MacLeod I.D., and Smith, B., (2017), Theoretical effects of industrial emissions on colour change at rock art sites on Burrup Peninsula, *J Archaeological Science*: *Reports* 12, 457-462.

Unpublished Reports

MacLeod, I.D., Haydock, P. and Ford, B (1991)- "Conservation research into the preservation of rock paintings in the West Kimberley region of Western Australia", Report to the Western Australian Heritage Committee, pp 1-89

MacLeod, I.D., Haydock, P & Charton, E., (1992) "The effects of avian guano on the preservation at *Walga Rock*". Report to the Australian Institute of Aboriginal and Torres Strait Islanders Studies, Canberra, pp 1-45.

MacLeod, I.D., Haydock, P and Ford, B (1994) *Conservation research into the preservation of rock paintings in the West Kimberley Region of Western Australia: Wet Season Report*. Report to the Heritage Council of WA, March 1994, pp-143.

MacLeod, I.D. and Haydock, P., (1996) *Research into the Conservation or rock paintings in the West Kimberley: Microclimate data analysis* Report to AIATSIS, May 1996, pp 1-132

Ford, B., Officer, K. and MacLeod, I.D., (1999) *A study of lichen invasion of Nursery Swamp II, Aboriginal Rock Art Site, Namadji National Park, Australian Capital Territory, Final Report May 1999*, Australian Capital Territory National Parks Association, Canberra 1999, pp. 1-28.

MacLeod, I.D., (2003) "The microenvironment of rocks on the Burrup: analysis of the relationships between nutrient supplies, surface pH and microflora – preliminary report, Report to the Minister of Culture and the Arts, pp 1-55.

MacLeod, I.D., (2017), "Report to the Murujuga Aboriginal Corporation; Impact of industrial emissions on the pH and Eh of engraved rock art on the Burrup peninsula", pp 1-17.

APPENDIX II: Chemical analysis of the wash solutions from the CSIRO monitoring sites August 2019.

Concentrations are in mg/L other than electrical conductivity which is in mS/m
Report no 19S0831

Name	Deep Gorge	Site 6 - Water Tanks	Site 22	Site 23	Site 5	Site 21	Site 4	Site 4a	Climbing Man
Sampled	'19 August	'19 August	'20 August	'20 August	'20 August	'21 August	'21 August	'21 August	'21 August
Al	0.014					0.022		0.053	
B	0.009								
Ba	0.0062	0.0013	0.0014	0.002	0.0094	0.0091	0.0009	0.005	0.001
Ca	2.5	0.7	0.5	1.8	1.4	3.5	0.2	1.2	0.3
Cl	17	1.7	2.1	3.7	19	82	0.9	4.5	3.1
Co	0.0001				0.0002			0.0004	
Cr	0.0006								
Cu	0.0011	0.0007	0.001	0.0006	0.0008	0.0014	0.0004	0.0015	0.0006
E. Cond.	12.7	1.6	1	2.4	9.2	35	0.5	3	1.6
Fe	0.025					0.033		0.063	
K	0.6	0.3	0.5	0.6	0.5	1.3	0.3	0.5	0.8
Mg	0.9			0.5	0.6	2.8		0.4	
Mn	0.018	0.0043	0.005	0.0055	0.012	0.011	0.0014	0.042	0.0017
NO$_3$	2.1	1	0.17	0.24	0.57	0.43		0.99	0.15
Na	4.4	1.3	1.3	3.8	6.1	28.9	0.8	4.5	2.1
S	1.3	0.2	0.1	1.2	1.5	3.6	0.2	1.6	0.1
SO$_4$	7.4	0.8	0.4	1.9	6.8	19.1	0.4	3.4	0.7
V	0.0003			0.0001	0.0002	0.0002		0.0005	
Zn	0.006	0.002	0.003	0.002	0.01	0.014	0.003	0.004	0.008

Sample volumes for the metal ion analyses were 200 ml and for the anions the volume was 100 ml
Samples were collected on the same rocks and stored in different containers which were kept cool with ice-bricks

APPENDIX III: Chemical analysis of the wash solutions from the CSIRO monitoring sites September 2018.

Concentrations are in mg/L other than electrical conductivity which is in mS/m
Report 18S0974

Chem Centre Id	Method Code	18S0974 /001	18S0974 /002	18S0974 /007	18S0974 /003	18S0974 /004	18S0974 /005	18S0974 /006
		Site 4	Site 5	Site 6	Site 7	Site 21	Site 22	Site 23
		7/09/18	4/09/18	3/09/18	4/09/18	5/09/18	5/09/18	6/09/18
Al	ICP	<0.005	<0.005	0.009	<0.005	<0.005	<0.005	<0.005
As	WCMS	<0.001	<0.001	<0.001	<0.001	<0.001	<0.001	<0.001
B	WCMS	<0.005	<0.005	0.007	<0.005	<0.005	<0.005	<0.005
Ba	WCMS	0.0019	0.0012	0.0023	0.0021	0.0024	0.0009	0.0011
Ca	ICP	0.9	0.3	2.2	0.9	0.7	0.2	0.4
Cd	WCMS	<0.0001	<0.0001	<0.0001	<0.0001	<0.0001	<0.0001	<0.0001
Cl	IC	1.3	2.1	2.2	2.5	5.4	1.8	1.8
Co	WCMS	<0.0001	<0.0001	<0.0001	<0.0001	<0.0001	<0.0001	<0.0001
Cr	WCMS	<0.0005	<0.0005	<0.0005	<0.0005	<0.0005	<0.0005	<0.0005
Cu	WCMS	0.0008	0.0012	0.0017	0.0009	0.0014	0.0011	0.0013
E.Cond.	WZSE	1.6	1.6	2.5	1.9	4	1.7	1.2
Fe	ICP	<0.005	<0.005	<0.005	<0.005	<0.005	<0.005	<0.005
K	ICP	0.7	0.8	0.3	0.4	0.5	2.1	0.6
Mg	ICP	0.1	<0.1	0.2	0.2	0.4	<0.1	<0.1
Mn	WCMS	0.0024	0.0013	0.0006	0.0041	0.0014	0.001	0.0014
NO2	WFIA	<0.1	<0.1	<0.1	<0.1	<0.1	<0.1	<0.1
NO3	WFIA	0.54	0.32	0.89	0.75	1.4	1	0.19
Na	ICP	1	1.5	1.6	1.4	5.3	1.1	1.2
Ni	WCMS	<0.001	<0.001	<0.001	<0.001	<0.001	<0.001	<0.001
Oxalate	IC	<0.2	<0.2	<0.2	<0.2	<0.2	<0.2	<0.2
Pb	WCMS	0.0001	<0.0001	<0.0001	<0.0001	<0.0001	<0.0001	0.0002
S	WCICP	0.7	0.3	0.7	0.4	0.6	0.1	0.2
SO4	IC	2	0.8	2.2	1.2	1.6	0.3	0.5
V	WCMS	0.0002	<0.0001	0.0002	0.0001	<0.0001	<0.0001	<0.0001
Zn	WCMS	0.003	0.006	<0.001	<0.001	0.006	0.005	0.002

Sample volumes for the metal ion analyses were 200 ml and for the anions the volume was 100 ml
Samples were collected on the same rocks and stored in different containers which were kept cool with ice-bricks

APPENDIX IV: Chemical analysis of the wash solutions from the CSIRO monitoring sites November 2017.

Concentrations are in mg/L other than electrical conductivity which is in mS/m

Report dated 7 December 2017

ChemCentre Id	Method Code	Limits of Reporting	17S2175-002	17S2175-001	17S2175-004	17S2175-005	17S2175-006	17S2175-003	17S2175-007
Client Id			Site 5	Site 6	Site 7	Site 21	Site 22	Site 23	Blank
Sampled			21/11/2017	20/11/2017	22/11/2017	22/11/2017	23/11/2017	21/11/2017	24/11/2017
Al	iMET1WCICP	0.005	<0.005	0.016	0.007	0.009	0.006	0.019	<0.005
As	iMET1WCMS	0.001	<0.001	<0.001	<0.001	<0.001	<0.001	<0.001	<0.001
B	iMET1WCMS	0.005	<0.005	0.008	<0.005	<0.005	<0.005	<0.005	<0.005
Ba	iMET1WCMS	0.0001	0.0061	0.011	0.0043	0.0097	0.0024	0.0064	0.0004
Ca	iMET1WCICP	0.1	1.1	11.5	3.2	2.5	0.5	5	0.1
Cd	iMET1WCMS	0.0001	<0.0001	<0.0001	<0.0001	<0.0001	<0.0001	<0.0001	<0.0001
Cl	iANIO1WAIC	0.5	3.2	5.3	3.9	7.4	3.3	13	<0.5
Co	iMET1WCMS	0.0001	<0.0001	<0.0001	<0.0001	<0.0001	<0.0001	<0.0001	<0.0001
Cr	iMET1WCMS	0.0005	<0.0005	<0.0005	<0.0005	<0.0005	<0.0005	<0.0005	<0.0005
Cu	iMET1WCMS	0.0001	0.0066	0.0016	0.0007	0.017	0.001	0.0021	0.0023
E Cond	iEC1WZSE	0.2	1.6	12.2	3.1	5.2	0.8	7.6	<0.2
Fe	iMET1WCICP	0.005	<0.005	0.012	0.008	0.011	0.005	0.01	<0.005
K	iMET1WCICP	0.1	0.5	0.6	0.4	1	0.2	0.7	0.2
Mg	iMET1WCICP	0.1	0.1	0.7	0.5	0.7	<0.1	0.6	<0.1
Mn	iMET1WCMS	0.0001	0.0026	0.0038	0.0051	0.006	0.0011	0.0009	0.0003
NO2	iNTR1WFIA	0.1	<0.1	<0.1	<0.1	<0.1	<0.1	<0.1	<0.1
NO3	iNTA1WFIA	0.05	0.25	0.46	0.38	1.9	1.1	0.22	0.15
Na	iMET1WCICP	0.1	1.2	7.2	1.6	5.2	1.4	9.3	0.3
Ni	iMET1WCMS	0.001	<0.001	<0.001	<0.001	<0.001	<0.001	<0.001	<0.001
Oxalate	iANIO1WAIC	0.1	<0.1	<0.1	<0.1	<0.1	<0.1	<0.1	
Pb	iMET1WCMS	0.0001	<0.0001	<0.0001	<0.0001	<0.0001	<0.0001	<0.0001	<0.0001
S	iMET1WCICP	0.1	1	2.6	2	2.5	0.3	3.2	<0.1
SO4	iANIO1WAIC	0.1	2.8	4.2	5.8	7.1	1.5	9.8	<0.1
V	iMET1WCMS	0.0001	0.0003	0.0006	0.0004	0.0004	0.0002	0.0006	<0.0001
Zn	iMET1WCMS	0.001	0.008	0.009	0.003	0.01	0.004	0.004	0.004

Sample volumes for the metal ion analyses were 200 ml and for the anions the volume was 100 ml
Samples were collected on the same rocks and stored in different containers which were kept cool with ice-bricks

APPENDIX V: Acidity and chlorinity measurements at the CSIRO monitoring sites November 2017

Site 6: Water Tanks   **20-Nov-17**

Location	pH	Cl ppm
1	5.61	134
2	5.72	195
3	5.83	
4	5.33	
5	5.85	
6	5.54	108
7	5.85	326
8	5.81	
9	5.28	
10	5.80	
mean	**5.66**	**191**
stdev	**0.22**	**97**

RH   49.9%

T air   31.4

T surface   45.9

T dew point   19.6

Date   21/11/2017

Site 5: Location off Burrup road

location	pH	Cl ppm
1	6.04	55
2	5.79	28
3	5.7	12
4	5.75	30
5	5.17	24
6	5.19	22
7	5.06	106
8	4.37	10
9	4.36	18
10	4.82	4.2
11	4.57	40
mean	**5.17**	**32**
stdev	**0.60**	**28**

Latitude   -20.62109

Longitude   116.76925

Time	07:15	08:45
RH	77%	42%
T air	23.7	34
T surface	25.7	32
T dew	19.2	
Ts-Td	8.4	

Location	pH	Cl ppm
1	5.68	4.5
2	5.75	6.2
3	5.62	15
4	4.45	55
5	5.49	8
6	6.39	42
7	4.42	26
8	5.47	6
9	5.76	6
10	5.93	16
mean pH	**5.50**	**18**
stdev pH	**0.62**	**17**

Site 23
Yara East
21/11/2017

	-
Latitude	20.6229
Longitude	116.797
Time	09:30
RH	37.3
T air	34.9
T surface	34.2
T dew	17.3
Ts-Td	17.6

Site 7 Deep Gorge

location	pH	Cl ppm
1	6.21	35
2	5.16	
3	5.53	32
4	5.93	30
5	4.92	
6	5.29	7.2
7	5.43	30
8	5.57	
9	5.3	12
10	5.9	34
11	5.32	
12	5.58	9
13	5.9	18
14	6.41	
15	5.09	8.2
mean pH	**5.57**	**22**
stdev pH	**0.42**	**12**

Date	**22-Nov-17**
Latitude	-20.63722
Longitude	116.78831
Time started	06:30
Time finished	08:30
Relative humidity	40.40%
Temperature air	31.4
Temperature surface	37.8
Temperature dew pt.	17
Ts-Td	21.3

Location no Site 21 Yara West **Date of measurements** **22-Nov-17**

Location	pH	Cl ppm
1	7.29	214
2	6.91	132
3	6.35	140
4	6.52	90
5	6.39	88
6	6.56	140
7	6.49	214
8	5.78	165
9	5.98	125
10	5.98	120
mean	6.43	143
stdev	0.45	44

Time of initiation   09:45

T air   38.6
T rock   38.8
T dew   11.3
Ts -Td   26

Site 22 **Date 23/11/2017**

Location	pH	Cl ppm
1	6.58	26.5
2	6.42	14.5
3	6.42	27.6
4	6.16	97
5	6.49	21
6	5.43	46
7	6.59	36
8	5.34	14.6
9	6.42	24
10	5.74	26
mean	6.16	33
stdev	0.48	24

Latitude   -20.6176
Longitude   116.7996

	Begin	End
Relative humidity	86.80%	15.20%
Temperature air	26.5	43.7
Temperature rock	30.8	33
T dew point	24.4	
Ts-Td	5.2	

APPENDIX VI: Acidity, chlorinity and redox measurements September 2018

Site 4: Woodside 35% RH, air 24.3º & rock 26.8º 7 Sept. 18

location no	pH	Cl	E vs Ag/AgCl
1	7.28	1.5	0.265
2	6.65	1.3	0.278
3	6.76	1.5	0.269
4	5.42	1.1	0.311
5	5.34	1.8	0.281
6	6.23	1.3	0.283
7	6.02	4.2	0.287
8	5.34	1.4	0.284
9	4.94	0.8	0.283
10	4.64	6.7	0.291
11	4.47	0.75	0.267
12	4.42	0.45	0.29
13	4.95	2.54	0.29
14	5.93	7	0.278
15	4.38	0.5	0.287
average	5.52	2.2	0.283
stdev	0.92	2.1	0.011

Site 5: Burrup Road 27% RH, air 33.2º, rock 39.5º 4 September 2018

location	pH	Cl ppm	E vs AgCl
1	3.97	14	0.254
2	4.65	1.4	0.256
3	4.66	1.88	0.256
4	4.88	4.59	0.259
5	5.58	2.7	0.259
6	5.15	3.8	0.269
7	5.41	4.1	0.271
8	5.33	3.1	0.273
9	5.18	2.65	0.251
10	4.87	3	0.274
11	5.17	6.9	0.283
12	4.87	1.2	0.277
mean	**4.98**	**4.1**	**0.265**
stdev	**0.43**	**3.5**	**0.011**

Site 6 on 3 September 2018

Reference no	pH	Cl	E V vs AgCl
1	6.11	0.76	0.156
2	6.08	1.7	0.173
3	6.38	1.15	0.193
4	6.09	1.8	0.175
5	5.52	0.34	0.186
6	6.40	0.9	0.208
7	6.37	0.41	0.201
8	6.37	1.22	0.201
9	6.27	6.9	0.201
10 a	4.70	1.51	0.215
10 b	4.70	11.6	0.224
10 c	4.70	0.82	
11	6.36	1.33	
Average	5.85	2.34	0.194
Stdev	0.70	3.24	0.020

Site 7: Deep Gorge, air 08:45 25.7°, rock 33.2° 4 September

Location ref	pH	Cl	E vs Ag/AgCl
1	7.02	17	0.231
2	7.02	37	0.216
3	7.20	18	0.178
4	6.40	14	0.23
5	6.20	15.6	0.202
6	6.66	14.6	0.23
7	6.68	25.3	0.243
8	6.06	18.6	0.260
9	6.53	17.6	0.258
10	7.04	8.2	0.221
average	6.68	18.6	0.227
stdev	0.39	7.8	0.025

Site 21: 5 Sept. 18 RH 25%, air 25.7º rock 29º

Location no	pH	Cl	E vs. Ag/Ag Cl
1	6.93	26	0.28
2	6.29	27.2	0.275
3	6.37	21	0.279
4	6.15	15.5	0.282
5	6.63	9.7	0.282
6	5.7	30	0.27
7	5.63	22	0.289
8	6.01	10.4	0.287
9	4.96	1.4	0.287
10	5.36	46.5	0.288
11	5.38	0.9	0.291
12	4.86	30.9	0.292
13	5.21	15	0.297
Average	5.81	19.7	0.285
stdev	0.65	12.8	0.007

site 22 Yara North East
5 September 18 RH
30%, rock 40º air 35º C

Location no	pH	Cl	E vs. Ag/Ag Cl
1	7.31	10.1	0.256
2	6.51	2.07	0.286
3	6.5	41	0.293
4	6.33	13.5	0.289
5	5.82	8.5	0.298
6	5.85	2.7	0.296
7	5.75	12.4	0.3
8	5.6	5.43	0.299
9	5.68	12.1	0.297
10	5.3	1.4	0.284
11	5.76	2.9	0.289
Mean	6.04	10.2	0.290
Stdev	0.57	11.2	0.012

Site 23: 6 Sept 2018 RH 22%, Temperature rock 35.9º, air 31.3º

Location no	pH	Cl	E vs. Ag/Ag Cl
1	5.59	53	0.264
2	5.25	27.5	0.272
3	4.75	55	0.281
4	4.5	23.6	0.289
5	4.36	26.4	0.293
6	4.4	65.2	0.294
7	4.63	40	0.278
8	4.16	17.2	0.287
9	4.37	28.5	0.238
10	4.37	17.5	0.285
11	6.31	11.5	0.282
12	4.63	11.7	0.287
13	5.48	14.5	0.295
14		22.9	0.306
mean	4.83	29.6	0.282
stdev	0.64	17.2	0.016

Climbing Man 22 August 2019

Climbing Man below main panel	pH	Cl ppm
Mean	4.62	14.4
Standard Error	0.05	3.0
Median	4.59	12.2
Mode	#N/A	4.6
Standard Deviation	0.16	10.5
Sample Variance	0.03	110.1
Kurtosis	0.41	2.1
Skewness	0.58	1.3
Range	0.56	35.5
Minimum	4.4	4.6
Maximum	4.96	40.1
Count	12	12

Climbing Man itself, just the pH due to safety risks
22 August 2019: Measurements ran left to right 1-5, then down approx. 12 cm for 6-10 then another 12 cm down for 11-15 going left to right.

	pH
Mean	4.36
Standard Error	0.13
Median	4.28
Mode	#N/A
Standard Deviation	0.50
Sample Variance	0.25
Kurtosis	0.08
Skewness	0.59
Range	1.78
Minimum	3.64
Maximum	5.42
Count	15

Site 4 North Withnell Bay Road

	pH	Cl	E NHE
Mean	5.14	4.9	0.397
Standard Error	0.04	0.6	0.004
Median	5.20	4.6	0.396
Mode	5.21	3.5	0.386
Standard Deviation	0.14	2.0	0.014
Sample Variance	0.02	4.0	0.000
Kurtosis	-0.75	5.2	0.692
Skewness	-0.59	2.0	0.099
Range	0.46	7.4	0.052
Minimum	4.86	3.0	0.370
Maximum	5.32	10.4	0.422
Count	12	12	12

site 4a, the rock 5 metres towards road from site 4, 22 August 2019

	pH	Cl ppm	E NHE
Mean	4.43	4.4	0.392
Standard Error	0.10	0.5	0.004
Median	4.48	3.8	0.389
Mode	4.48	2.8	0.376
Standard Deviation	0.35	1.9	0.015
Sample Variance	0.12	3.6	0.000
Kurtosis	-0.97	0.8	-2.028
Skewness	-0.33	1.3	0.162
Range	1.12	5.9	0.037
Minimum	3.83	2.6	0.375
Maximum	4.95	8.5	0.412
Count	12	12	12

site 5 Burrup Road West 20 August 2019

	pH	Cl ppm	E NHE
Mean	4.79	6.3	0.391
Standard Error	0.05	0.8	0.011
Median	4.72	5.8	0.394
Mode	4.72	4.6	0.377
Standard Deviation	0.17	2.5	0.038
Sample Variance	0.03	6.2	0.001
Kurtosis	0.27	5.5	0.149
Skewness	1.20	2.2	-0.525
Range	0.49	8.6	0.131
Minimum	4.63	4.4	0.318
Maximum	5.12	13	0.449
Number	11	11	11

Water Tanks, Site 6, 19 August 2019

	pH	Cl ppm	E NHE
Mean	4.67	9.7	0.391
Standard Error	0.05	1.8	0.005
Median	4.64	8.5	0.390
Mode	4.59	#N/A	#N/A
Standard Deviation	0.18	6.3	0.017
Sample Variance	0.03	39.7	0.000
Kurtosis	-0.97	1.4	-1.204
Skewness	0.39	1.3	0.314
Range	0.58	21	0.050
Minimum	4.43	3	0.369
Maximum	5.01	24	0.419
Count	12	12	12

Deep Gorge site 7, 19 August 2019

Deep Gorge site 7	pH	Cl	Eh
Mean	4.42	8.6	0.368
Standard Error	0.13	1.1	0.006
Median	4.52	7.2	0.366
Mode	#N/A	6.9	0.355
Standard Deviation	0.44	3.8	0.020
Sample Variance	0.19	14.7	0.000
Kurtosis	3.40	1.2	-1.083
Skewness	-1.5	1.3	0.245
Range	1.67	13	0.061
Minimum	3.31	4.3	0.339
Maximum	4.98	17.3	0.400
Count	12	12	12

Site 21, Yara West, 21 August 2019

	pH	Cl ppm	E NHE
Mean	5.16	95	0.369
Standard Error	0.09	20	0.005
Median	5.21	68	0.369
Mode	5.21	25	#N/A
Standard Deviation	0.30	70	0.018
Sample Variance	0.09	4918	0.000
Kurtosis	0.04	1	0.369
Skewness	-0.78	1	0.501
Range	0.97	225	0.066
Minimum	4.60	25	0.340
Maximum	5.57	250	0.406
Sum	61.93	1140	4.432
Count	12	12	12

Site 22, Yara North East
Sampled on 20 August 2019

	pH	*Cl*	*Eh*
Mean	4.62	30.3	0.382
Standard Error	0.03	1.4	0.005
Median	4.61	30.0	0.387
Mode	4.55	33.0	0.388
Standard Deviation	0.10	4.9	0.018
Sample Variance	0.01	24.4	0.000
Kurtosis	2.64	0.0	-0.197
Skewness	1.26	-0.1	-0.787
Range	0.37	18.0	0.059
Minimum	4.48	21	0.348
Maximum	4.85	39	0.407
Count	12	12	12

Site 23: Yara East, sampled 20 August 2019

	pH	Cl	Eh
Mean	4.47	30.4	0.397
Standard Error	0.08	2.8	0.006
Median	4.60	30.0	0.395
Mode	4.62	32.0	0.395
Standard Deviation	0.28	9.7	0.019
Sample Variance	0.08	94.4	0.000
Kurtosis	1.95	4.4	-0.221
Skewness	-1.63	1.6	-0.138
Range	0.91	40	0.064
Minimum	3.8	16	0.361
Maximum	4.71	56	0.425
Count	12	12	12

APPENDIX VIII: Surface pH measurements 2003-2004 in the Burrup

	17-Jun-03	28-Aug-03	23-Feb-04	
Location		pH	pH	
Dampier W1		5.03	4.90	
Dampier W1		4.85	4.82	
Dampier W1		5.14	4.77	
Dampier W1		5.13	5.18	
Dampier W1		4.61	4.47	
Dampier W1		4.95	4.59	
Dampier W1		4.37	4.80	
Dampier W1		4.10	4.88	
Dampier W1		4.49	4.76	
Dampier W1			4.71	
Dampier W1			4.64	
Dampier W1 mean		**4.74**	**4.77**	
Dampier W1 st. dev.		**0.37**	**0.19**	
Dampier W2		4.30	4.41	
Dampier W2		4.34	4.32	
Dampier W2		4.96	4.61	
Dampier W2		4.80	4.63	
Dampier W2		4.86	4.40	
Dampier W2		4.72	4.27	
Dampier W2		4.78	4.16	
Dampier W2		4.94	4.78	
Dampier W2		4.82	4.50	
Dampier W2		4.33	4.68	
Dampier W2 mean		**4.7**	**4.5**	
Dampier W2 st. dev.		**0.3**	**0.2**	
				27-Feb-04
Burrup SW1		4.70	4.43	4.63
Burrup SW1		4.69	5.33	4.76
Burrup SW1		4.94	4.52	4.97
Burrup SW1		4.49	4.89	4.79
Burrup SW1		4.96	4.68	4.78
Burrup SW1		4.16	4.60	4.92
Burrup SW1		4.42	4.92	3.89
Burrup SW1		4.66	4.98	4.94
Burrup SW1			5.01	4.94
Burrup SW1			4.65	5.02
Burrup SW1 mean		**4.63**	**4.80**	**4.76**
Burrup SW1 st. dev.		**0.27**	**0.27**	**0.33**

27-Feb-04

Burrup SW2		5.39	4.88	4.87
Burrup SW2		5.32	4.49	4.68
Burrup SW2		4.64	4.82	4.83
Burrup SW2		4.44	4.83	5.16
Burrup SW2		4.60	4.72	4.83
Burrup SW2		5.43	4.69	4.80
Burrup SW2		5.00	4.65	4.98
Burrup SW2		5.40	4.72	5.00
Burrup SW2		5.38	4.63	5.19
Burrup SW2			4.59	5.24
Burrup SW2 mean		**5.07**	**4.70**	**4.96**
Burrup SW2 st. dev.		**0.40**	**0.12**	**0.19**

				27-Feb-04
King Bay 1		4.89	4.61	4.91
King Bay 1		4.37	5.34	4.73
King Bay 1		5.27	5.15	4.46
King Bay 1		4.98	4.69	4.79
King Bay 1		5.41	4.39	4.64
King Bay 1		5.30	4.70	4.98
King Bay 1		4.85	5.02	4.80
King Bay 1		4.94	5.00	4.87
King Bay 1		6.04	5.12	4.93
King Bay 1		5.33	4.93	4.88
King Bay 1		5.36		4.91
King Bay 1		5.17		
King Bay 1 mean		**5.16**	**4.90**	**4.81**
King Bay 1 st. dev.		**0.41**	**0.29**	**0.15**

				27-Feb-04
King Bay 2		5.27	4.85	4.61
King Bay 2		5.24	4.89	4.75
King Bay 2		5.27	4.89	4.80
King Bay 2		5.41	4.74	4.95
King Bay 2		5.31	5.29	4.86
King Bay 2		4.59	4.77	5.30
King Bay 2		4.88	5.22	4.78
King Bay 2		3.82	5.41	4.76
King Bay 2		5.05	4.93	5.02
King Bay 2		4.91	5.17	3.54
King Bay 2		5.48		5.02
King Bay 2		5.44		4.78
King Bay 2 mean		**5.06**	**5.02**	**4.76**
King Bay 2 st. dev.		**0.5**	**0.2**	**0.42**

Withnell Bay		5.15	5.02
Withnell Bay		4.95	5.01

Withnell Bay		5.18	5.27
Withnell Bay		4.95	4.97
Withnell Bay		4.98	4.73
Withnell Bay		4.79	5.19
Withnell Bay		4.47	4.82
Withnell Bay		4.70	5.50
Withnell Bay		4.85	5.04
Withnell Bay		4.46	4.55
Withnell Bay		4.91	5.01
Withnell Bay mean		**4.85**	**5.01**
Withnell Bay st. dev.		**0.24**	**0.26**

Withnell Bay 2		4.92	5.76
Withnell Bay 2		4.73	5.28
Withnell Bay 2		4.26	5.52
Withnell Bay 2		4.45	5.52
Withnell Bay 2		4.89	5.24
Withnell Bay 2		4.97	5.26
Withnell Bay 2		4.78	5.44
Withnell Bay 2		4.83	5.26
Withnell Bay 2		4.93	5.50
Withnell Bay 2		4.66	5.68
Withnell Bay 2 mean		**4.74**	**5.45**
Withnell Bay 2 st. dev.		**0.23**	**0.18**

North Withnell Bay 1		4.48	4.66
North Withnell Bay 1		4.59	4.80
North Withnell Bay 1		4.17	4.85
North Withnell Bay 1		4.86	4.62
North Withnell Bay 1		4.37	4.66
North Withnell Bay 1		4.54	4.75
North Withnell Bay 1		4.29	4.76
North Withnell Bay 1		4.51	5.03
North Withnell Bay 1			5.16
North Withnell Bay 1			4.89
North Withnell Bay 1			
North Withnell Bay 1			
North Withnell Bay 1			
North Withnell Bay 1 mean		**4.48**	**4.82**
North Withnell Bay 1 st. dev.		**0.21**	**0.17**

North Withnell Bay 2		4.77	4.65
North Withnell Bay 2		4.74	3.45 soil area

North Withnell Bay 2		4.66	4.87
North Withnell Bay 2		4.31	4.79
North Withnell Bay 2		4.83	5.09
North Withnell Bay 2		4.65	4.76
North Withnell Bay 2		4.58	4.88
North Withnell Bay 2		4.50	5.13
North Withnell Bay 2		4.63	5.05
North Withnell Bay 2			4.73
North Withnell Bay 2			5.03
North Withnell Bay 2 mean, no soil		4.63	4.90
North Withnell Bay 2 st. dev. no soil		0.15	0.17
North Withnell Bay 2 mean			**4.9**
North Withnell Bay 2 st. dev.			**0.2**

Deep Gorge 1		4.91	4.71
Deep Gorge 1		4.54	5.06
Deep Gorge 1		4.87	4.74
Deep Gorge 1		4.72	4.87
Deep Gorge 1		4.89	4.90
Deep Gorge 1		4.10	5.14
Deep Gorge 1		4.32	4.98
Deep Gorge 1		4.06	4.80
Deep Gorge 1		5.19	4.80
Deep Gorge 1		4.17	5.07
Deep Gorge 1		4.14	
Deep Gorge 1 mean		**4.54**	**4.91**
Deep Gorge 1 st. dev.		**0.40**	**0.15**

Deep Gorge 2		4.59	4.69
Deep Gorge 2		4.93	4.97
Deep Gorge 2		4.46	5.45
Deep Gorge 2		4.63	5.31
Deep Gorge 2		4.57	5.20
Deep Gorge 2		4.79	5.04
Deep Gorge 2		4.71	5.16
Deep Gorge 2		4.36	5.12
Deep Gorge 2		4.70	5.31
Deep Gorge 2			3.85
Deep Gorge 2			
Deep Gorge 2 mean		**4.64**	**5.01**
Deep Gorge 2 st. dev.		**0.17**	**0.46**

Deep Gorge 3			5.19
Deep Gorge 3			4.91
Deep Gorge 3			5.06
Deep Gorge 3			4.73
Deep Gorge 3			4.78
Deep Gorge 3			4.91
Deep Gorge 3			5.39
Deep Gorge 3			5.27
Deep Gorge 3			5.23
Deep Gorge 3			5.10
Deep Gorge 3 mean			**5.06**
Deep Gorge 3 st. dev.			**0.22**

Climbing Man Gully 1		5.37	4.96
Climbing Man Gully 1		5.53	4.80
Climbing Man Gully 1		5.39	5.03
Climbing Man Gully 1		4.84	4.78
Climbing Man Gully 1		5.41	4.97
Climbing Man Gully 1		4.83	4.63
Climbing Man Gully 1		4.81	4.93
Climbing Man Gully 1		5.70	5.03
Climbing Man Gully 1		3.04	5.37
Climbing Man Gully 1		5.55	4.22
Climbing Man Gully 1		5.42	5.53
Climbing Man Gully 1		4.62	4.26
Climbing Man Gully 1			4.58
Climbing Man Gully 1 mean		**5.0**	**4.9**
Climbing Man Gully 1 st. dev.		**0.7**	**0.4**
Climbing Man Gully 1 mean (-acid spot)		5.22	
Climbing Man Gully 1 st. dev. (-acid spot)		0.37	

Climbing Man Gully 1-1		5.05	4.92
Climbing Man Gully 1-1		4.85	5.00
Climbing Man Gully 1-1		5.03	3.95
Climbing Man Gully 1-1		5.97	4.45
Climbing Man Gully 1-1		5.78	3.94
Climbing Man Gully 1-1		5.46	3.83
Climbing Man Gully 1-1		5.79	3.97
Climbing Man Gully 1-1		5.45	3.68
Climbing Man Gully 1-1		5.23	4.94
Climbing Man Gully 1-1		5.31	3.85
Climbing Man Gully 1-1 mean		**5.39**	**4.25**
Climbing Man Gully 1-1 st. dev.		**0.37**	**0.52**

June 03 Adjacent to Climbing Man	3.74		4.86

Feb 04 Climbing Man itself	4.31		4.85
Feb 04 Climbing Man itself	4.54		3.91
Feb 04 Climbing Man itself	4.19		3.61
Feb 04 Climbing Man itself	4.1		4.87
Feb 04 Climbing Man itself	4.27		3.75
Feb 04 Climbing Man itself	4.78		4.86
Feb 04 Climbing Man itself	4.55		4.82
Feb 04 Climbing Man itself	3.58		4.68
Feb 04 Climbing Man itself			5.13
Feb 04 Climbing Man itself			4.68
Feb 04 Climbing Man itself mean	**4.23**		**4.55**
Feb 04 Climbing Man itself st. dev.	**0.39**		**0.53**

Climbing Man gully 2B			5.19
Climbing Man gully 2B			5.04
Climbing Man gully 2B			5.23
Climbing Man gully 2B			5.28
Climbing Man gully 2B			5.21
Climbing Man gully 2B			5.06
Climbing Man gully 2B			5.35
Climbing Man gully 2B			5.43
Climbing Man gully 2B			5.29
Climbing Man gully 2B			5.53
Climbing Man gully 2B mean			**5.26**
Climbing Man gully 2B st. dev.			**0.15**

Compound, off site up hill		4.88	3.81
Compound, off site up hill		4.49	5.06
Compound, off site up hill		4.76	4.94
Compound, off site up hill		4.33	4.76
Compound, off site up hill		5.17	5.67
Compound, off site up hill		4.17	4.65
Compound, off site up hill		4.16	3.88
Compound, off site up hill		4.73	3.86
Compound, off site up hill		4.61	4.59
Compound, off site up hill		4.67	4.40
Compound, off site up hill		4.64	
Compound, off site, uphill, mean		**4.60**	**4.56**
Compound, off site, uphill st. dev.		**0.30**	**0.60**

Compound off site, 2			3.85
Compound off site, 2			4.62
Compound off site, 2			3.82
Compound off site, 2			4.66
Compound off site, 2			4.58
Compound off site, 2			4.91
Compound off site, 2			4.51
Compound off site, 2			4.52
Compound off site, 2			4.83
Compound off site, 2			3.94
Compound off site, 2 mean			**4.42**
Compound off site, 2 st. dev.			**0.40**

Rock 3	4.67		4.46
Rock 3	4.76		4.79
Rock 3			4.63
Rock 3			5.03
Rock 3			4.40
Rock 3			4.16
Rock 3			4.71
Rock 3			4.69
Rock 3			4.82
Rock 3			4.54
Rock 3 mean	**4.72**		**4.62**
Rock 3 st. dev.	**0.06**		**0.25**

Rock 86	4.56	4.71	4.98
Rock 86	4.67	4.72	4.95
Rock 86	4.46	4.62	5.09
Rock 86	4.63	5.04	5.08
Rock 86	5.57	4.89	4.86
Rock 86	5.3	4.96	5.10
Rock 86	5.12	5.22	4.90
Rock 86		4.99	4.92
Rock 86		4.96	4.64
Rock 86		5.05	5.21
Rock 86			5.05
Rock 86 mean	**4.90**	**4.92**	**4.98**
Rock 86 st. dev.	**0.43**	**0.18**	**0.15**

Rock 97	5.21		4.87
Rock 97	5.26		5.30
Rock 97	5.74		5.11
Rock 97			5.03
Rock 97			6.06
Rock 97			5.68
Rock 97			5.34
Rock 97			5.41
Rock 97			5.67
Rock 97			5.00
Rock 97 mean	**5.40**		**5.35**
Rock 97 st. dev.	**0.29**		**0.37**

Rock 162	4.92	4.72	4.88
Rock 162	5.87	4.63	4.82
Rock 162	5.29	4.86	4.81
Rock 162		4.73	4.88
Rock 162		4.68	5.21
Rock 162		4.50	5.41
Rock 162		4.54	5.12
Rock 162		4.68	5.14
Rock 162		4.71	5.21
Rock 162			5.06
Rock 162 mean	**5.36**	**4.67**	**5.05**
Rock 162 st. dev.	**0.48**	**0.11**	**0.20**

Rock 938		3.97	5.83
Rock 938		4.38	5.12
Rock 938		4.75	5.06
Rock 938		5.15	4.83
Rock 938		4.87	5.45
Rock 938		4.57	4.56
Rock 938		4.64	5.75
Rock 938		5.20	4.35
Rock 938		4.50	4.47
Rock 938		4.80	3.98
Rock 938		5.00	
Rock 938		4.85	
Rock 938		5.63	
Rock 938		**4.7**	
Rock 938		**5.4**	
Rock 938 mean		**4.82**	**4.94**
Rock 938 st. dev.		**0.41**	**0.61**

Rock 1681	5.63	4.57	4.14
Rock 1681	5.36	4.43	5.18
Rock 1681	5.53	4.38	4.93
Rock 1681	5.59	4.17	4.40
Rock 1681	5.28	4.29	4.88
Rock 1681	5.45	4.43	4.8
Rock 1681	5.40	4.21	4.93
Rock 1681	4.86	4.76	4.73
Rock 1681	5.34	4.32	4.85
Rock 1681	4.90	4.10	4.63
Rock 1681	5.64	4.15	
Rock 1681	5.67	3.92	
Rock 1681	4.74	3.86	
Rock 1681	5.81	3.85	
Rock 1681 mean	**5.37**	**4.25**	**4.75**
Rock 1681 st. dev.	**0.33**	**0.26**	**0.30**

Gidley Island 1			25-Feb-04
Gidley Island 1			10:00
Gidley Island 1			4.45
Gidley Island 1			4.81
Gidley Island 1			5.09
Gidley Island 1			4.96
Gidley Island 1			5.06
Gidley Island 1			4.93
Gidley Island 1			4.86
Gidley Island 1			5.08
Gidley Island 1			4.63
Gidley Island 1 mean			**4.17**
Gidley Island 1 st. dev.			**1.67**

Gidley Island 2			25-Feb-04
Gidley Island 2			10:30
Gidley Island 2			4.73
Gidley Island 2			4.52
Gidley Island 2			4.68
Gidley Island 2			4.67
Gidley Island 2			5.24
Gidley Island 2			4.94
Gidley Island 2			4.65
Gidley Island 2			4.78
Gidley Island 2			4.76
Gidley Island 2			5.00
Gidley Island 2			4.57
Gidley Island 2 mean			**4.78**
Gidley Island 2 st. dev.			**0.21**

Gidley Island 3			25-Feb-04
Gidley Island 3			11:00
Gidley Island 3			4.61
Gidley Island 3			5.54
Gidley Island 3			4.70
Gidley Island 3			5.10
Gidley Island 3			4.50
Gidley Island 3			4.92
Gidley Island 3			5.25
Gidley Island 3			5.26
Gidley Island 3			5.50
Gidley Island 3			4.21
Gidley Island 3 mean			**4.96**
Gidley Island 3 st. dev.			**0.45**

Dolphin Island 1			25-Feb-04
Dolphin Island 1			12:10
Dolphin Island 1			4.93
Dolphin Island 1			4.85
Dolphin Island 1			4.72
Dolphin Island 1			4.63
Dolphin Island 1			4.61
Dolphin Island 1			5.05
Dolphin Island 1			4.86
Dolphin Island 1			4.71
Dolphin Island 1			5.08
Dolphin Island 1			4.95
Dolphin Island 1			4.52
Dolphin Island 1 mean			**4.81**
Dolphin Island 1 st. dev.			**0.19**

Dolphin Island 2			25-Feb-04
Dolphin Island 2			12:35
Dolphin Island 2			5.14
Dolphin Island 2			4.91
Dolphin Island 2			4.89
Dolphin Island 2			3.68
Dolphin Island 2			3.74
Dolphin Island 2			5.04
Dolphin Island 2			4.85
Dolphin Island 2			5.07
Dolphin Island 2			4.79
Dolphin Island 2			5.04
Dolphin Island 2			4.72
Dolphin Island 2			0.54
Dolphin Island 2			
Dolphin Island 2 mean			**4.97**
Dolphin Island 2 st. dev.			**0.12**

Dolphin Island 3			25-Feb-04
Dolphin Island 3			12:55
Dolphin Island 3			5.22
Dolphin Island 3			5.32
Dolphin Island 3			5.15
Dolphin Island 3			5.66
Dolphin Island 3			5.07
Dolphin Island 3			4.65
Dolphin Island 3			3.87
Dolphin Island 3			4.81
Dolphin Island 3			5.25
Dolphin Island 3			5.07
Dolphin Island 3			5.22
Dolphin Island 3 mean			**5.03**
Dolphin Island 3 st. dev.			**0.46**

Appendix IX: Colour measurements in 2018

Location	Engraved L*	Engraved a*	Engraved b*	Parent L*	Parent a*	Parent b*	ΔL*	E-P Δa*	Δb*
S4Spot1	33.97	15.73	18.49	30.20	13.79	14.48	3.77	1.94	4.01
S4Spot2	33.95	15.38	19.03	32.46	14.82	15.73	1.49	0.56	3.30
S4Spot3	35.41	16.58	19.49	32.86	14.44	16.61	2.55	2.14	2.88
S4Spot4	33.61	15.81	18.32	32.76	14.37	15.33	0.85	1.44	2.99
S5spot1	37.64	19.06	22.58	34.47	13.72	14.57	3.17	5.34	8.01
S5spot2	37.28	19.72	23.12	32.14	14.81	15.72	5.14	4.91	7.40
S5spot3	33.16	15.23	17.55	29.22	13.69	14.62	3.94	1.54	2.93
S5spot4	36.87	19.26	22.09	30.40	14.55	15.64	6.47	4.71	6.45
S6spot1	40.23	12.00	17.82	38.50	13.40	17.62	1.73	-1.40	0.20
S6spot2	39.15	11.43	16.89	37.50	12.45	16.16	1.65	-1.02	0.73
S6spot3	39.56	10.64	15.62	37.51	13.30	16.93	2.05	-2.66	-1.31
S6spot4	40.31	10.70	16.25	39.17	13.64	17.83	1.14	-2.94	-1.58
S7spot1	33.03	13.64	17.13	29.26	14.41	15.50	3.77	-0.77	1.63
S7spot2	31.56	14.49	16.47	29.76	13.75	14.21	1.80	0.74	2.26
S7spot3	31.78	13.49	16.34	25.52	11.09	12.35	6.26	2.40	3.99
S7spot4	33.89	14.11	18.33	27.67	13.46	14.79	6.22	0.65	3.54
S21spot1	39.67	16.71	22.50	31.27	12.72	12.83	8.40	3.99	9.67
S21spot2	38.56	15.73	21.47	34.75	14.37	16.03	3.81	1.36	5.44
S21spot3	37.76	16.98	22.38	33.89	14.54	17.80	3.87	2.44	4.58
S21spot4	39.04	15.98	21.85	32.71	12.27	14.16	6.33	3.71	7.69
S22spot1	35.49	12.49	16.32	33.18	12.06	12.60	2.31	0.43	3.72
S22spot2	33.99	13.60	15.90	33.11	12.75	14.16	0.88	0.85	1.74
S22spot3	37.31	14.47	19.11	34.48	13.22	15.24	2.83	1.25	3.87
S22spot4	37.28	14.03	19.13	33.94	12.55	14.01	3.34	1.48	5.12
S23spot1	37.77	10.78	16.58	33.88	12.32	16.05	3.89	-1.54	0.53
S23spot2	33.29	12.07	17.90	38.15	14.21	19.41	-4.86	-2.14	-1.51
S23spot3	34.93	10.97	17.32	32.04	13.91	15.80	2.89	-2.94	1.52
S23spot4	34.76	10.42	16.45	32.39	8.62	12.03	2.37	1.80	4.42

Appendix X: Colour measurements on rocks August 2019

Colour differences (**Bold**) between background and engravings on each of the monitoring sites

	L*	a*	b*	L*	a*	b*	L*	a*	b*
Site 4 spot 1	30.85	14.18	14.84	34.20	15.84	18.87	**3.35**	**1.66**	**4.03**
Site 4 spot 2	29.61	13.19	14.30	31.39	14.51	16.32	**1.78**	**1.32**	**2.02**
Site 4 spot 3	32.85	14.68	15.18	33.59	15.37	17.65	**0.74**	**0.69**	**2.47**
Site 4 spot 4	33.58	14.69	15.84	33.78	14.92	17.48	**0.19**	**0.23**	**1.63**
Site 5 spot 1	34.55	13.39	14.23	37.15	18.06	21.51	**2.60**	**4.67**	**7.28**
Site 5 spot 2	29.81	14.06	14.78	35.97	19.21	22.39	**6.16**	**5.15**	**7.61**
Site 5 spot 3	33.36	10.60	11.03	40.26	19.45	24.01	**6.91**	**8.85**	**12.99**
Site 5 spot 4	32.44	16.21	17.49	38.26	20.25	23.21	**7.83**	**3.24**	**6.53**
Site 6 spot 1	38.26	12.75	17.24	40.20	11.91	17.69	**1.94**	**-0.84**	**0.45**
Site 6 spot 2	38.37	11.73	16.23	37.67	12.55	16.93	**-0.69**	**0.83**	**0.71**
Site 6 spot 3	37.96	12.43	16.80	39.73	12.21	16.74	**1.77**	**-0.23**	**-0.06**
Site 6 spot 4	39.53	12.31	16.86	40.25	10.22	16.08	**0.72**	**-2.09**	**-0.78**
Site 7 spot 1	27.84	13.14	14.52	31.73	13.88	17.65	**3.89**	**0.74**	**3.13**
Site 7 spot 2	28.82	12.38	13.11	31.55	15.16	16.79	**2.73**	**2.78**	**3.68**
Site 7 spot 3	26.64	11.95	13.02	31.80	15.45	17.98	**5.15**	**3.50**	**4.95**
Site 7 spot 4	25.55	12.70	14.00	30.90	13.60	16.79	**5.34**	**0.90**	**2.79**
Site 21 spot 1	33.30	13.63	15.81	37.44	16.45	21.28	**4.15**	**2.82**	**5.48**
Site 21 spot 2	32.62	13.64	15.38	38.02	15.64	20.88	**5.40**	**2.00**	**5.50**
Site 21 spot 3	32.77	14.62	16.39	36.13	16.63	21.55	**3.36**	**2.01**	**5.16**
Site 21 spot 4	33.82	13.54	15.71	39.41	15.54	20.87	**5.58**	**2.00**	**5.16**
Site 22 spot 1	34.44	13.36	14.68	34.73	13.08	15.94	**0.28**	**-0.28**	**1.27**
Site 22 spot 2	31.50	12.55	14.08	34.26	13.72	16.92	**2.75**	**1.16**	**2.84**
Site 22 spot 3	32.85	12.31	13.52	35.08	13.95	16.75	**2.23**	**1.65**	**3.24**
Site 22 spot 4	30.81	11.46	11.94	35.39	13.29	18.17	**4.59**	**1.84**	**6.23**
Site 23 spot 1	35.59	11.59	16.00	38.96	9.82	16.19	**3.37**	**-1.77**	**0.19**
Site 23 spot 2	35.56	13.02	17.98	34.79	12.32	19.21	**-0.77**	**-0.70**	**1.23**
Site 23 spot 3	32.81	12.56	17.70	32.71	11.73	18.47	**-0.09**	**-0.83**	**0.77**
Site 23 spot 4	32.35	9.07	12.45	36.65	10.93	17.37	**4.30**	**1.85**	**4.92**